



National Library
of Canada

Bibliothèque nationale
du Canada

Canadian Theses Service

Service des thèses canadiennes

Ottawa, Canada
K1A 0N4

NOTICE

The quality of this microform is heavily dependent upon the quality of the original thesis submitted for microfilming. Every effort has been made to ensure the highest quality of reproduction possible.

If pages are missing, contact the university which granted the degree.

Some pages may have indistinct print especially if the original pages were typed with a poor typewriter ribbon or if the university sent us an inferior photocopy.

Reproduction in full or in part of this microform is governed by the Canadian Copyright Act, R.S.C. 1970, c. C-30, and subsequent amendments.

AVIS

La qualité de cette microforme dépend grandement de la qualité de la thèse soumise au microfilmage. Nous avons tout fait pour assurer une qualité supérieure de reproduction.

S'il manque des pages, veuillez communiquer avec l'université qui a conféré le grade.

La qualité d'impression de certaines pages peut laisser à désirer, surtout si les pages originales ont été dactylographiées à l'aide d'un ruban usé ou si l'université nous a fait parvenir une photocopie de qualité inférieure.

La reproduction, même partielle, de cette microforme est soumise à la Loi canadienne sur le droit d'auteur, SRC 1970, c. C-30, et ses amendements subséquents.

UNIVERSITY OF ALBERTA

**NUTRIENT FLUCTUATIONS IN FED-BATCH
FERMENTATIONS OF BAKER'S YEAST**

By

PRADYUMNA KUMAR NAMDEV

**A Thesis submitted to the Faculty of Graduate Studies and Research in partial
fulfillment of the requirements for the degree of DOCTOR OF PHILOSOPHY**

DEPARTMENT OF CHEMICAL ENGINEERING

**EDMONTON, ALBERTA
SPRING 1992**



National Library
of Canada

Bibliothèque nationale
du Canada

Canadian Theses Service Service des thèses canadiennes

Ottawa, Canada
K1A 0N4

The author has granted an irrevocable non-exclusive licence allowing the National Library of Canada to reproduce, loan, distribute or sell copies of his/her thesis by any means and in any form or format, making this thesis available to interested persons.

The author retains ownership of the copyright in his/her thesis. Neither the thesis nor substantial extracts from it may be printed or otherwise reproduced without his/her permission.

L'auteur a accordé une licence irrévocable et non exclusive permettant à la Bibliothèque nationale du Canada de reproduire, prêter, distribuer ou vendre des copies de sa thèse de quelque manière et sous quelque forme que ce soit pour mettre des exemplaires de cette thèse à la disposition des personnes intéressées.

L'auteur conserve la propriété du droit d'auteur qui protège sa thèse. Ni la thèse ni des extraits substantiels de celle-ci ne doivent être imprimés ou autrement reproduits sans son autorisation.

ISBN 0-315-73035-8

Canada

UNIVERSITY OF ALBERTA
RELEASE FORM

NAME OF AUTHOR: PRADYUMNA KUMAR NAMDEV

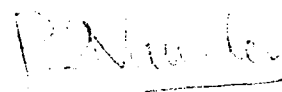
TITLE OF THESIS: Nutrient Fluctuations In Fed-batch Fermentations Of
Baker's Yeast.

DEGREE: Doctor of Philosophy

YEAR THIS DEGREE GRANTED: Spring, 1992

Permission is hereby granted to the University of Alberta Library to reproduce single copies of this thesis and to lend or sell such copies for private, scholarly, or scientific research purposes only.

The author reserves all other publication and other rights in association with the copyright in the thesis, and except as hereinbefore provided neither the thesis nor any substantial portion thereof may be printed or otherwise reproduced in any material from whatever without the author's written permission.


.....

B29, J.R. Hospital Qtrs.
Maratha Mandir Road
Bombay 400 008, INDIA

DATE: January 13th 1992

UNIVERSITY OF ALBERTA

FACULTY OF GRADUATE STUDIES AND RESEARCH

The undersigned certify that they have read, and recommend to the Faculty of Graduate Studies and Research for acceptance, a thesis entitled **Nutrient Fluctuations in Fed-batch Fermentations of Baker's Yeast** submitted by **Pradyumna K. Namdev** in partial fulfillment of the requirements for the degree of Doctor Of Philosophy.

.....
M. R. Gray, Supervisor

.....
B. G. Thompson, Co-supervisor

.....
S. E. Wanke

.....
D. T. Lynch

.....
H. Anwar

.....
E. H. Dunlop

Date: January 13th, 1992

This thesis is dedicated to my mother.

ABSTRACT

Production-scale fermentors exhibit spatial gradients in nutrient concentrations due to poor mixing between the 'feed zone' where feed is added at the top of the vessel and the bulk of liquid where nutrients are consumed. Frequent exposure of cells to these concentration gradients can result in unexpected effects on productivity. These effects were studied by pulsed addition of feed to an aerobic culture of *Saccharomyces cerevisiae* in a 2 L fermentor with pulse-on interval of 5 s. The pulse-off interval, from 3 s to 39 s, was controlled by a Monte Carlo method to give a log-normal distribution with a mean of 20 s and a standard deviation of 8.9 s. A circulation time distribution of this log-normal type characterises the mixing patterns in a production vessel of size about 150 m³. The effect of feed zone was simulated by the Monte Carlo addition of feed to a recycle loop, where the broth circulated between the recycle loop and the fermentor to give a range of residence times in the loop from 0.5 to 12 min.

Monte Carlo experiments with a complex medium showed no feed zone effect on biomass yields, whereas 10% higher biomass yields were obtained in defined-medium experiments. Correspondingly, up to 50% less ethanol was consumed in complex-media experiments due to fluctuations in nutrient supply, whereas defined-media experiments showed no effect on ethanol. Experiments with periodic addition of feed with pulse-off time of 15 s produced a synchronous response of the culture for both defined- and complex-media fermentations. These differences in results proved that the range of circulation times and complex nature of media are important parameters in evaluating the feed zone effect.

A synchronous culture in the chemostat produced non-harmonic oscillations in the CO₂ fraction of the off-gas. These CO₂-cycles continued for five cycles during an exponential fed-batch fermentation, whereas Monte Carlo fermentation produced a chaotic response in CO₂ and disrupted synchrony. These results showed that synchrony cannot be established in a production fermentor. A structured model was proposed for synchrony, with the segregation of the population accounted for in the delay of uptake of storage carbohydrates. The model predicted certain experimental results, including the stable oscillations of chemostat and fast and random fluctuations of CO₂ during the Monte Carlo fermentations. These results from the model indicated that storage carbohydrates may play a role in generation of synchrony.

ACKNOWLEDGEMENTS

I would like to express my sincere gratitude to my thesis supervisor, Dr. Murray Gray, for providing constant encouragement, technical guidance and insightful direction throughout the course of this research project. I learned the philosophy and approach to the engineering research and teaching through continuous discussions with Dr. Gray, for which I will remain thankful to him.

I take this opportunity to thank my thesis co-supervisor, Dr. B.G. Thompson, for his comments, encouragement and the use of the excellent research facilities at the Alberta Research Council.

Many people helped to make my work at the Alberta Research Council easier and enjoyable. I wish to express my thanks to Dr. Dennis Ward, for help with the computer monitoring and control system; Dr. Alan Jones, for showing me a microbiologist's view of fermentation; Graeme Macaloney and Robert Carmichael, for stimulating discussion on a range of topics; Twyla Malcolm, Indira Draper and Mike Brandingen, for their technical assistance.

My fellow research group members, P.K. Yegneswaran and Jan Bloemkolk, helped to create an atmosphere of intellectual stimulation and friendship which made my years in Edmonton enjoyable and memorable.

I would like to thank the National Science and Engineering Research Council of Canada and the University of Alberta for the funding of this project and my presentations of this research work at various national and international meetings.

I especially thank my parents for their unwavering support, encouragement and blessing throughout my life and helping me to recognize the value of education and achieve this distinction.

TABLE OF CONTENTS

Chapter	Page
List of Tables	x
List of Figures	xiii
List of Symbols	xix
Glossary	xxiii
1. INTRODUCTION	1
References	10
2. EXPERIMENTAL SIMULATION OF LARGE-SCALE BIOREACTOR ENVIRONMENTS USING A MONTE CARLO METHOD	15
Introduction	15
Theory	19
Materials and Methods	22
Results and Discussion	29
Conclusions	36
References	37

Chapter		Page
3.	THE EFFECT OF FEED—ZONE IN FED—BATCH FERMENTATION OF <i>SACCHAROMYCES CEREVISIAE</i>	40
	Introduction	40
	Theory	45
	Materials and Methods	57
	Results and Discussion	65
	Conclusions	80
	References	81
4.	EFFECTS OF GLUCOSE FLUCTUATIONS ON SYNCHRONY IN FED—BATCH FERMENTATION OF <i>SACCHAROMYCES CEREVISIAE</i>	85
	Introduction	85
	Materials and Methods	88
	Results and Discussion	91
	Conclusions	106
	References	107
5.	MODELLING THE SYNCHRONY IN CHEMOSTAT AND FED—BATCH FERMENTATIONS OF <i>SACCHAROMYCES CEREVISIAE</i>	110
	Introduction	110
	The Model	114
	Results	124
	Discussion	137
	Conclusions	139
	References	140

Chapter		Page
6.	CONCLUSIONS AND RECOMMENDATIONS	143
APPENDIX A	Calibration Equations For Biomass	147
APPENDIX B	Data From Repeated Experiments For Fed–Batch Fermentations With Complex Medium	149
APPENDIX C	CTD Calculation And Data From Repeated Experiments For Fed–Batch Fermentations With Complex And Defined Media	155
APPENDIX D	Calculation Of Synchrony Fraction And Data From Repeated Experiments For Fed–Batch Fermentations With Defined Medium	167

LIST OF TABLES

Table	Page
1.1 Experimental evaluation of the effects of concentration gradients in bench-scale fermentations	6
2.1 Circulation times (t_c) obtained from Figure 2.3 and used in the Monte Carlo fermentation.	26
2.2 Concentrations of biomass, ethanol, and glucose from <i>S.cerevisiae</i> fermentations with continuous, Monte Carlo and periodic supply of nutrients.	32
3.1 Composition of media used in fermentations with <i>S.cerevisiae</i> ATCC 32167.	58
3.2 Initial and final levels of biomass, ethanol and acetic acid for experiments with <i>S.cerevisiae</i> NCYC 1018 grown on complex medium.	66
3.3 Final levels of biomass and ethanol for experiments with <i>S.cerevisiae</i> ATCC 32167 grown on defined medium	76
5.1 Operating conditions used in the simulations following experiments described in Chapter 4.	125
5.2 Model parameters used in the simulations following Strassle <i>et al.</i> (1988).	126

Table		Page
A.1	Dry cell weight vs optical density for <i>S.cerevisiae</i> NCYC 1018 grown on complex medium during fed–batch fermentations.	147
A.2	Dry cell weight vs optical density for <i>S.cerevisiae</i> ATCC 32167 grown on defined medium during fed–batch fermentations.	148
B.1	DCW and ethanol data for continuous fed–batch fermentations with <i>S.cerevisiae</i> NCYC 1018 grown on complex medium	150
B.2	DCW and ethanol data for Monte Carlo fed–batch fermentations with <i>S.cerevisiae</i> NCYC 1018 grown on complex medium	151
B.3	DCW and ethanol data for periodic fed–batch fermentations with <i>S.cerevisiae</i> NCYC 1018 grown on complex medium	152
C2.1	DCW, ethanol and acetate data for continuous fed–batch fermentations with <i>S.cerevisiae</i> NCYC 1018 grown on complex medium and in fermentor–loop system	158
C2.2	DCW, ethanol and acetate data for Monte Carlo fed–batch fermentations with <i>S.cerevisiae</i> NCYC 1018 grown on complex medium and in fermentor–loop system	159
C3.1	DCW and ethanol data for continuous fed–batch fermentations with <i>S.cerevisiae</i> ATCC 32167 grown on defined medium	160

Table	Page
C3.2 DCW and ethanol data for Monte Carlo fed–batch fermentations with <i>S.cerevisiae</i> ATCC 32167 grown on defined medium	161
C3.3 DCW and ethanol data for periodic fed–batch fermentations with <i>S.cerevisiae</i> ATCC 32167 grown on defined medium	162
C4.1 DCW and ethanol data for continuous and Monte Carlo fed–batch fermentations with <i>S.cerevisiae</i> ATCC 32167 grown on complex medium	164
D.1 Budded fraction data for chemostat ($D=0.2\text{ h}^{-1}$) to continuous fed–batch fermentation	170
D.2 Budded fraction data for chemostat ($D=0.2\text{ h}^{-1}$) to Monte Carlo fed–batch fermentation	171
D.3 Budded fraction data for chemostat at $D = 0.1\text{ h}^{-1}$	173

LIST OF FIGURES

Figure		Page
2.1	Schematic diagram of a single cycle in the Monte Carlo experiment	21
2.2	Fermentor monitoring and control system	23
2.3	A log-normal CTD ($\bar{t}_c = 20$ s, $\sigma = 8.9$ s) with area under the curve divided into 25 equal probability sections	25
2.4	Monte Carlo algorithm to simulate a CTD in a bench-scale fermentor	28
2.5	Ethanol and biomass profiles from fed-batch fermentation of <i>S. cerevisiae</i> with different feeding strategies	30
2.6	Oxygen uptake rate and carbon dioxide evolution rate during fed-batch fermentation of <i>S. cerevisiae</i> with Monte Carlo and continuous supply of substrate	31
2.7	Oscillations in DO level after 13 h of fed-batch fermentation of <i>S. cerevisiae</i> with periodic feeding	35

Figure		Page
3.1	Three-zone mixing model for a fed-batch fermentor	46
3.2	Network-of-zones 'stochastic' model following Mann <i>et al.</i> (1981)	49
3.3	Types of 'flow-cell' used in Network-of-zones 'stochastic' model following Mann <i>et al.</i> (1981)	50
3.4	Prediction of a CTD for feed zone and a fit with RTD for a single passage through a recycle flow model	51
3.5	Experimental simulation of feed zone effects	55
3.6	A schematic of mixing bulb used to mix fresh feed with recirculating culture broth	63
3.7	A comparison of biomass profiles for experiments with complex medium and recycle loop of volume = 50 mL	67
3.8	Comparison of theoretical demand of glucose equivalent required for observed growth with the glucose supplied during continuous and Monte Carlo experiments with complex medium. The feed rate in Monte Carlo experiments is an instantaneous rate to the recycle loop during the pulse-on period of 5 s	69
3.9	Net amount of ethanol (symbols), maltose (symbols), and glucose (line) consumed during experiments with complex medium and recycle loop of volume of 50 mL	70

Figure		Page
3.10	Net amount of ethanol consumed (circles), and acetic acid produced (triangles) during experiments with complex medium. A recirculation rate of 0.25 L/h and recycle loop of volume 50 mL were used	72
3.11	Comparison of biomass (open symbols), and ethanol (closed symbols) produced during experiments with <i>S.cerevisiae</i> ATCC 32167 on defined medium	75
4.1	Effect of dilution rate on oscillations of dissolved oxygen and CO ₂ fraction in off-gas. t_s represents period for single-cell phase and t_b represents period for budding-cell phase. G1, S, G2 and M represent the four phases of the cell-cycle of yeast	92
4.2	Correlation between budded fraction of yeast population and CO ₂ fraction in off-gas during chemostat operation	93
4.3	Profile of CO ₂ fraction in off-gas for a complete experiment consisting of batch, chemostat and fed-batch operations	97
4.4	Comparison of profiles of budded fraction for the continuous fed-batch fermentation and the Monte Carlo fed-batch fermentation	99
4.5	Comparison of profiles of CO ₂ fraction in off-gas for the three types of fed-batch experiments: continuous, Monte Carlo, and periodic	102

Figure		Page
4.6	Comparison of profiles of dissolved oxygen for the three types of fed–batch experiments: continuous, Monte Carlo, and periodic	103
5.1	A cell–cycle model showing the interaction between the cell–cycle events and the nutrient environment	115
5.2	The metabolic network scheme used to model the synchrony in chemostat culture of <i>S.cerevisiae</i>	117
5.3	Prediction of the stable oscillations in chemostat culture of <i>S.cerevisiae</i> at $D = 0.2 \text{ h}^{-1}$, $G_{\text{in}} = 5 \text{ g/L}$	127
5.4	Predictions for the continuous fed–batch fermentation at an exponentially increasing rate, $F_{\text{in}} = 8 \exp(0.16t)$ with $G_{\text{in}} = 100 \text{ g/L}$	130
5.5	Comparison of model predictions for Monte Carlo with continuous fed–batch fermentations	131
5.6	Predictions of CO_2 and DO profiles for the Monte Carlo fed–batch fermentation	133
5.7	Comparison of model predictions for periodic with continuous fed–batch fermentation	134
5.8	Predictions of CO_2 and DO profiles for the periodic fed–batch fermentation	135

Figure		Page
B.1	Comparison of RQ profiles for continuous fed–batch with Monte Carlo fed–batch fermentations with <i>S.cerevisiae</i> , NCYC 1018 grown on complex medium.	153
B.2	Comparison of DO profiles for continuous fed–batch with Monte Carlo fed–batch fermentations with <i>S.cerevisiae</i> , NCYC 1018 grown on complex medium.	154
C1.1	An algorithm to calculate a CTD for a reference zone using the ‘Network–of–Zones’ stochastic model.	156
C1.2	A CTD calculated for the impeller zone.	157
C3.1	Reproducibility of biomass profiles for continuous and Monte Carlo fed–batch fermentations with <i>S.cerevisiae</i> NCYC 1018, grown on defined medium.	163
C4.1	Comparison of CER profiles for fermentations of <i>S.cerevisiae</i> ATCC 32167, grown on complex medium.	165
C4.1	Comparison of DO profiles for fermentations of <i>S.cerevisiae</i> ATCC 32167, grown on complex medium.	166
D.1	Reproducibility of CO ₂ profiles for chemostat ($D=0.2\text{ h}^{-1}$) <i>S.cerevisiae</i> ATCC 32167 grown on defined medium	174
D.2	CO ₂ –cycles during chemostat fermentations ($D=0.2\text{ h}^{-1}$) as a measure of synchrony, with <i>S.cerevisiae</i> ATCC 32167 grown on defined medium	175
D.3	Profile of dissolved oxygen during a chemostat ($D=0.2\text{ h}^{-1}$) <i>S.cerevisiae</i> ATCC 32167 grown on defined medium	176

Figure		Page
D.4	Profile of pH during a chemostat at $D = 0.2 \text{ h}^{-1}$ with <i>S.cerevisiae</i> ATCC 32167 grown on defined medium	177
D.5	Profile of CO_2 in a continuous fed–batch fermentation with <i>S.cerevisiae</i> ATCC 32167 grown on defined medium	178
D.6	Profile of CO_2 for a Monte Carlo fed–batch fermentation <i>S.cerevisiae</i> ATCC 32167 grown on defined medium	179
D.7	Profile of O_2 during a batch–chemostat–continuous fed–batch fermentation with <i>S.cerevisiae</i> ATCC 32167 grown on defined medium	180
D.8	Profile of O_2 during a batch–chemostat–Monte Carlo fed–batch fermentation with <i>S.cerevisiae</i> ATCC 32167 grown on defined medium	181
D.9	Profile of pH during a batch–chemostat–continuous fed–batch fermentation with <i>S.cerevisiae</i> ATCC 32167 grown on defined medium	182
D.10	Profile of pH during a batch–chemostat–Monte Carlo fed–batch fermentation with <i>S.cerevisiae</i> ATCC 32167 grown on defined medium	183
D.11	Cell number density in chemostat–continuous fed–batch fermentation with <i>S.cerevisiae</i> ATCC 32167 grown on defined medium	184
D.12	Cell number density in chemostat–Monte Carlo fed–batch fermentation with <i>S.cerevisiae</i> ATCC 32167 grown on defined medium	185

LIST OF SYMBOLS

BF	ratio of number of budded cells to total number of cells
CO _{2g}	molar fraction of carbon dioxide in off-gas, (%)
CPR	carbon dioxide production rate by the cells, [mmol/(L-h)]
D	dilution rate, (h ⁻¹)
DCW	dry cell weight, (g/L)
DO	dissolved oxygen relative to saturation condition, (%)
E	concentration of ethanol in the liquid phase, (g/L)
f	circulation time distribution function, (s ⁻¹)
F	volumetric flow rate, (L/h)
G	concentration of glucose in the liquid phase, (g/L)
H _{O2}	solubility constant for oxygen, (mmol/L)
K _i	saturation constant for the species i, (g/L)
k _L a	volumetric mass transfer coefficient, (1/h)
K _{O2}	saturation constant for oxygen, (mmol/L)
K _t	parameter in the kinetics for uptake of storage carbohydrates, (g/g)
K _{tinh}	a parameter in the kinetics of storage carbohydrates formation, (h-g/g)
m _{x/s}	maintenance coefficient for the yeast culture, [g/(g-h)]
N	number of cells per unit volume, (L ⁻¹)
O _{2g}	molar fraction of oxygen in off-gas, (%)
O _{2L}	concentration of oxygen in the liquid phase, (mmol/L)
OUR	oxygen uptake rate by the cells, [mmol/(L-h)]
P	probability of entering recycle loop as given by f(t _c) in Equation (1) Chapter 3, (s ⁻¹)
Q _{gtm}	a parameter in the kinetics for storage carbohydrate, [g/(g-h)]

Q_i	specific flux for the species i , [g/(g–h)]
Q_{o2m}	maximum specific oxygen uptake rate, [mmol/(g–h)]
Q_{qo}	a parameter in the kinetics for uptake of storage carbohydrates
Q_r	recirculation rate of broth between fermentor and recycle loop (L/h)
R_g	theoretical demand of glucose for observed growth (Equation 10 in Chapter 3), (g/h)
R_n	normally distributed random number
R_u	uniformly distributed random number
t	time, (h)
t_c	circulation time, (s)
\bar{t}_c	mean circulation time, (s)
t_{lag}	lag time as defined by Equation (1) in Chapter 3, (s)
t_p	pulse–off interval during the Monte Carlo fed–batch fermentation, (s)
T_r	concentration of storage carbohydrates (internal glucose), (g/L)
T_c	period of a CO ₂ –cycle during chemostat fermentation, (h)
V	total volume of broth in the fermentor, (L)
X	residual biomass or biomass without the storage carbohydrates, (g/L)
X^T	total biomass, (g/L)
y_s	fraction of synchronised sub–population in the fermentor
Y_{ce1}	yield coefficient for CO ₂ on ethanol uptake, (mmol/g)
Y_{ce2}	yield coefficient for CO ₂ on ethanol secretion, (mmol/g)
Y_{cgo}	yield coefficient of CO ₂ on oxidative glucose uptake, (mmol/g)
Y_{oe}	yield coefficient of oxygen on ethanol uptake, (mmol/g)
Y_{og}	yield coefficient of oxygen on glucose uptake, (mmol/g)
Y_{xe}	yield coefficient of X on ethanol, (g/g)
Y_{xgo}	yield coefficient of X on oxidative glucose uptake, (g/g)
Y_{xgr}	yield coefficient of X on reductive glucose uptake, (g/g)

Greek Letters

α	reduction in probability P as defined by equation (6)
β	reduction in probability P as defined by equation (8)
μ	specific growth rate of biomass, (hr ⁻¹)
μ_1	log—mean circulation time, (s)
ρ	molar density of air, (mmol/L)
σ	standard deviation of circulation time, (s)
σ_l	log—mean standard deviation, (s)
σ_θ	normalized standard deviation
τ	the delay interval or duration of the budding—cell phase, (h)
ψ	fraction of the heterogeneous population in budding phase

Subscripts

air	air
b	fermentor broth
crit	limiting respiratory capacity
e	ethanol
g	glucose
gg	glucose flux through glycolysis
go	glucose uptake in oxidative mode
gr	glucose uptake in reductive mode
h	non-synchronous sub-population in the fermentor
in	inlet condition to the fermentor
m	maximum flux
mc	Monte Carlo
o	conditions at the start of the fed-batch fermentation
out	exit condition from the fermentor
o ₂	oxygen
p	recycle loop
s	synchronous sub-population in the fermentor
t	storage carbohydrates
x	biomass without storage carbohydrates

GLOSSARY¹

aerobes	microorganisms whose growth requires the presence of air or free oxygen
allosteric control	control by enzymes with a binding and catalytic site for the substrate and a different site where a modulator acts
assimilation	the incorporation of nutrients into the biomass of an organism
ATCC	American Type Culture Collection
ATP	adenosine triphosphate, a major carrier of phosphate and energy in biological systems, composed of adenosine and three phosphate groups; the free energy released from the hydrolysis of ATP is used to drive many energy requiring reactions in biological systems
β -galactosidase	an enzyme catalysing the hydrolysis of β -linked galactose within dimers or polymers
budding	a form of asexual reproduction in which a daughter cell develops from a small outgrowth or protrusion of the parent cell; the daughter cell is smaller than the parent cell
catabolism	reactions involving the enzymatic degradation of organic compounds to simpler organic or inorganic compounds with the release of free energy

¹Atlas, R.M. *Microbiology, Fundamentals and Applications*. Macmillan Publishing Company: New York, 1984. A-6.

catabolite— repression	repression of the transcription of genes coding for certain inducible enzyme systems by glucose or other readily utilisable carbon sources
cell—cycle	growth cycle of a cell
chemostat	an apparatus used for continuous—flow culture to maintain bacterial cultures in the log phase of growth based on maintaining a continuous supply of a solution containing a nutrient in limiting quantities that controls the growth rate of the culture
culture	a growth of particular types of microorganisms on or within a medium as a result of inoculation and incubation
defined medium	the material supporting the microbial growth in which all the constituents, including trace substances, are quantitatively known; a mixture of known composition used for culturing microorganisms.
diauxie	the phenomena in which, given two carbon sources, an organism preferentially metabolizes one completely before utilising the other
eukaryotes	cellular organisms having a membrane—bound nucleus within which the genome of the cell is stored as chromosomes composed of DNA; eukaryotic organisms include algae, fungi, protozoa, plants, and animal
fermentation	a mode of energy—yielding metabolism that involves a sequence of oxidation—reduction reactions in which an organic substrate and the organic compounds derived from that substrate serve as the primary electron donor and the terminal electron acceptor; in contrast to

respiration, there is no requirement for an external electron acceptor to terminate the metabolic sequences; also, routinely used to represent a process to grow the cells in suspension with external supply of air

fermenter

an organism that carries out the fermentation

fermentor

a reaction chamber for growing microorganisms in suspension

glucose-effect

saturation of respiratory capacity of yeast cells due to excess of glucose in the medium; the excess is fermented into ethanol

glycolysis

an aerobic process of glucose dissemination by a sequence of enzyme-catalyzed reactions to a pyruvic acid

induction

an increase in the rate of synthesis of an enzyme; the turning on of enzyme synthesis in response to environmental conditions

medium

the material that supports the growth/reproduction of microorganisms

metabolism

the sum total of all chemical reactions by which energy is provided for the vital processes and new substances are assimilated

metabolites

chemical participating in metabolism; nutrients

microorganisms

microscopic organisms, including algae, bacteria, fungi, protozoa, and viruses

mRNA

the RNA that carries information from DNA to ribosomes where it specifies the amino acid sequence for a particular polypeptide chain

NAD	a coenzyme used as an electron acceptor in oxidation–reduction reactions
NADH	reduced NAD
NCYC	National Collection Of Yeast Cultures
prokaryotes	cells whose genomes are not contained within a nucleus; the bacteria
rDNA proteins	recombinant DNA technology products: proteins produced by microorganism by deliberately modifying the genetic properties of the producing microorganisms
respiration	a mode of energy–yielding metabolism requiring a terminal electron acceptor for substrate oxidation, with oxygen frequently used as the terminal electron acceptor
segregated–models	models for behaviour of a culture which consider heterogeneity of the population in the culture
structured–models	models for behaviour of a culture which differentiate a single cell into various components
synchrony	a phenomena in which, all cells of the culture are in the same phase of the cell–cycle at any given time
transcription–control	control of transcription of genetic information on mRNA level
yeasts	a category of fungi defined in terms of morphological and physiological criteria, typically a unicellular, saprophytic organism that characteristically ferments a range of carbohydrates and in which asexual reproduction occurs by budding

CHAPTER 1

INTRODUCTION

Scope and Significance

Industrial fermentations are routinely operated in a fed–batch mode whereby the nutrients are fed to the fermentors according to a predetermined strategy (Whitaker, 1980). These fermentation processes include production of baker's yeast, antibiotics, recombinant proteins, amino acids, enzymes and vitamins. The fermentation cultures show a high degree of sensitivity to the concentration of nutrients in the fermentor, so that the feed rate of nutrients is manipulated to achieve high productivity. In production of baker's yeast, for example, molasses and ammonia are fed at an increasing rate to obtain a high cell density, up to 50 g/L (Reed, 1982). The molasses supply is decreased towards the end of baker's yeast fermentation to achieve a product with a higher level of rising capability and storage capability. Glucose is fed according to a profile in production of penicillin to extend the growth and antibiotic production periods (Mou, 1982). Therapeutic proteins are produced from genetically modified microorganisms by achieving high cell density, up to 60 g/L, in fed–batch fermentation (Zabriskie and Arcuri, 1986).

The cost associated with the fermentation step usually ranges from 15% to 60% of the cost for the overall process (Hacking, 1986). The process economics for most of the bulk products, such as baker's yeast and antibiotics, dictate the use of large fermentors of volumes in the range of 150 m³ to 600 m³. The wealth of experience and rules of thumb on scale–up methods, and more recently government regulations, make the stirred fermentor a favourite choice of industry (Sittig, 1982).

The major issues considered during the scale–up of fermentors are as follows:

the interaction of the hydrodynamics with the microbial metabolism, strain degeneration, media degradation, and interaction of the fermentation step with the down-stream processing step. Engineering techniques are used to tackle the first issue by devising scale-up methods for the selection of vessel size, impellers, configuration of the internals in the vessel and operating conditions. The major operating costs for typical large-scale stirred fermentors include agitation, compression of air and nutrients (Hacking, 1986). The design and operating conditions associated with these variables are obtained from scale-up studies involving a range of fermentors, from 2 L to 20,000 L in the laboratory and the pilot-plant.

Scale-up methods

The simplest approach to scale-up of fermentors is a step-wise empirical approach in which the size of the fermentor is increased in successive stages. This approach usually results in cost and time before satisfactory fermentor design conditions are obtained. Consequently, a number of empirical and semi-empirical methods have been proposed and widely used to reduce the cost and the time associated with scale-up. These methods include rules of thumb (Charles, 1985), regime analysis (Sweere *et al.*, 1987) and the total environment approach (Young, 1979).

The engineering variables, including power per unit volume, mass transfer coefficient for oxygen, tip speed of the impeller and mixing time are used to obtain rules of thumb. The scale-up is performed by keeping one of the engineering variables constant. A number of empirical correlations are used to estimate the other operating variables. Regime analysis is performed to determine the rate limiting step from among the many relevant mechanisms, including mass-transfer of oxygen, bulk-phase mixing and nutrient consumption rates. The regime analysis

method is used to select the relevant rule of thumb for scale-up. The total environmental approach to scale-up involves reproducing profiles of all the environmental variables at each fermentor capacity so that the desired performance can be reproduced. These methods are usually insufficient for *a priori* analysis, especially when more than one variable controls the fermentation. For example, in antibiotic production, shear sensitivity of the mycelial microorganism and flooding of the impeller by gas put limits on the agitation and aeration rate, respectively, thus causing poor mixing of the bulk. For fed-batch fermentations, the location and delivery of feed also affect the distribution of fresh nutrients in the medium. A rational strategy is, therefore, needed to aid in scale-up of fermentors.

Importance of Micro-environment

In production vessels, there are limitations on power supply to the impellers (1 to 4 kW/m³), aeration (10 to 60 m³/(h-m³)) and the type of impeller (Sittig, 1982). The viscosity of the broth in biomass production is low (< 40 mPa-s) but could be up to 2 Pa-s of apparent viscosity during antibiotic fermentation. These limitations on operating conditions and high viscosity would produce spatial variation in the intensity of mixing in the production vessel. The uptake of nutrients and oxygen coupled with localised supply of air and nutrients under imperfect mixing conditions, therefore, leads to spatial heterogeneity in the fermentor. Among these variables are pH, temperature, shear stress, dissolved oxygen, dissolved carbon dioxide and nutrient concentrations (Lilly, 1983).

As a microbial cell, embedded in its microenvironment, circulates in the fermentor, it would be exposed to a range of concentrations and other variables in its microenvironment. The sizes of microenvironments (50 – 300 μm) in typical industrial fermentors are much larger than the size of microbial cells which range from 1 to 5 μm (Dunlop and Ye, 1990). The overall performance of the fermentor

would depend on the response of individual cells to their respective microenvironment. The traditional rules of thumb for scale-up neglect the interaction of the cells with their microenvironment by averaging the hydrodynamics through the use of the engineering variables.

Various microorganisms show a range of sensitivities to different physical and chemical variables in their microenvironment (Lilly, 1983). Shear stress affects growth and productivity of various mycelial organisms and microbial polysaccharide production. The control of temperature can be a serious problem for fermentations with fast growing organisms such as *Saccharomyces cerevisiae* and *Escherichia coli*. Low dissolved oxygen levels and high nutrient concentrations cause reductions in the yields of biomass, for example in baker's yeast production, and antibiotics, such as penicillin. Numerous articles on scale-up have indicated that the gradients in dissolved oxygen and nutrients are the major factors affecting the performance of microbial fermentation (Reuss and Brammer, 1985).

The effects of concentration gradients on productivity would be critical if a significant proportion of the microbial population is exposed to extreme concentrations for sufficient periods. Mixing time and circulation time measurements in stirred vessels have shown that the cells could spend times exceeding one minute away from the fully aerated zone of the impeller and the location of nutrient addition (Bryant, 1977). Few metabolic studies have been done to demonstrate that the microbial cells could have response times of less than a minute to the changes in nutrient levels (Einsele *et al.*, 1978; Brooks & Meers, 1973; Petrik *et al.*, 1983). A rational strategy to aid scale-up studies, therefore, should be based on the evaluation of interactions of microbial cells with the concentrations in their microenvironment.

Previous Attempts

Both theoretical and experimental investigations have been performed to

evaluate the effect of varying concentrations on fermentation. Recycle-flow models were used to partition the production fermentor into a number of compartments (Sinclair and Brown, 1970; Bajpai and Reuss, 1982; Tanner *et al.*, 1985; Yu and Bajpai, 1986; Bajpai and Sohn, 1987). These simulations were limited in their implications as the metabolic models used in the simulations were not suitable for transient conditions. In the experimental studies, three types of experimental system were used to impose concentration gradients on the culture: a single stirred fermentor with varying input, a single loop fermentor with varying feed location, and two fermentors with recirculation of broth between them. These experimental studies are summarised in Table 1.1 according to the experimental apparatus, perturbations in feed, and the microorganism used. No realistic mixing model or parameters were used to design the experimental set-up and operating conditions in these experimental studies. The gradients in nutrient and dissolved oxygen imposed in these experimental studies were, therefore, not representative of large fermentors. Also, most of these studies used the chemostat mode of operation, whereas fed-batch fermentation is routinely used in industry. Although mixing intensity at the point of feeding has been shown to affect the yield of biomass, the experiments were not correlated with production scale fermentation conditions (Hansford and Humphrey, 1966; Dunlop and Ye, 1990). Nevertheless, these studies showed that concentration fluctuations with characteristic times in less than few minutes would interfere with the metabolism of cells and thus affect the productivity.

Selection of a suitable microorganisms is important to test the effects of concentrations fluctuations on the metabolism of cells. Table I shows that *Saccharomyces cerevisiae* or baker's yeast was often used in previous studies. *S.cerevisiae* is sensitive to low levels of glucose and oxygen (Kappeli and Sonnleitner, 1986). For example, if glucose concentration in the medium exceeds 0.5 g/L, ethanol is excreted and the yield of biomass is reduced. Also, chemostat

TABLE 1.1: Experimental evaluation of the effects of concentration gradients in bench-scale fermentations

Fermentor Type	Mode of Operation	Perturbations	Time Constant (s)	Microorganisms	Reference
S T R ¹	Chemostat	Periodic Methanol Feed	20 – 100	<i>Pseudomonas methylophilus</i>	Brooks & Meer (1973)
S T R	Chemostat	Periodic Glucose Feed	0.5 – 240	<i>Saccharomyces cerevisiae</i>	Welles & Blanch (1976)
S T R	Chemostat	Periodic Air & Glucose Feed	20 – 500	<i>S. cerevisiae</i>	Heinze et al. (1981)
S T R	Chemostat	Periodic Glucose Feed	10 – 100	<i>S. cerevisiae</i>	Heinze et al. (1985)
S T R	Chemostat	PRBS ² Methanol Feed	4 – 25	<i>Pseudomonas methylophilus</i>	Roberts & Slater (1986)
S T R	Batch	Agitation	NA	<i>Bacillus subtilis</i>	Griot et al. (1986)
S T R	Batch	Periodic Pressure	120	<i>Penicillium chrysogenum</i>	Vardar & Lilly (1982)
S T R	Batch	Periodic Air/N ₂	20 – 180	<i>Gluconobacter oxydans</i>	Oosterhuis et al. (1985)
S T R	Batch	Periodic Air/N ₂	60 – 600	<i>S. cerevisiae</i>	Sweere et al. (1988a)

1. S T R: Stirred Tank Reactor, 2. PRBS: Pseudo Random Binary Sequence

TABLE 1.1 (continued)

Fermentor Type	Mode of Operation	Perturbations	Time Constants (s)	Microorganisms	Reference
Tubular Loop	Chemostat	Recirculation in the Loop	300	<i>Candida tropicalis</i>	Katanger (1976)
Tubular Loop	Fed-batch	Glucose Feed Location	5 – 25	<i>S. cerevisiae</i>	Heinze <i>et al.</i> (1981)
Tubular Loop	Batch	Recirculation in the Loop	15 – 59	<i>Aureobasidium pullulans</i>	Kristiansen & Mcneil (1987)
Tubular Loop	Batch	Recirculation in the Loop	10 – 100	<i>S. cerevisiae</i>	McNeil <i>et al.</i> (1990)
Air-Lift	Fed-batch	Methanol Feed Location	–	<i>Methylophilus methylotrophus</i>	Fields & Slater (1984)
Two STR	Batch	Periodic Air/N ₂	30 – 120	<i>G. oxydans</i>	Oosterhuis <i>et al.</i> (1985)
Two STR	Batch	D.O. Control	150 – 372	<i>B. subtilis</i>	Griot <i>et al.</i> (1986)
STR-Loop	Batch	Air to STR N ₂ to Loop	60 – 600	<i>P. chrysogenum</i> <i>Escherichia coli</i>	Larsson & Enfors (1988)
Two STR	Chemostat	Air to STR I N ₂ to STR II	60 – 270	<i>S. cerevisiae</i>	Sweere <i>et al.</i> (1988b)
Two STR	Fed-batch	Feed to STR I	60 – 378	<i>S. cerevisiae</i>	Sweere <i>et al.</i> (1988c)
STR-Loop	Chemostat	Glucose Feed into the Loop	6.4	<i>S. cerevisiae</i>	Fowler & Dunlop (1989)

cultures of *S.cerevisiae* have a tendency to partially synchronize under perfect mixing and aerobic conditions (Strassle *et al.*, 1988). Regular oscillations in the various measurements were observed due to the partial synchrony of *S.cerevisiae* in chemostat cultures. Low concentrations of ethanol (< 0.1 g/L) and perfectly mixed conditions in the fermentor were cited as prerequisites for this oscillatory behaviour. The oscillatory behaviour of a yeast culture would be, therefore, susceptible to elimination by poor mixing conditions in the fermentor. The large number of metabolic studies and industrial applications of *S.cerevisiae* make it a suitable choice to evaluate the effects of mixing on growth.

Objectives

The objective of this thesis is to systematically evaluate the effect of gradients in the nutrient concentrations on the metabolism of *S.cerevisiae* during fed–batch fermentation. The experimental apparatus and the profiles of feed rates were designed such that fluctuations in nutrient concentrations representative of a larger stirred fermentor were reproduced.

A novel approach, based on a Monte Carlo method is developed in Chapter 2 of this thesis to recreate the concentration gradients from a large–scale fermentor in the bench–scale fermentor. The strategy was implemented experimentally using a fed–batch culture of *S.cerevisiae*. A complex media and a log–normal distribution of circulation times were used, which are characteristic of production conditions. In Chapter 3, the effect of a nutrient–rich ‘feed–zone’ on the fed–batch fermentation of *S.cerevisiae* in a complex and a defined medium is described. Such a feed–zone could exist in production vessels as the nutrients are usually fed at the top of the fermentor. In the experiments, the broth was recirculated between a recycle loop and a bench–scale fermentor, and feed was supplied intermittently into the loop according to the Monte Carlo method.

The effect of transient fed-batch conditions and fluctuations in the glucose feed on a synchronously dividing culture of *S.cerevisiae* is discussed in Chapter 4. Chemostat and exponential fed-batch fermentations of *S.cerevisiae* were performed using a defined media. The response from the *S.cerevisiae* culture to the transient conditions in various types of fed-batch fermentations provided a sensitive and severe test to discriminate between the models for spontaneous synchrony. In Chapter 5, a metabolically structured model with a time delay was used to simulate the synchrony in a chemostat with one adjustable parameter. The synchrony model, consisting of four ordinary differential equations, is used to test the mechanism of synchrony by simulating the fed-batch fermentations. The standard curves, derivation and data from repeated experiments for Chapters 2, 3 and 4 are given in Appendices A, B, C and D.

REFERENCES

- Bajpai, R.K. and Reuss, M. Coupling of mixing and microbial kinetics for evaluating the performance of bioreactors. *Can. J. Chem. Eng.* **1982**, *60*, 384–392.
- Bajpai, R.K. and Sohn, P.U. In *Biotechnology progress, Mixing and scale-up*; Ho, C.S. and Oldshue, J.Y., Eds.; AIChE symposium, Miami, **1987**, pp 13–21.
- Brooks, J.D., Meers, J.L. The effect of discontinuous methanol addition on the growth of a carbon-limited culture of *Pseudomonas* sp.. *J. Gen. Microbiol.*, **1973**, *77*, 513–519.
- Bryant, J. Characterization of mixing in fermentors. *Adv. Biochem. Eng.* **1977**, *5*, 101–123.
- Charles, M. In *Comprehensive Biotechnology*, Moo-Young, M., Ed. in-chief; Pergamon Press:Oxford, **1985**, *2*, pp 57–75.
- Dunlop, E.H., Ye, S.J. Micromixing in fermentors: Metabolic changes in *Saccharomyces cerevisiae* and their relationship to fluid turbulence. *Biotechnol. Bioeng.* **1990**, *36*, 854–864.
- Einsele, A. Scaling of bioreactors. *Process Biochem.*, **1978**, *July*, 13–14.
- Fields, P.R., Slater, N.K.H. The influence of fluid mixing upon respiratory patterns for extended growth of a methylotroph in an air-lift fermenter. *Biotechnol. Bioeng.* **1984**, *26*, 719–726.
- Fowler, J.D., Dunlop, E.H. Effects of reactant heterogeneity and mixing on catabolite repression in cultures of *Saccharomyces cerevisiae*. *Biotechnol. Bioeng.* **1989**, *33*, 1039–1046.
- Griot, M., Moes, J., Heinzle, E., Dunn, I.J., Bourne, J.R. A microbial culture for the measurement of macro and micro mixing phenomena in biological

- reactors. *Int. Conf. Bioreactor Fluid Dynamics*. Cambridge, UK, 1986, paper 16, 203–216.
- Hacking, A.J. *Economic aspects of biotechnology*. Cambridge University Press, Cambridge; 1986, pp 276–287.
- Hansford, G.S., Humphrey, A.E. The effect of equipment scale and degree of mixing on continuous fermentation yield at low dilution rates. *Biotechnol. Bioeng.* 1966, 8, 85–96.
- Heinzle, E., Nishizawa, Y., Dunn, I.J., Bourne, J.R. Dynamic and steady-state effects of cyclic feeding of oxygen and glucose in an ethanol-producing yeast culture. *Ann. N.Y. Acad. Sci.* 1981, 369, 159–166.
- Heinzle, E., Moes, J., Dunn, I.J. The influence of cyclic glucose feeding on a continuous baker's yeast culture. *Biotechnol. Lett.*, 1985, 7(4), 235–240.
- Kappeli, O. and Sonnleitner, B. Regulation of sugar metabolism in *Saccharomyces* type yeast: Experimental and conceptual considerations. *CRC Crit. Rev. in Biotechnol.* 1986, 4(3), 299–325.
- Katinger, H.W.D. Physiological response of *Candida tropicalis* grown on n-Paraffin to mixing in a tubular closed loop fermenter. *Eur. J. Appl. Microbiol.*, 1976, 3, 103–114.
- Kristiansen, B., McNeil, B. The design of a tubular loop for scale-up and scale-down of fermentation processes. In the *Intl. conf. on bioreactors and biotransformations*, Moody, G.W. and Baker, P.B., Ed., Gleneagles, Scotland, UK, 1987, 321–334.
- Larsson, G. and Enfors, S.-O. Kinetics of microbial response to insufficient mixing in bioreactors. *Sixth Eur. Congr. on Mixing*, Pavia, Italy. 1988, 443–450.
- Lilly, M.D. In *Bioactive Microbial Products 2, Development and Production*, Nisbet, L.J. and Winstanley, D.J., Eds.; Academic Press: New York, 1983, pp 79–89.

- McNeil, B., Kristiansen, B. Simulated scale-up of a yeast fermentation using a loop bioreactor. *Biotechnol. Lett.* **1990**, *12*(1), 39–44.
- Mou, D.G. In *Antibiotics containing the β -lactam structure*. Demain, A.L. and Solomon, N.A., Eds.; **1983**, pp 255–284.
- Oosterhuis, N.M.G., Kossen, N.W.F., Olivier, A.P.C., Schenk, E.S. Scale-down and optimization studies of the gluconic acid fermentation by *Gluconobacter oxydans*. *Biotechnol. Bioeng.* **1985**, *27*, 711–720.
- Petrik, M., Kappeli, O., Fiechter, A. An expanded concept for the glucose effect in the yeast *Saccharomyces uvarum*: Involvement of short- and long-term regulation. *J. Gen. Microbiol.* **1983**, *129*, 43–49.
- Reed G. In *Prescott & Dunn's Industrial Microbiology*; Reed, G., Ed.; AVI Publishing Company, Inc.: Westport, Connecticut, **1982**, pp 593–633.
- Reuss, M. and Brammer, U. Influence of substrate distribution on productivities in computer controlled baker's yeast production. *Proc. IFAC Conf. on Modelling and Control of Biotechnological Processes*, Noordwijkerhout, **1985**, 145–150.
- Roberts, J.A.E. and Slater, N.K.H. Simulation of a methylotroph's behaviour in an imperfectly mixed fermentor. *Int. Conf. Bioreactor Fluid Dynamics*. Cambridge, UK, **1986**, paper 19, 257–267.
- Sinclair, C.G. and Brown, D.E. Effect of incomplete mixing on the analysis of the static behaviour of continuous cultures, *Biotechnol. Bioeng.*, **1970**, *12*, 1001–1017.
- Sittig, W. The present state of fermentation reactors. *J. Chem. Tech. Biotechnol.* **1982**, *32*, 47–58.
- Strassle, C., Sonnleitner, B., Fiechter, A. A predictive model for the spontaneous synchronisation of *Saccharomyces cerevisiae* grown in continuous culture I. Concept. *J. Biotechnol.* **1988**, *7*, 299–318.

- Sweere, A.P.J., Mesters, L. Janse, L., Luyben, K.Ch.M., Kossen, N.W.F.
Experimental simulation of oxygen profiles and their influence on baker's yeast production: I. One fermentor system. *Biotechnol. Bioeng.* 1988a, 31, 567–578.
- Sweere, A.P.J., Janse, L., Luyben, K.Ch.A.M., Kossen, N.W.F. Experimental simulation of oxygen profiles and their influence on baker's yeast production:II. Two fermentor system. *Biotechnol. Bioeng.* 1988b, 31, 579–586.
- Sweere, A.P.J., Matla, Y.A., Zandvliet, J., Luyben, K.Ch.A.M. and Kossen, N.W.F.
Experimental simulation of glucose fluctuations: The influence of continually changing glucose concentrations on the fed–batch baker's yeast fermentation. *Appl. Microbiol. Biotechnol.*, 1988c, 28, 219–224.
- Sweere, A.P.J., Luyben, K.Ch.M., Kossen, N.W.F. Regime analysis and scale–down: tools to investigate the performance of bioreactors. *Enzyme Microbiol. Biotechnol.* 1987, 9, 386–398.
- Tanner, R.D., Dunn, I.J., Bourne, J.R., Klu, M.K. The effect of imperfect mixing on an idealised kinetic fermentation model. *Chem. Eng. Sci.* 1985, 40(7), 1213–1219.
- Vardar, F., Lilly, M.D. Effect of cycling dissolved oxygen concentrations on product formation in penicillin fermentations. *Eur. J. Appl. Microbiol. Biotechnol.* 1982, 14, 203–211.
- Welles, J.B., Blanch, H.W. The effect of discontinuous feeding on ethanol production by *Saccharomyces cerevisiae*. *Biotechnol. Bioeng.* 1976, 28, 129–132.
- Whitaker, A. Fed–batch culture, *Process Biochem*, 1980, 15, 10–15.
- Young, T.B. Fermentation scale–up: Industrial experience with a total environmental approach. *Annal. New York Acad. Sci.* 1979, 326, 165–180.

Yu, M., Bajpai, R. Role of mixing in stirred bioreactors. *Biotechnol. Bioeng.* **1986**, *symp. no. 17*, 673–681.

Zabriskie, D.W., Arcuri, E.J. Factors influencing productivity of fermentations employing recombinant microorganisms. *Enzyme Microb. Technol.* **1986**, *8*, 706–717.

CHAPTER 2

EXPERIMENTAL SIMULATION OF LARGE-SCALE BIOREACTOR ENVIRONMENTS USING A MONTE CARLO METHOD¹

INTRODUCTION

Production-scale bioreactors range from 0.02–1.5 m³ for animal cells and up to 600 m³ for antibiotics and yeast production. As cells circulate in these agitated vessels, their local environment is primarily mixed and replenished near the impellers, and then left largely unmixed as the cells circulate into the peripheral volume. During the residency time in these poorly mixed zones, the cells can alter the local operating conditions. The cells in a large vessel, therefore, undergo fluctuations in local conditions which are dictated by the interaction between imperfect mixing and cell metabolism (Einsele *et al.*, 1978). Such fluctuations in the immediate environment of the cells can account for the difficulty in scaling up the production of many microbial cultures (Oosterhuis, 1984).

Fed-batch fermentation is commonly used for production of secondary metabolites. The biomass can be provided with the appropriate nutrients and precursors at each stage of the fermentation, and fed-batch fermentation technology also offers operational benefits. For example, continuous addition of fresh medium can prolong production of antibiotic from *Cephalosporium acremonium*, and reduce

¹A version of this chapter was published as a part of the paper: Namdev *et al.*, *Can. J. Chem. Eng.* 1991, 69, 513–519.

catabolite repression (Trilli *et al.*, 1977; Matsumura *et al.*, 1981). In the production of yeast, the glucose is fed continuously to minimize the 'glucose effect' (Reuss and Brammer, 1985). As fluid elements circulate in a large fermentor, the substrate will be mixed in at the impellers, and be depleted as the elements circulate through the vessel (Bajpai and Reuss, 1982). Occasionally the cells would be exposed to much higher concentrations as they pass the zone where the substrate is added (Fowler and Dunlop, 1989). A significant complication is the routine use of inexpensive complex media in industrial fermentation, which supply multiple carbon and nitrogen sources (Whitaker, 1980). In industrial fermentors, the local supply of substrates, therefore, can be influenced by mixing characteristics during fermentation.

A common method for characterizing circulation in stirred vessels is the mixing time, defined as the time for a pulse of tracer to mix with the bulk fluid (Nagata, 1975). Mixing times can be relatively long in production systems; as high as 104 s in a 160 m³ fermentor (Charles, 1978). The circulation time distribution (CTD) is an alternative method of characterizing circulation within a stirred vessel, and is measured by determining the probability for each possible time interval that a fluid element takes to return to a fixed reference position, which is usually selected as the impeller region. The CTD for water in typical fermentors follows a log-normal distribution, with a mean time and a variance (Bryant, 1977; Middleton, 1979; Mann *et al.*, 1981; Mukataka *et al.*, 1981; Reuss, 1982; van Barneveldt *et al.*, 1987). This log-normal distribution is consistent with meandering flow paths away from the impeller region (Mann *et al.*, 1981). The mean circulation time increases with the size of the fermentor, up to 20 or 30 s for a 100–120 m³ volume (Oosterhuis, 1984; Bryant, 1977; Middleton, 1979). With a mean time of 20 s, times from 10 s to 80 s would be observed for each pass around the fermentor. The breadth of the distribution of circulation times tends to increase with the

viscosity of liquid, so that viscous fermentation media can give a bimodal distribution, indicating the development of stagnant zones in the vessel (Funahashi *et al.*, 1987).

One of the challenges for understanding and defining scale-up of microbial cultures, intended for processes carried out in large-scale stirred vessels, is to replicate the characteristics of this circulation distribution which have the largest impact on the cells. Such a scale-up method would use simple, small-scale equipment so that scale-up can be examined cheaply and systematically on the lab bench before moving to the production plant.

Several techniques have been proposed to investigate the effects of mixing and fluctuating local environment on growth and productivity of cells. The use of periodic oscillations in substrate concentration (Heinzle *et al.*, 1985) has been proposed as methods to evaluate the effects of poor mixing in fermentors. Substrate would be supplied every 20 s, for example, to mimic a production fermentor with a mean circulation time of 20 s. Circulation times in vessels are distributed over a range of values, however, and are not fixed at the single mean value. For example, two similar mixing times of 23 s and 28 s have been shown to be equivalent to two significantly different circulation time distributions characterised by ($\bar{t}_c = 5$ s, $\sigma = 0.8$ s) and ($\bar{t}_c = 20$ s, $\sigma = 8.9$ s) respectively (Bajpai and Reuss, 1982). Furthermore, periodic oscillations in substrate concentration in chemostats can induce synchrony and shifts in metabolism which would not be characteristic of industrial fed-batch operation.

A two-fermentor system has been used to study the effects of fluctuations in glucose on *Saccharomyces cerevisiae* (Sweere *et al.*, 1988). By maintaining a high concentration in one tank, and low in another, continuous recirculation of fluid between the two tanks can approximate circulation modes in a large fermentor. The two-tank approach is suggested by mass transfer studies which indicate that most

micromixing occurs in a small zone near the impeller, with segregated flow in the remaining volume (Bajpai and Reuss, 1982; Wilhelm *et al.*, 1966). This two-tank experimental method suffers from several limitations. First, two fermentors must be kept in sterile operation, and the flow between the two cannot be measured directly so that tracer methods must be used (Oosterhuis *et al.*, 1985). Second, the lowest concentration in the second vessel is dependent on both the activity of the culture and the rate of recirculation between the two tanks. Furthermore, the cells are exposed to only two concentrations rather than a continuous range. The third limitation is that the circulation time distribution (as in the residence-time distribution for two tanks in series) do not follow a log-normal distribution. Hence the cells do not experience the same fluctuations that they would in a large vessel. The method cannot simulate the bimodal circulation observed for high viscosity systems (Funahashi *et al.*, 1987). Clearly, an alternative and more flexible method for studying mixing interactions is required.

This study presents a systematic method for designing small-scale experiments, in a single fermentor, to simulate the interaction between mixing and growth which is characteristic of large-scale production fermentors. The use of a Monte Carlo method to control the inputs to a small fermentor exposes the growing culture to representative fluctuations in local concentration. Experimental results are given for Monte Carlo cycling of nutrients to cultures of *S. cerevisiae*. These experiments were conducted using a complex medium to better represent industrial fermentations with multiple carbon and nitrogen sources (Whitaker, 1980).

THEORY

Bajpai and Reuss (1982) proposed a method for simulating the interaction between mixing and growth, following the mixing model of Manning *et al.* (1965). In this system, the agitated tank was split into a micromixing zone, a small portion of the tank volume in the vicinity of the impeller where all fluid elements were combined, and a macromixing zone (the remaining volume of the tank) where the elements were segregated. The time of passage through the macromixing zone and back to the micromixing zone was described by the following log-normal probability distribution:

$$f(t_c) = (1/\sqrt{2\pi} \sigma t_c) \exp[-(\ln(t_c) - \mu_l)^2 / 2\sigma^2] \quad (1)$$

$$\bar{t}_c = \exp[\mu_l + (\sigma^2/2)] \quad (2)$$

$$\sigma_\theta^2 = [\sigma^2 / \bar{t}_c^2] = \exp(\sigma_l^2) - 1 \quad (3)$$

where μ_l and σ_l are the mean and deviation of the normally distributed variable y ($\equiv \ln t_c$). The distribution was divided into discrete elements, with \bar{t}_c and σ obtained from the literature, and the model was used to simulate the effect of circulation on growth of yeast in a chemostat. This method is limited by the availability of valid models for growth and product formation, therefore a direct experimental method is required.

A simple approach to scale-up is to manipulate a small fermentor to directly simulate large-scale fluctuations. Hence, we consider the circulation of a single cell from a Lagrangian reference frame and make the small fermentor a representative fluid element in a much larger system. A cycle of the representative fluid element

through the fermenter is as follows: the fluid element starts in the micromixing zone, where the concentration of air or nutrient is replenished. The remainder of the circulation time (t_c) is in the macromixing zone, where the cells in the fluid element are left to depend on the local concentration of oxygen or nutrient. For example, by turning the feed supply on and off, the cells in a small fermenter are alternately exposed to excess of nutrients and growth-driven nutrient depletion, analogous to a large-scale system. The Monte Carlo method provides a straightforward technique for controlling the on-off cycles to mimic the circulation-time distribution in a much larger vessel: a random number can be used to select the circulation time (t_c) from the log-normal probability distribution as follows:

$$t_c = \exp(R_n \sigma_l + \mu_l) \quad (4)$$

In practice \bar{t}_c and σ are calculated from experimental data, then μ_l and σ_l are obtained by solving equations (2) and (3). The disadvantage of equation (4) is that very long cycle times are calculated, which may not be observed experimentally. Alternately, equation (1) can be discretized into n elements of equal probability, each with a corresponding circulation time which is log-normally distributed as in Figure 2.1. A uniform random number, R_u , is then used to select the current value of t_c . In the present study the distribution was divided into discrete elements, and \bar{t}_c and σ were obtained from the literature. Note that any probability distribution could be studied by this discrete method. Over a large number of cycles the cells experience the log-normal distribution of circulation times. Because the circulation times are short with respect to the growth rate of the cells, the outcome of an experiment is not sensitive to the order of the cycles. Over the course of their growth the cells would experience thousands of these random cycles, so that no one circulation time would be dominant, unlike the case of periodic oscillations.

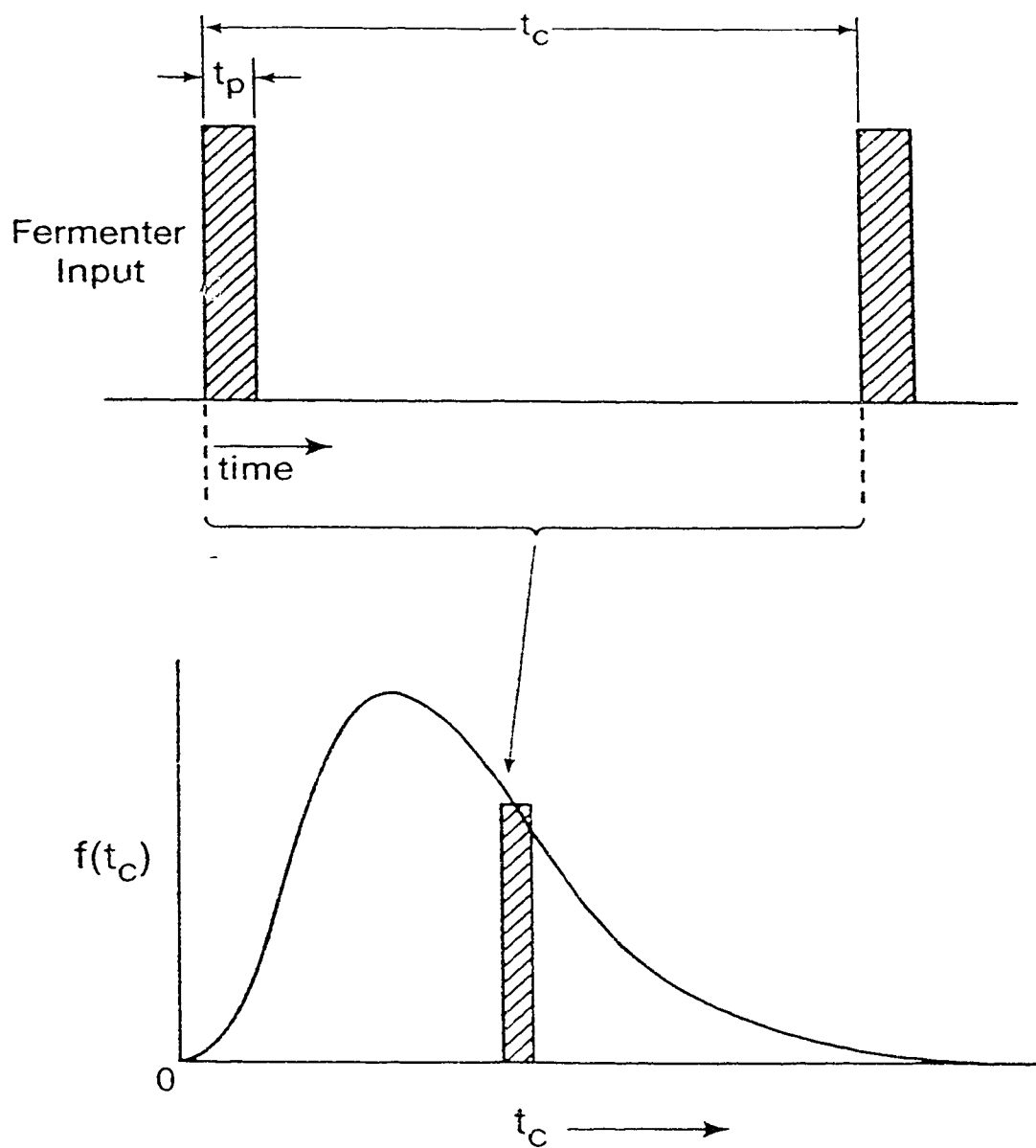


FIGURE 2.1 Schematic diagram of a single cycle in the Monte Carlo experiment. Nutrient is supplied for time t_p , then the feed is turned off for the remainder of the circulation time t_c . The values of t_c for successive periods are randomly selected from the log-normal distribution, $f(t_c)$.

MATERIALS AND METHODS

Microorganism and Medium

The organism used in this study was *S. cerevisiae* NCYC 1018. The organism was maintained on a YD medium (yeast extract and dextrose) slants. The composition of the medium used for shake flask and fermentor culture was as follows: dextrose, 10 g/L; yeast extract, 3 g/L; malt extract, 3 g/L; peptone, 5 g/L (all Difco). The feed composition for fed-batch runs was as following: dextrose, 100 g/L; yeast extract, 30 g/L; malt extract, 30 g/L; peptone, 50 g/L (all Difco). RO water was used for the preparation of medium.

Equipment

The studies on fluctuations in oxygen and substrate concentration were conducted using a 2 L New Brunswick Multigen fermentor, equipped for computer monitoring and control (Figure 2.2). Sensors for pH (Phoenix autoclavable double-reference electrode), amount of acid and base added, temperature (Omega), and dissolved oxygen (Ingold autoclavable DO probe) were connected to a microcomputer via an OPTO-22 data-acquisition system. The pH was controlled by an Omega PHCN-36 pH/ORP controller. The fermentor off-gas was analyzed for O₂, CO₂ and N₂ by a Perkin Elmer Mass Spectrometer. A Tylan Mass flow controller system and peristaltic pumps (Pharmacia model P1; 0.6–500 mL/h) were used to regulate the flows of air and nutrients to the fermentor, respectively.

Cultures and Assays

The inoculum (50mL) was grown to exponential phase for 24 h at 30°C and 250 rpm in a 250ml shake flask. The fermentation was carried out with 2% (v/v) inoculum and initial content of 1 L at 30°C, 500 rpm, and air supply of 1 L/min.

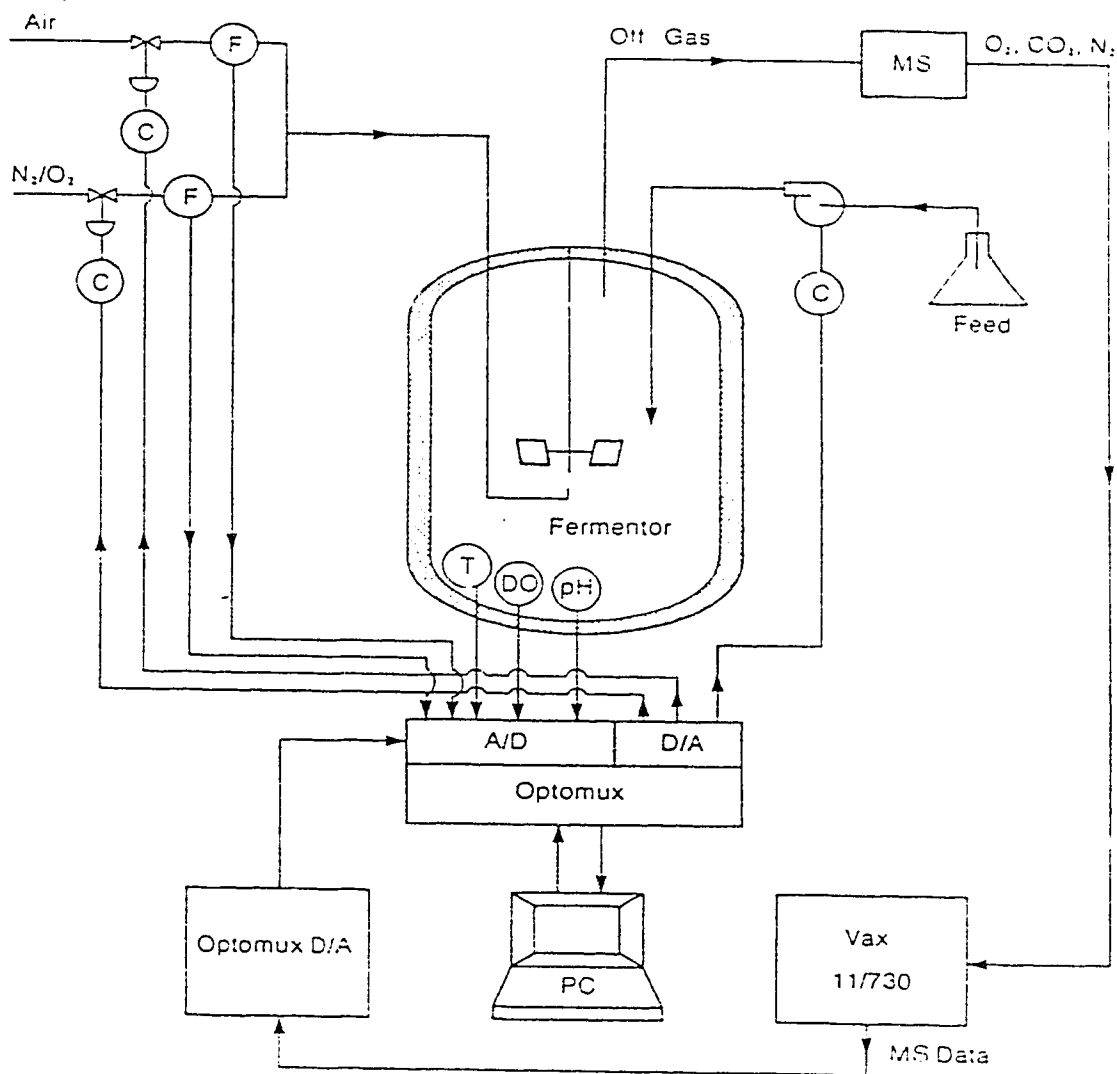


FIGURE 2.2 Fermentor monitoring and control system.

The pH was continuously controlled between 4.5 and 4.8 by using 2N HCl and 2N NaOH. The foam was controlled using 2% (w/v) antifoam SAG 471 (Union Carbide). All fed–batch experiments were fed the feed medium at a rate of 13.5 mL/h. Feeding was started when the carbon dioxide evolution rate (CER) was 5–5.1 mmol/(L–h) and the glucose level was close to zero, after about 11 h of growth. At this stage the culture was switching from aerobic fermentation on glucose to respiration on ethanol.

Samples were taken aseptically every 3 h in the fed–batch experiments. The biomass was measured by absorbance at 620 nm using a Spectronic 21 spectrophotometer. A linear correlation between dry weight and absorbance was obtained (Appendix A). The sample was filtered using 0.45 μ m, 25 mm diameter Sartorius cellulose nitrate filters. Glucose in the supernatant was analyzed using a YSI (model 27) Glucose Analyzer with a precision of ± 3 mg/L and minimum value of 10 mg/L. Ethanol and acetic acid was measured within 5% precision using Spectra Physics GC equipped with 80/120 carbopack B/6.6% carbowax 20M column and a flame ionization detector.

Design of Cycling Experiments

Each cycle of a Monte Carlo experiment followed a set pattern, as illustrated by a pulse of nutrient in Figure 2.1. The pulse time (t_p) was constant in all cycles, with a value of approximately half of the shortest circulation time. A log–normal distribution was used with parameters $\bar{t}_c = 20$ s and $\sigma = 8.9$ s, which characterize the circulation time distribution typical of a large fermentor (Bajpai and Reuss, 1982). The area under the distribution curve was divided into 25 elements (Figure 2.3), each of equal probability and represented by a particular circulation time (Table 2.1). The log–normal distribution was discretized in this manner to avoid extremely large values of t_c , which would occasionally result from equation (4).

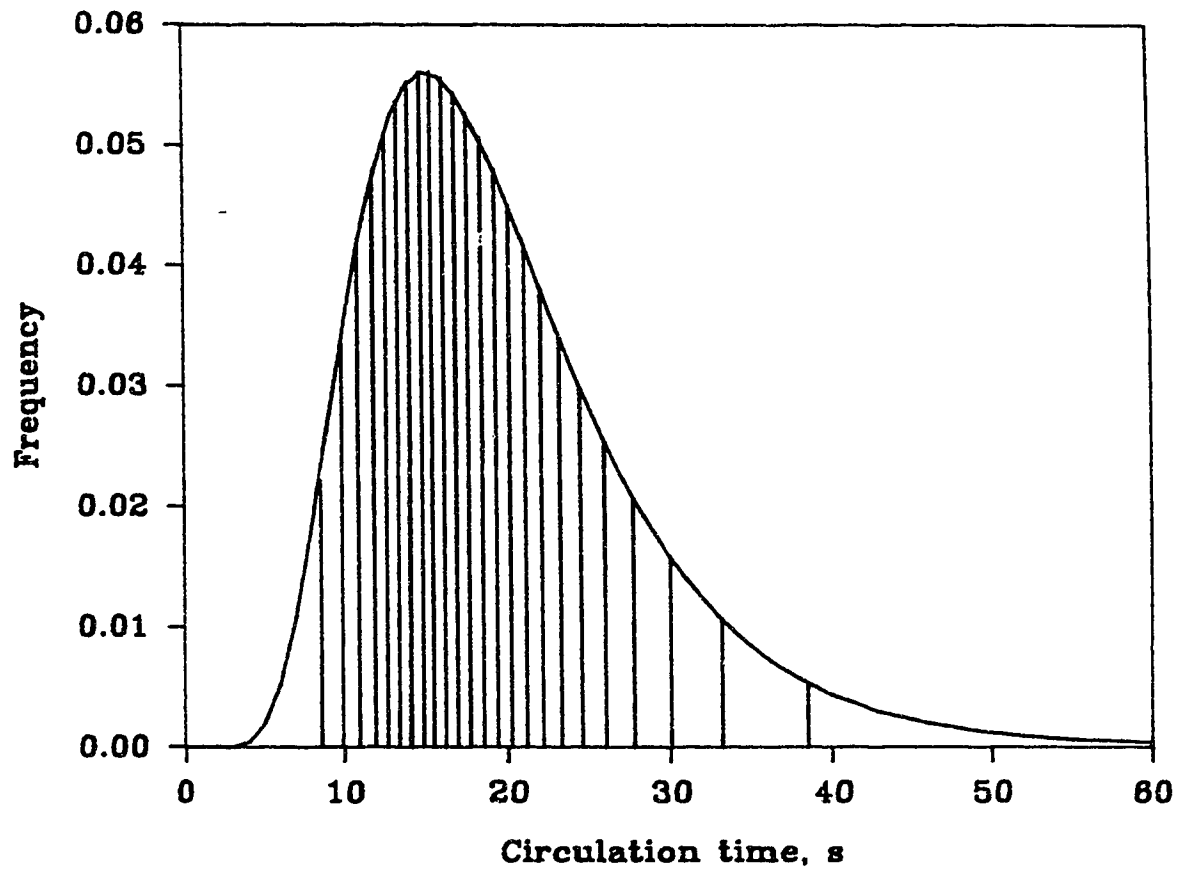


FIGURE 2.3: A log-normal CTD ($\bar{t}_c = 20$ s and $\sigma = 8.9$ s) with area under the curve divided into 25 equal probability sections.

TABLE 2.1 Circulation times (t_c) obtained from Figure 2.3 and used in the Monte Carlo fermentation.

Number	Circulation Time (s)
1	8
2	9
3	10
4	11
5	12
6	13
7	14
8	15
9	15
10	16
11	17
12	17
13	18
14	19
15	20
16	21
17	22
18	23
19	24
20	25
21	27
22	29
23	31
24	35
25	44

After the input of each pulse, one of the 25 circulation times ($8 \text{ s} < t_c < 44 \text{ s}$) was randomly selected as the next total cycle time (t_c) from Table 2.1. The algorithm used to implement the Monte Carlo method for control of nutrients supply is given in Figure 2.4. The fed-batch experiments were conducted for 15 h of feeding time, encompassing a total of 2700 cycles. The large number of cycles gave a good approximation to the log-normal distribution.

The effect of fluctuations in the nutrient level was evaluated by comparing the Monte Carlo fed-batch experiments with continuous fed-batch and periodic fed-batch experiments (control runs). The peristaltic feed pumps were switched on and off based on the Monte Carlo algorithm, running on a microcomputer. A pulse time of 3 s for the periodic feed and Monte Carlo fed-batch was selected based on minimum time required for actuating the feed pumps. Periodic fed-batch experiments were performed with a fixed cycle time equal to the mean circulation time of 20 s. To ensure that the same amount of nutrient was fed in all fed-batch runs, the amount of nutrient in each pulse was equal to the amount which was fed in the continuous fed-batch run during the time t_c . This feeding strategy simulated the addition of nutrient as a fluid element passes through the impeller zone; it would not simulate the process of mixing near the feed point of a large fermenter.

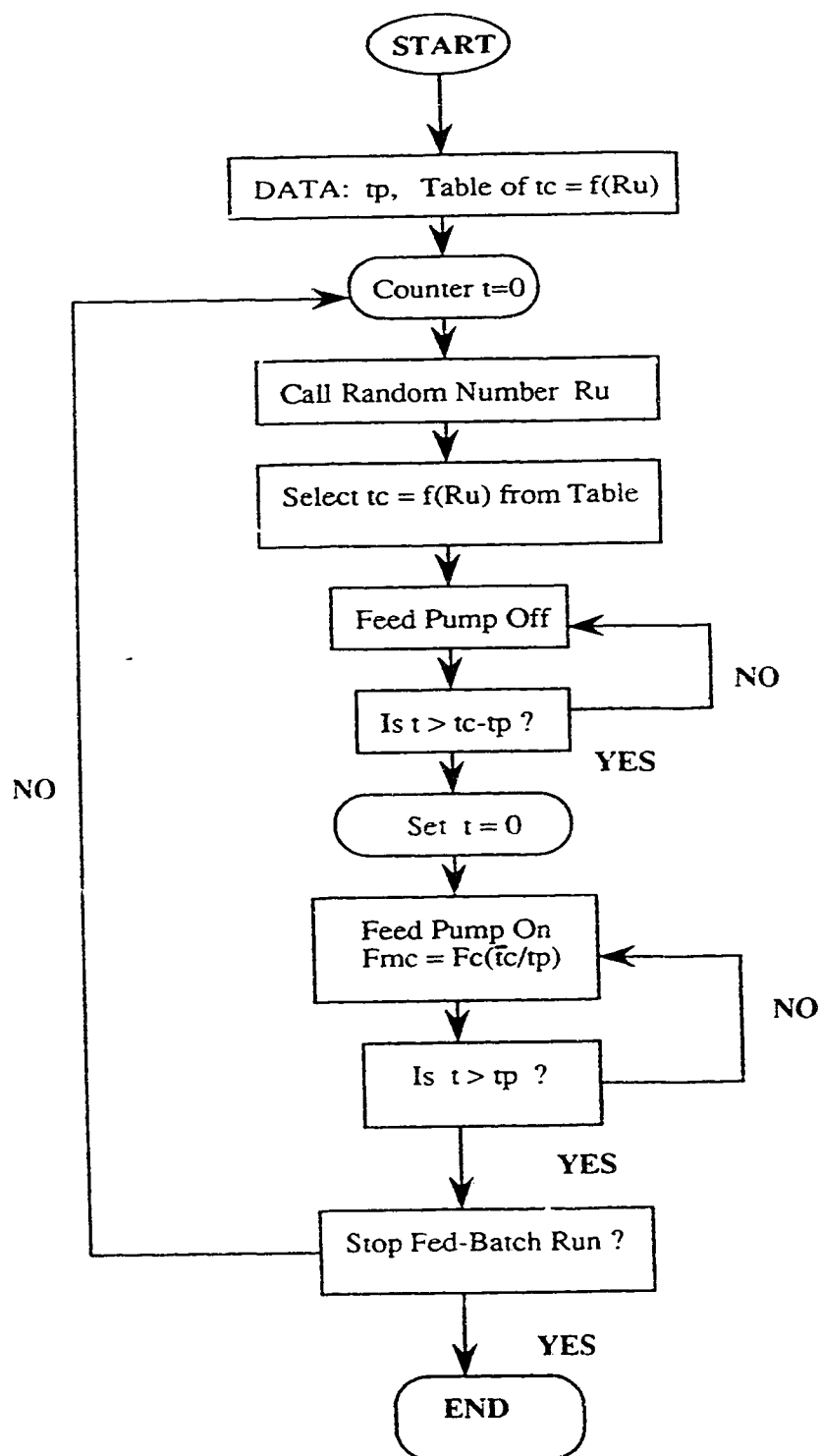


FIGURE 2.4 Monte Carlo algorithm to simulate a CTD in a bench-scale fermentor.

RESULTS AND DISCUSSION

The Monte Carlo fed-batch runs were compared with two control runs: periodic feed and continuous feed. Figure 2.5 shows representative data for biomass and ethanol during the three types of fed-batch runs, and corresponding profiles of CER and OUR are shown in Figure 2.6. Data from repeated experiments and profiles of dissolved oxygen and respiratory quotient ($RQ = CER/OUR$) are given in Appendix B. Figure 2.5 shows that the biomass level in Monte Carlo fed-batch runs was higher than the control runs (continuous and periodic feeds) after approximately 3 h, with a difference of 0.8 g/L at the end of the experiments. This difference in DCW was relatively small, but was significant in comparison to the reproducibility of the experiments, which was about ± 0.1 g/L (Table 2.2). Although the maximum and terminal levels of ethanol achieved in all fed-batch runs were comparable (Table 2.2), the consumption of ethanol between 6 and 12 h during the Monte Carlo and periodic fed-batch runs was lower (Figure 2.5). In all runs, the demand for glucose exceeded the rate of addition at 5 to 5.5 h, and the metabolism switched from fermentation on glucose to simultaneous respiration on glucose and ethanol. This switching of metabolism was indicated by net ethanol consumption (Figure 2.5) and OUR becoming greater than CER (Figure 2.6). Glucose levels in all the cases remained below 0.5 g/L and close to the detection limit of 0.1 g/L, while acetate was less than 0.1 g/L in all samples.

As illustrated in Figure 2.6, higher carbon dioxide evolution rate (CER) and oxygen uptake rate (OUR) were observed during the Monte Carlo fed-batch run, compared to the control runs. The profiles of CER and OUR were reproducible for each type of experiment to within 2 mmol/(L-h). The respiratory quotient, RQ profiles were similar (Figure B.1 in Appendix B). The maximal values of CER and OUR in the Monte Carlo runs occurred about 1 h earlier than in control runs, after

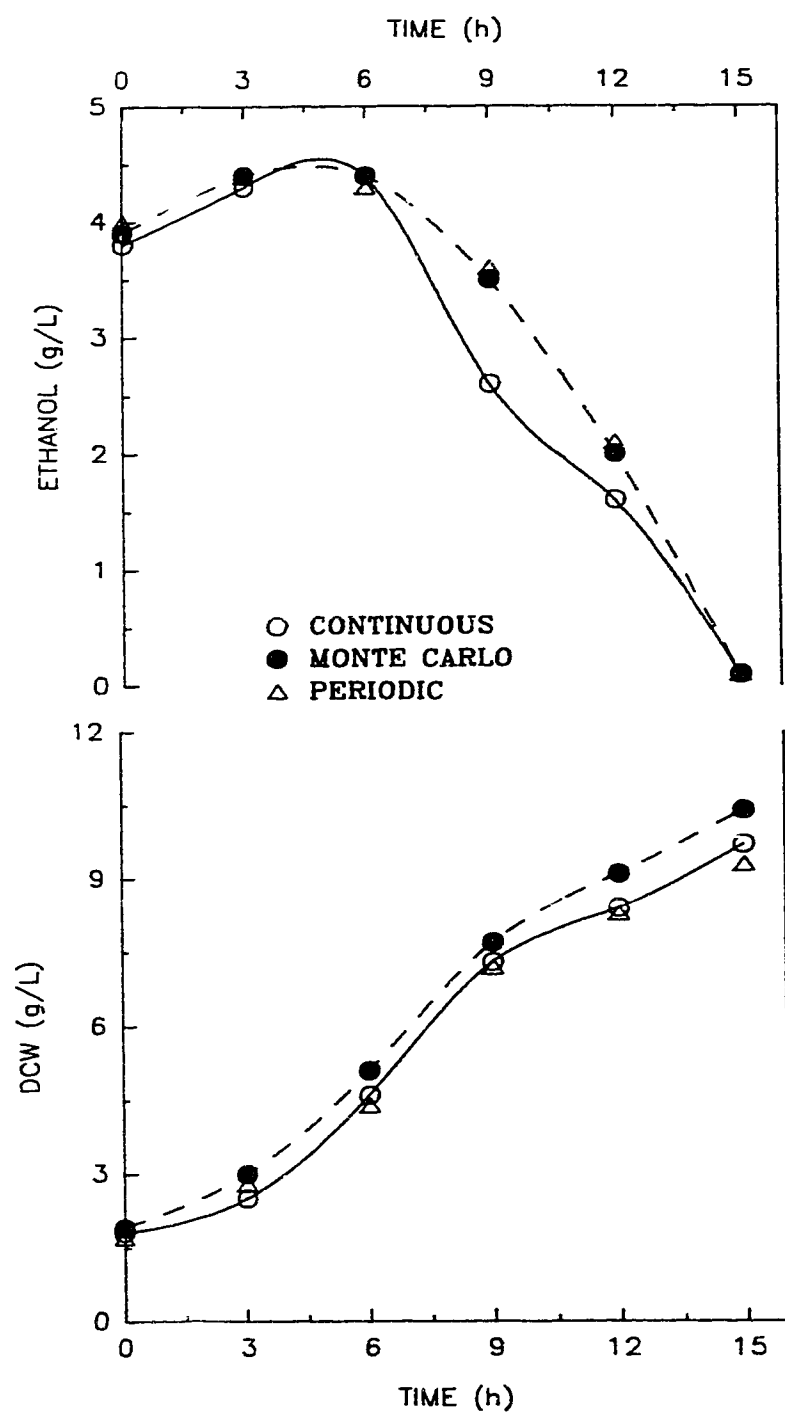


FIGURE 2.5: Ethanol and biomass profiles from fed-batch fermentations of *S.cerevisiae* with different feeding strategies.

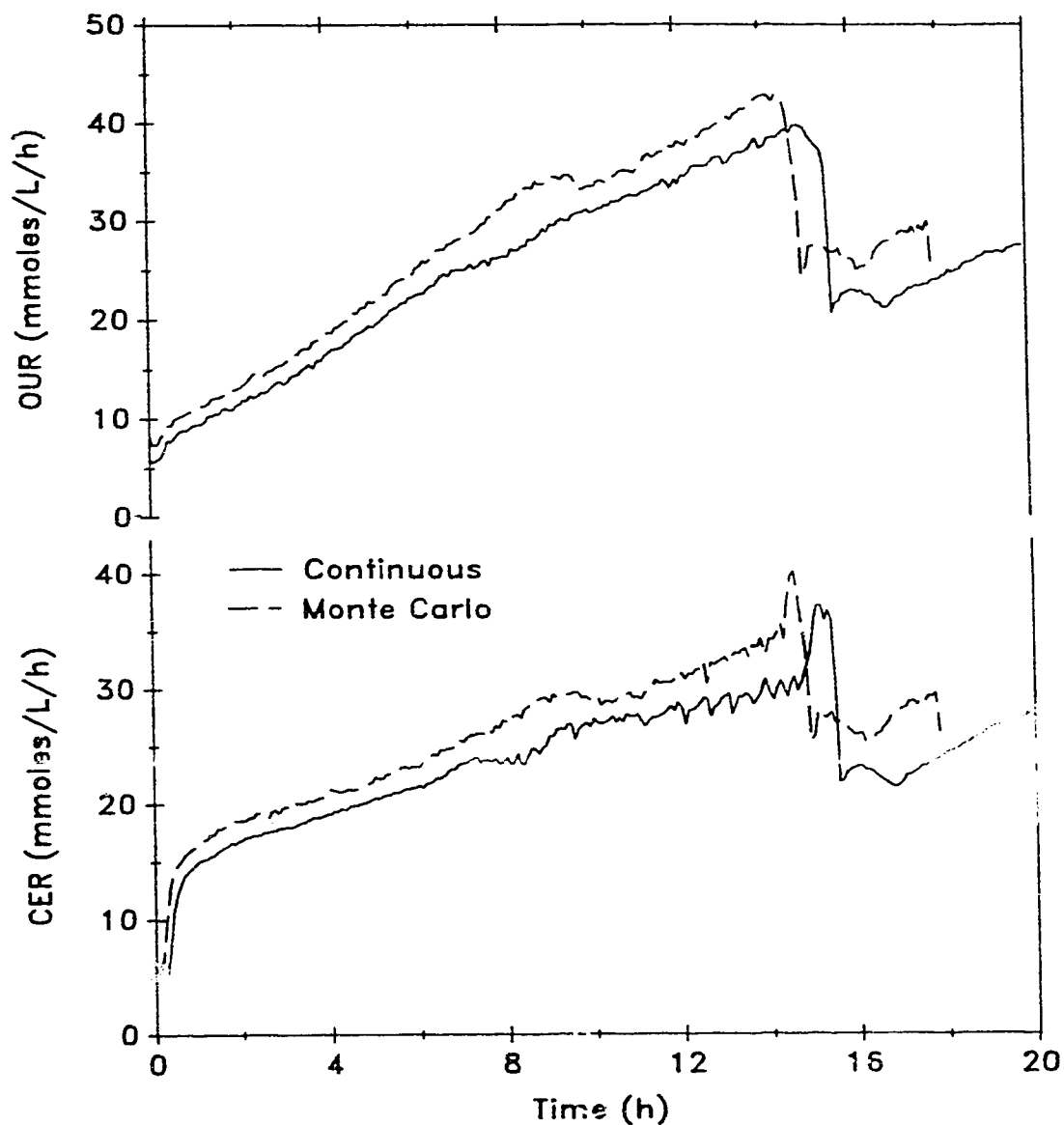


FIGURE 2.6: Oxygen uptake rate (OUR) and Carbon dioxide evolution rate (CER) during fed-batch fermentations of *S.cerevisiae* with Monte Carlo and continuous supply of nutrients.

TABLE 2.2 Concentrations of Biomass, Ethanol, and Glucose from *S. cerevisiae* fermentations with continuous, Monte Carlo and periodic supply of nutrients.

	Run	Terminal Biomass (g/L) (15 h)	Maximum Ethanol (g/L) (3 h)	Terminal Ethanol (g/L) (15 h)	Terminal Glucose (g/L) (15 h)
Continuous	1	9.6	—	0.1	0.5
Fed-Batch	2	9.5	4.4	0.5	0.48
	3	9.7	4.3	0.1	0.54
Periodic	1	9.2	4.2	0.1	0.52
Fed-Batch	2	9.3	4.4	0.1	0.47
Monte Carlo	1	10.4	4.4	0.1	0.6
Fed-Batch	2	10.3	4.7	0.4	0.61

which the culture entered a stationary phase and ceased growing. The higher levels of both CER and OUR, the earlier switch to stationary phase, and the higher yield of biomass in the Monte Carlo fed-batch experiments all confirm a higher level of metabolic activity, as compared to the continuous and periodic fed-batch runs.

Previous studies (Sweere *et al.*, 1988; Reuss and Brammer, 1985) on the effect of fluctuations in the nutrient levels on the fed-batch culture of *S. cerevisiae* showed a significant drop in the biomass level and higher ethanol production due to the 'glucose effect'. Sweere *et al.* (1988) also reported production of acetate and glycerol up to 1.5 g/L. These results of previous studies seem contrary to the present work. Unlike the present study, Sweere *et al.* (1988) used glucose as the sole carbon source, and continuous recirculation between two fermentors. In the present study, diauxic phenomena were likely dominant due to the use of a complex medium. A carbon balance on biomass, ethanol, glucose and CER in the present study leads to the inference that an extra source of carbon is being utilized in the Monte Carlo fed-batch experiments, other than glucose and ethanol. The complex feed medium in the present study contained 0.15 g of maltose for every 1 g of available glucose, as well as smaller quantities of other potential carbon sources. The increased yield of biomass in Monte Carlo fed-batch runs was, therefore, likely due to enhanced utilization of maltose (and possibly other compounds) compared to control runs. D'Amore *et al.* (1989) reported that the maltose uptake is repressed in the presence of glucose, but at lower concentration of glucose simultaneous consumption of glucose and maltose does take place. In experiments with continuous feeding, the culture would use the maltose less efficiently, because the preferred glucose feed was always supplied, and consequently, lower biomass yield would be obtained than in Monte Carlo experiments.

Heinze *et al.* (1981; 1985) used periodic feeding of glucose to a chemostat culture of *S. cerevisiae*, and observed a slight decrease in the yield of ethanol and a

corresponding increase in the biomass yield when the cycle time was increased from 0 to 500 s. In the present study, periodic feeding with a cycle time of 20 s showed no significant difference in biomass, CER or OUR profiles compared to the continuous fed–batch run (Figure 2.6). Oscillations in DO values of around 7% were induced during the last 6 h of the experiments (Figure 2.7), however, implying a synchronous response of the culture to periodic oscillations in nutrient supply. This observation suggests that the use of periodic feeding to evaluate effects of inhomogeneous substrate concentrations, as suggested in the literature, gives a different response from the more realistic approach of Monte Carlo feeding.

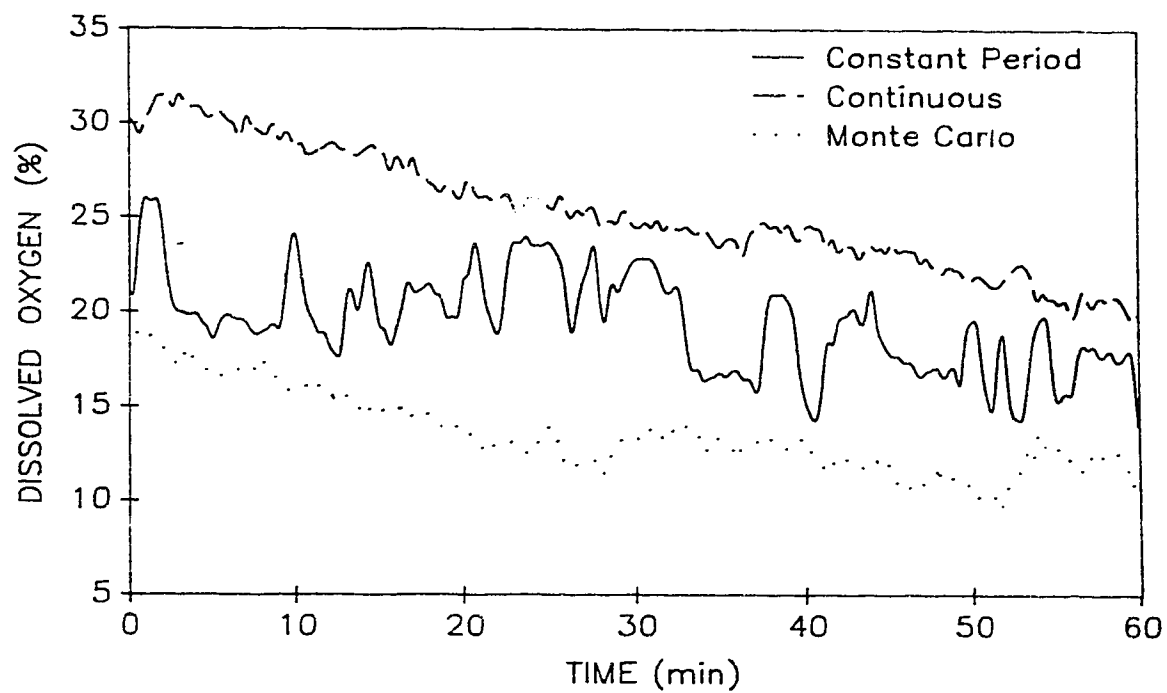


FIGURE 2.7: Oscillations in dissolved oxygen levels after 13 h of fed-batch fermentation of *S.cerevisiae* with periodic feeding.

CONCLUSIONS

1. An experimental technique for evaluating the effects of circulation in stirred production bioreactors was developed based on a Monte Carlo method for duplicating the circulation time distribution on a small scale.
2. Monte Carlo cycling substrate to *S. cerevisiae* cultures gave experimental results different from both periodic cycling and continuous supply.
3. The Monte Carlo experiments were quite reproducible because the randomly selected circulation times were much shorter than the length of the experiments.

REFERENCES

- D'Amore, T., Russell, I., and Stewart, G.G. Sugar utilization by yeast during fermentation. *J. Ind. Microbiol.*, **1989**, *4*, 315–324 .
- Bajpai, R.K. and Reuss, M. Coupling of mixing and microbial kinetics for evaluating the performance of bioreactors. *Can. J. Chem. Eng.*, **1982**, *60*, 384–392.
- Bryant, J. Characterization of mixing in fermenters. *Adv. Biochem. Eng.*, **1977**, *5*, 101–123.
- Charles, M. Technical aspects of the rheological properties of microbial cultures. *Adv. Biochem. Eng.*, **1978**, *8*, 1–63.
- Einsele, A., Ristroph, D.L., and Humphrey, A. Mixing times and glucose uptake measured with a fluorometer. *Biotechnol. Bioeng.*, **1978**, *20*, 1487–1492.
- Fowler, J.D. and Dunlop, E.H. Effects of reactant heterogeneity and mixing on catabolite repression in cultures of *Saccharomyces cerevisiae*. *Biotechnol. Bioeng.*, **1989**, *33*, 1039–1046.
- Funahashi, H., Harada, H., Taguchi, H. and Yoshida, T. Circulation time distribution and volume of mixing regions in highly viscous xanthan gum solution in a stirred vessel. *J. Ferment. Technol.* **1987**, *20*, 277–282.
- Heinzle, E., Nishizawa, Y., Dunn, I.J., and Bourne, J.R. Dynamic and steady-state effects of cyclic feeding of oxygen and glucose in an ethanol-producing yeast culture. *Ann. N.Y. Acad. Sci.*, **1981**, *369*, 159–166.
- Heinzle, E., Moes, J., Dunn, I.J. The influence of cyclic glucose feeding on a continuous baker's yeast culture. *Biotechnol. Lett.*, **1985**, *7*, 235–240.
- Mann, R., Mavros, P.P., and Middleton, J.C. A structured stochastic flow model for interpreting flow-follower data from a stirred vessel., *Trans. Instn. Chem. Eng.*, **1981**, *59*, 271–278.

- Manning, F.S., Wolf, D. and Keairns, D.L. Model simulation of stirred tank reactors. *AIChE J.*, **1965**, *11*, 723–727.
- Matsumura, M., Imanaka, T., Yoshida, T., and Taguchi, H. Modelling of cephalosporin C production and its application to fed–batch culture. *J. Ferment. Technol.*, **1981**, *59*, 115–123.
- Middleton, J.C. Measurement of circulation within large mixing vessels. *Proc. 3rd Eur. Conf. on Mixing*, York, **1979**, 15–36.
- Mukataka, S., Kataoka, H., and Takahashi, J. Circulation time and degree of fluid exchange between upper and lower circulation regions in a stirred vessel with a dual impeller., *J. Ferment. Technol.*, **1981**, *59*, 303–307.
- Nagata, S. In *Mixing: Principles and Applications*, Wiley, New York, **1975**.
- Oosterhuis, N.M.G. Scale–up of Bioreactors, a scale down approach, Ph.D. Thesis, Delft University of Technology, Delft, The Netherlands, **1984**.
- Reuss, M. Mathematical models of coupled oxygen transfer and microbial kinetics in bioreactors. *Proc. IFAC Conf. on Modelling and Control of Biotechnol. Processes*, Helsinki, Finland, **1982**, 42–55.
- Reuss, M. and Brammer, U. Influence of substrate distribution on productivities in computer controlled baker's yeast production. *Proc. IFAC Conf. on Modelling and Control of Biotechnol. Processes*, Noordwijkerhout, **1985**, 145–150.
- Sweere, A.P.J., Matla, Y.A., Zandvliet, J., Luyben, K.Ch.A.M., Kossen, N.W.F. Experimental simulation of glucose fluctuations: The influence of continually changing glucose concentrations on the fed–batch baker's yeast fermentation. *Appl. Microbiol. Biotechnol.*, **1988**, *28*, 109–115.
- Trilli, A., Michelini, V., Mantovani, V. and Pirt, S.J. Estimation of productivities in repeated fed–batch cephalosporin fermentation. *J. appl. Chem. Biotechnol.* **1977**, *27*, 219–224.

- Van Barneveldt, J., Smit, W., Oosterhuis, N.M.G., and Pragt, H.J. Measuring the liquid circulation time in a large gas-liquid contactor by means of a radio pill. 2. Circulation time distribution. *Ind. Eng. Chem. Res.*, 1987, 26, 2192-2195.
- Whitaker, A. Fed-batch culture. *Process Biochem.*, 1980, 15, 10-15.
- Wilhelm, R.H., Donohue, W.A., Valesano, D.J., and Brown, G.A. Gas absorption in a stirred vessel: Locale of transfer action. *Biotechnol. Bioeng.*, 1966, 8, 55-69.

CHAPTER 3

THE EFFECT OF FEED ZONE IN FED-BATCH FERMENTATIONS OF SACCHAROMYCES CEREVISIAE¹

INTRODUCTION

The fed-batch mode of operation of industrial fermentors is usually accomplished by feeding a concentrated nutrient solution at the top of the vessel (Anderson *et al.*, 1982). Fed-batch operation is well suited for baker's yeast (Rosen, 1987), antibiotics (Mou, 1983), and rDNA (Zabriskie and Arcuri, 1986) fermentations, where the growth and product formation are optimized by controlling a limiting nutrient, such as glucose, below a critical level. The nutrient solution is fed to match the demand due to growth and desired product formation, while avoiding undesired metabolic effects. The fermentation industry often employs baffled and sparged vessels as large as 300 m³, agitated with impellers. The limitation on power input to the impellers (≤ 4 kW/m³), and high apparent viscosity (≤ 2 Pa s), lead to poor mixing of the contents of the fermentor (Anderson *et al.*, 1982; Sittig, 1982). For example, the time taken to homogenize a pulse of tracer in a 150 m³ stirred vessel can be on the order of several minutes (Einsele, 1978). The inhomogeneity in nutrient levels in the fermentor caused by poor mixing has a deleterious effect on the control of nutrient levels, and often results in

¹A part of this chapter was published in the *Proceedings of 5th European Congress on Biotechnology*, Vol. 2, Copenhagen, Denmark, July 1990, pp 805–808.

difficulties during scale-up (Anderson *et al.*, 1982; Lilly, 1983).

In large fed-batch fermentors, the transfer of fluid elements loaded with fresh feed from the feeding point to any point in the fermenter occurs through the pumping action of impellers. A zone of concentrated nutrients, or 'feed zone', would be created close to the feeding point due to incomplete mixing. This feed zone is defined as the region of fermentor where a threshold concentration of nutrients is exceeded. The threshold concentration depends on the nutrient effect of interest, for example, catabolite repression in yeast (Fowler and Dunlop, 1989; Petrik *et al.*, 1983). The effects of short but repeated exposure of the microbial cells to high concentrations in the feed zone on the productivity of a production-scale fermentor will depend on the volume of the feed zone, which in turn depends on the number of feeding ports and the degree of turbulence at each feeding port. No experimental estimate of volume of the feed zone in a production fermentor is yet available, but bench-scale experiments have been performed to evaluate the effect of the feed zone on yields. Variation in the position of nutrient addition to a chemostat culture of *Saccharomyces cerevisiae* was shown to affect the yield of biomass (Hansford and Humphrey, 1966). A higher yield of biomass was obtained in the ICI process for single cell protein in a 1,500 m³ fermentor when multiple entry points were used for methanol feed instead of a single point (Senior and Windass, 1980). The feed blending problem was considered in the analysis of poor mixing in a chemical reactor (Fasano and Penney, 1991), a chemostat (Fowler and Dunlop, 1989), and a fed-batch fermentor (Reuss and Brammer, 1985). The segregation of the feed zone from rest of the fluid content was shown to be essential to evaluate the interaction between non-linear reaction kinetics and mixing in both cases. A critical requirement for any fermentation to be sensitive to mixing intensities is that the response time of key metabolic steps is not significantly longer than the time spent in regions where extreme substrate concentrations exist (Fowler and Dunlop, 1989).

The characteristic-time analysis of microbial metabolism shows that two mechanisms, allosteric control of enzyme activity and transcription control of enzyme synthesis, may be affected by concentration gradients in the fermentor environment (Roels, 1982). For example, addition of pulses of lactose to glucose-limited cultures of *Escherichia coli* gave immediate induction of mRNA synthesis for β -galactosidase production (Contesse *et al.*, 1970). During pulse addition of glucose to the culture of *Saccharomyces uvarum*, ethanol and acetic acid were secreted as waste products due to short term regulation of enzymes responsible for availability of precursors for respiratory pathway (Petrik *et al.*, 1983). This short term regulation by excess glucose, known as the 'glucose effect', is caused by saturation of respiratory capacity (Kappeli and Sonnleitner, 1986). NADH measurements showed a response time of 4.4 s for glucose uptake by starved *S.cerevisiae* cells exposed to a pulse of 100 mg/L of glucose (Einsele *et al.*, 1978). These studies were limited to characterizing response times of cells to a single carbon source in defined media, whereas a production scale fermentation usually utilizes complex media with multiple carbon and nitrogen sources. Nevertheless, they show that key metabolic steps can respond in less than one minute to gradients in nutrient levels.

As a microbial cell circulates in the vessel, it will experience a range of concentrations. The overall performance of a fermentation system can be best predicted by reproducing the microenvironment around the cells in the fermentor, and their response to this microenvironment. A two compartment mixing model (Manning *et al.*, 1965), consisting of an impeller region with complete micromixing and a bulk region with complete segregation, has been used to model the non-ideal behavior of stirred fermenters (Bajpai and Reuss, 1982). Several experimental studies have been performed to simulate these micro-environments. Periodic pulse feeding of a carbon source to various continuous cultures has been used to mimic the

fluctuations characteristic of large fermentors (Brooks and Meers, 1973; Heinzle *et al.*, 1985; Roberts and Slater, 1986), but such regular fluctuations in concentrations are not experienced by cells in a large fermentor. The recirculation of broth between two fermentors with addition of fresh feed to one fermenter was used to evaluate the effects of two extreme glucose levels on the fed-batch culture of *S.cerevisiae* (Sweere *et al.*, 1988). These experimental studies are limited in their relevance as the effects of two extreme concentrations, rather than a range of concentrations, were simulated. The segregation of the feed zone was also not considered, in that the two compartment mixing model was used with the assumption that feed is added to the impeller region in the production vessel. Fowler and Dunlop (1989) evaluated the effects of nutrient heterogeneity in the feed-entry region of a chemostat culture by using a static mixer to mix fresh feed with recirculating broth. The values of design parameters, such as volume of static mixer, the intensity of mixing, and recirculating rate, were not based on any characterization of the mixing in production fermentors.

All these experimental studies used defined medium with a single carbon source for fermentation, whereas typical production-scale fermentation utilize complex medium with multiple carbon sources. In Chapter 2, an experimental strategy was proposed whereby representative concentration gradients were reproduced in a bench-scale fermenter by using a Monte Carlo method to simulate the circulation time distribution of a large fermentor. They assumed that the feed was added into the impeller region of the production vessel, and hence the zone of high concentration of nutrients close to the feeding point was not considered. A experimental methodology is, therefore, required which simulates the effect of feed zone on the performance of a fed-batch fermentation using a complex medium.

The objective of this chapter was to determine the effects of nutrient fluctuations on production-scale fed-batch fermentation by systematically carrying

out bench-scale experiments. An aerobic fed-batch culture of *S.cerevisiae*, grown on a complex media, was selected as the model culture. A simple constant-feed rate strategy was used because it was simple to implement with ill-defined yield coefficients on complex media. The effect of high concentration in the feed zone was evaluated by intermittently supplying the concentrated feed into the entrance of a recycle loop coupled with a 1 L of fermentor culture. An exact estimate of the volume of feed zone in a production fermentor was not available, therefore, the recirculation rate of the broth was varied from 0.25 to 6 L/h, and recycle loop volumes of 15 and 50 mL were selected. These experimental conditions produced glucose fluctuations in the experimental system ranging from 0.3 g/L in the fermentor to 11 g/L in the recycle loop. For comparison with literature studies, fed-batch fermentations were also performed with an exponentially increasing supply of a defined medium.

THEORY

Mixing Model

Two modes of mixing occur in the liquid or bulk-phase of a stirred tank: macromixing controlled by convective bulk diffusion and eddy diffusion; and micromixing controlled by molecular diffusion (Brodkey, 1981). The stirred tank can be divided into two regions based on the mode of mixing: the bulk zone, where macromixing controls the circulation patterns; and the impeller zone, where micromixing is rate limiting (Manning *et al.*, 1965). In fed-batch operation, the circulation patterns in the macromixed zone control the dispersion of nutrients from the feeding point into the fermentor. Addition of feed to a single point at the top of the fermentor creates a plume of concentrated nutrients, which extends from the feeding point into the macromixed zone. This plume, or feed zone, may extend down to the impeller zone due to macromixing and relatively slow uptake kinetics. For example, during addition of acid to a stirred tank filled with base, a plume of acid was shown to exist (Knysh and Mann, 1984).

As the fluid elements circulate in the fermentor, the microorganisms will be exposed to high concentrations of nutrients in the feed zone. In the impeller region, the fluid elements loaded with fresh feed from the feed zone will be micromixed with other elements. The fluid elements leaving the impeller region will have a lower average concentration than the concentration in the feed zone. The micro-macromixer or two-zone mixing model (Bajpai and Reuss, 1982) assumes that the feed is added into the impeller zone, which makes it difficult to evaluate the effect of transient exposure to high concentration in the feed zone on culture metabolism. This feed zone effect can be evaluated by segregating the feed zone from the bulk zone and the impeller zone. This extension of the two-zone mixing model to a three-zone mixing model is shown in Figure 3.1.

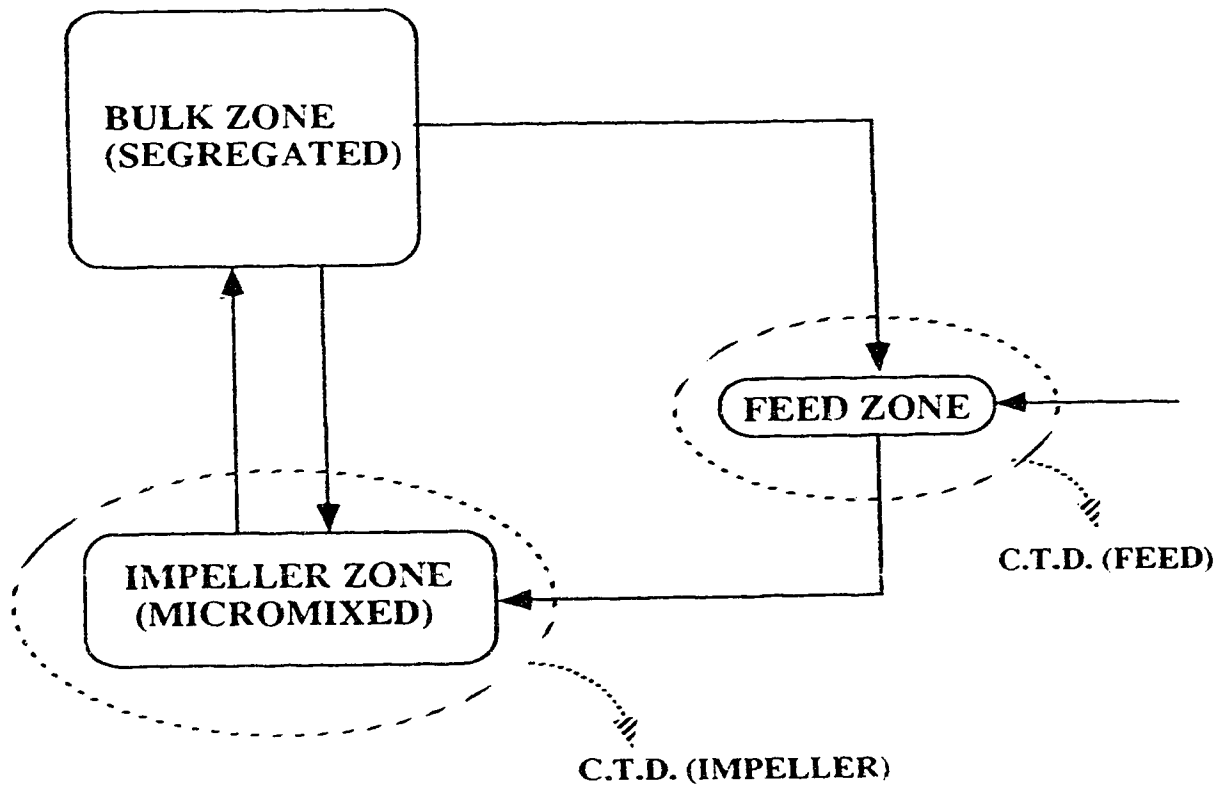


Figure 3.1 Three-zone mixing model for a fed-batch fermentor.

Circulation Time Distribution

The overall performance of the culture will depend upon the response of each microbial cell to its micro-environment during its circulation in the large fermenter. The micro-environments encountered by microbial cells depend on their residence times in the bulk zone, and frequencies of visits to the feed and impeller zones. These frequencies and residence times are controlled by macromixing, and are quantified by a 'circulation time distribution' or CTD. The CTD is obtained by measuring the probability for each possible time interval that a fluid element takes to return to a fixed reference zone. Usually the impeller zone is chosen as a reference to measure a CTD by a flow-follower method (Bryant, 1977). This CTD describes the frequency of visit by a fluid element to the impeller zone and total time spent by that fluid element away from the impeller zone. A CTD of log-normal type with a mean, \bar{t}_c , of 20 s and a standard deviation, σ , of 8.9 s was used by Bajpai and Reuss (1982) to numerically simulate a large-scale baker's yeast fermentation. From the experiments of Middleton (1979), this CTD characterises the bulk circulation pattern for a 4.4 m³ stirred tank of water with a single turbine impeller agitated at 100 rpm and no aeration. A 300 m³ tank filled with a Newtonian medium and agitated at 220 rpm with no aeration would give a similar CTD (Middleton, 1979). A log-normal CTD with a mean of 20 s and a standard deviation of 8.9 s was, therefore, selected in the present study to characterise the macromixing of the bulk liquid in a typical 300 m³ stirred fermentor used for baker's yeast production.

The frequency of a fluid element visiting the feed zone is characterized by a CTD with respect to the feeding point. No experimental measurement of CTD with respect to the feeding point is available. Mann *et al.* (1981) have successfully predicted the CTD with respect to the impeller zone, for a 0.6 m³ tank, stirred at 250 rpm with no aeration, by using a 'network-of-zones' stochastic model (Appendix C.1). This model divides the bulk flow into different circulation loops or

zones, established by the mean flow field. Each zone is sub-divided into a series of perfectly plug-flow elements or 'flow-cells'. The model assumes radial symmetry, and hence each cell is annular. Thus, the 'network-of-zones' model divides a given stirred tank into 10X20 flow-cells of equal volume. A flow velocity and a switching probability are associated with each flow-cell to model the convection between the adjacent cells in the same circulation loop (Figure 3.2), and the eddy diffusion between cells of adjacent loops (Figure 3.3), respectively. The time spent by a fluid element in each flow-cell depends upon the flow velocity associated with that flow-cell, and its movement into the next flow-cell is decided by the average velocity pattern and the switching probability. A circulation time, t_c , can be obtained by summing the residence times spent in all flow-cells encountered during each circulation pass.

The network-of-zones model was used to predict the CTD with respect to the feeding point. The velocity profile and switching probability parameters followed Mann *et al.* (1981). The pumping capacity used by Mann *et al.* (1981) was scaled-up to simulate a log-normal type CTD with respect to the impeller zone with a mean of 20 s, characteristic of a production-scale fermentor. The feed was assumed to be added into one flow-cell at the top left corner of the vessel, which was selected as a reference. The circulation time distribution was determined by simulating 5000 circulations with respect to the reference flow-cell at the feeding point. The resulting CTD for the feed zone, $f(t_c)$ as shown in Figure 3.4, has the form of a time delay of 19.3 s with an exponential decay. The peak in CTD of $2.3 \times 10^{-3} \text{ s}^{-1}$ denotes the maximum probability of entering the reference flow-cell. The time delay in the CTD is the shortest duration of circulation to return to the reference flow-cell.

Simulation of Feed Zone Effects

A recycle-flow model can be selected such that its residence time distribution

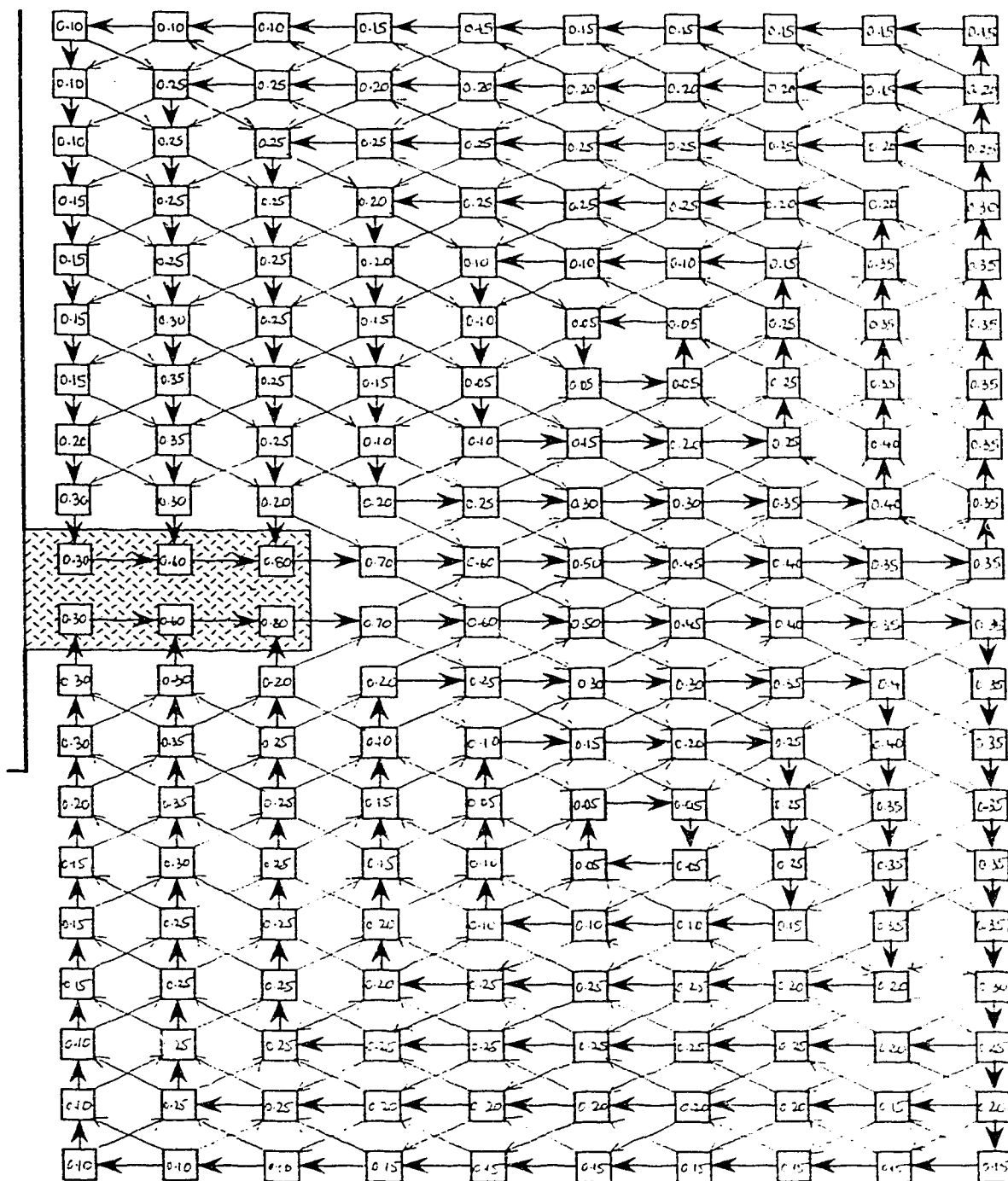


Figure 3.2 'Network-of-zones' stochastic model following Mann *et al.* (1981).
The number inside each cell represents the proportion of flow rate passing through that cell.

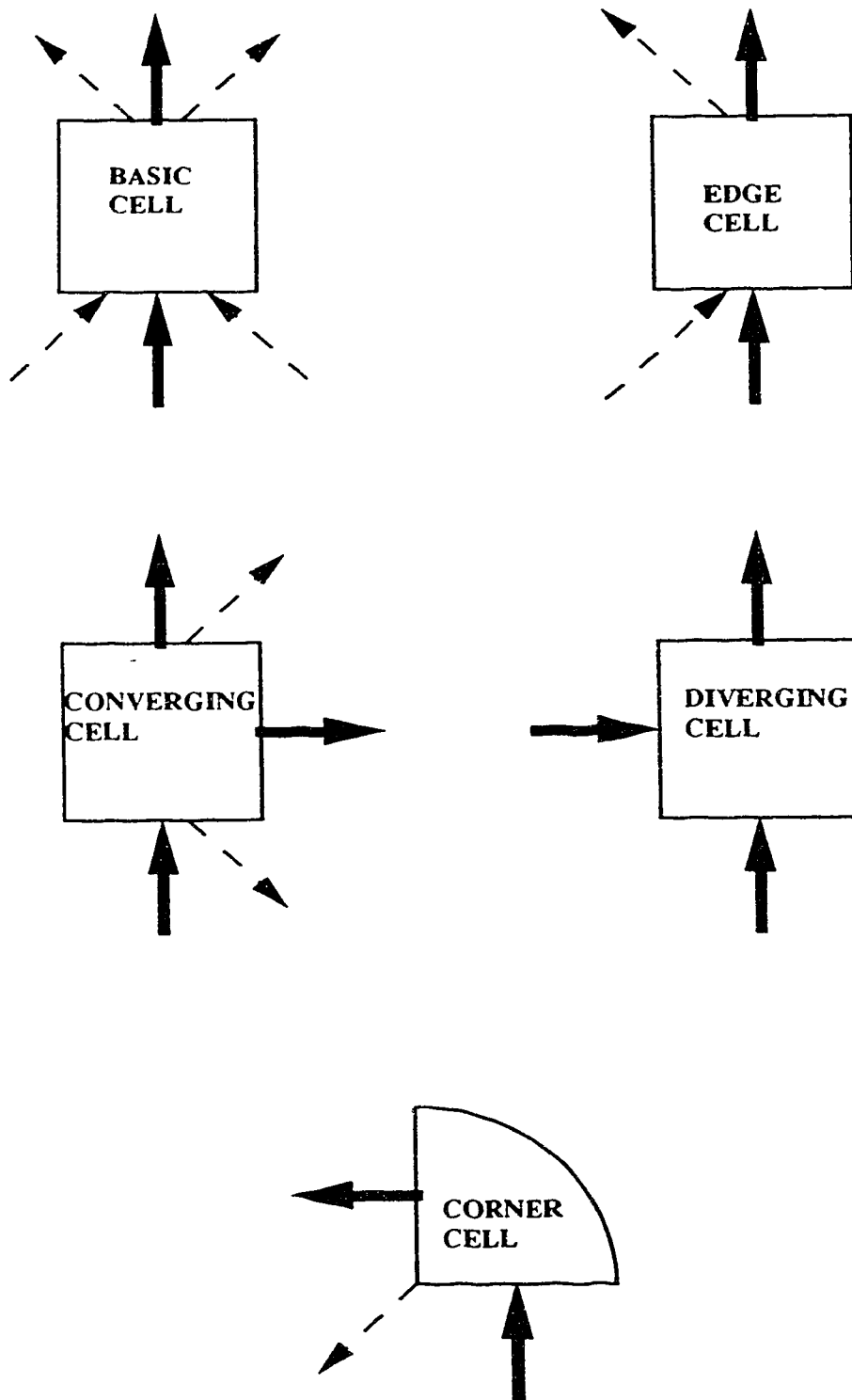


Figure 3.3 Types of 'flow-cell' used in 'network-of-zones' stochastic model following Mann *et al.* (1981).

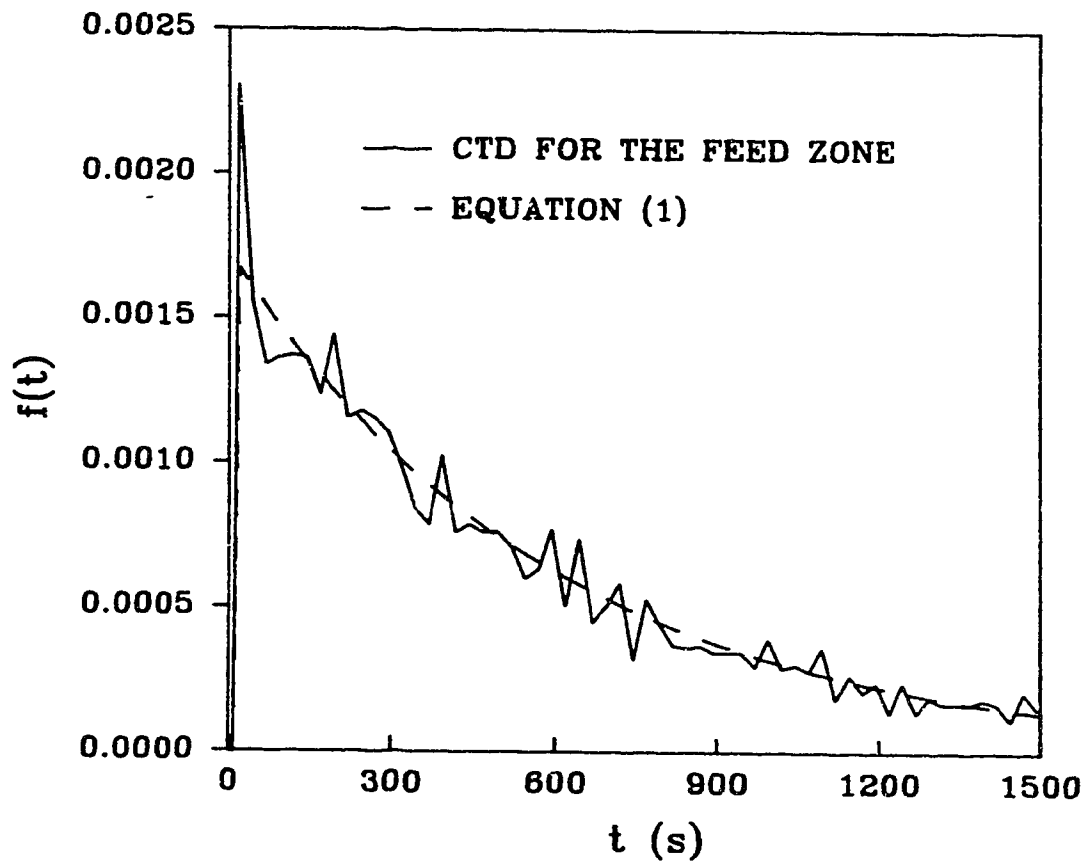


Figure 3.4 Prediction of a CTD for feed zone, $f(t_c)$, and a fit with RTD, $f(t)$, for a single passage through a recycle flow model (equation 1).

will be equivalent to the CTD, $f(t_c)$ (Khang and Levenspiel, 1976). A model comprised of a stirred tank of volume V_b and a plug flow recycle loop of volume V_p , with a recirculation rate of Q_r , will give the desired CTD, $f(t_c)$, according to the following equation (Levenspiel, 1972):

$$f(t) = P \exp[-P(t-t_{lag})] \quad (1)$$

where P represents the maximum probability of entering the recycle loop and t_{lag} represents the residence time in the loop as follows:

$$P = Q_r/V_b \quad (2)$$

$$t_{lag} = V_p/Q_r \quad (3)$$

The recycle-flow model suggests that the feed zone effect can be simulated by employing a well mixed bench-scale fermenter with a recycle loop, where the feed is added into the recycle loop. The recirculation rate, Q_r , fixes the probability of cells entering the recycle loop for a given bench-scale fermentor (V_b). This probability is equivalent to the probability of a fluid element visiting the feed zone in the production fermentor. The time spent by the culture broth in recycle loop simulates the high concentration experienced a fluid element in the feed zone of the production fermentor. Mixing of the recirculating broth carrying the fresh feed with the rest of broth in the bench-scale fermentor simulates the micromixing in the impeller zone of the production fermentor.

The values of the three experimental design parameters recirculation rate, Q_r , recycle loop volume, V_p , and fermentor volume, V_b , depend on the CTD, $f(t_c)$, according to equations (2) and (3). The CTD, $f(t_c)$, was obtained by using a

'flow-cell' as a reference zone. The network-of-zones model assumes radial symmetry, but the feed is added to a single point in the production fermentor. The CTD $f(t_c)$, therefore, indicates the upper limit on the probability of visiting the feed zone, P . The value of t_{lag} from the network-of-zones model is the shortest possible time for a fluid element to leave the feed zone, circulate in the bulk fluid via the impeller, and return to the feed zone. The minimum time that a fluid element spends in the nutrient-rich plume from the feeding point is $t_{lag}/2$, the minimum to reach the impeller. The best fit of equation (1) to the CTD, $f(t_c)$, gave an upper limit on the parameter P , as $(P)_{max} = 1.7 \times 10^{-3}$ and the lower limit on the time delay of $(t_{lag})_{min} = 9.64$ s. The design parameters Q_r and V_b were bounded by equation (2) and $(P)_{max}$. A lower limit on V_p was set by using equation (3) and $(t_{lag})_{min}$ where the residence time in the loop is $(t_{lag})_{min}/2$. For example, if we select the bench-scale fermentor content (V_b) of 1L then the upper limit of recirculation rate, or $(Q_r)_{max}$, will be 6.12 L/h and the lower limit of recycle loop volume, or $(V_p)_{min}$, will be 8.2 mL. These bounds on Q_r , and V_p can be used to select suitable ranges of lower recirculation rate and higher volume of the recycle loop. Selecting a recirculation rate, Q_r , less than $(Q_r)_{max}$ reduces the maximum probability of exposure to the feed zone, P , by a factor α given by,

$$\alpha = Q_r / (Q_r)_{max} \quad (4)$$

On leaving the impeller zone in the large fermentor, fluid elements with an average content of nutrients are assumed to be completely segregated in the bulk zone. During their circulations in the bulk zone, the cells in each fluid element have access to their respective micro-environments for nutrient supply. These circulations of fluid elements away from the impeller zone are characterized by the CTD with respect to the impeller zone. If the feed is assumed to be added into the

impeller zone, then these circulations can be simulated by intermittently feeding the nutrients into the bench-scale fermentor, according to a Monte Carlo method from Chapter 2. Consider the content of the bench-scale fermentor to be equivalent to a fluid element of the large fermentor. The duration of pulse-on (t_p) of feed to the bench-scale fermentor represents the circulation of the fluid element in the impeller zone, and the duration of pulse-off ($t_c - t_p$) represents the circulation of the fluid element through the bulk zone. The Monte Carlo method selects a circulation time t_c from a given CTD with respect to the impeller zone. For example, consider a CTD which has a form of log-normal distribution with a log mean circulation time μ_1 , and a log-mean standard deviation σ_1 . The Monte Carlo method can use a normalized random number, R_n , to select the circulation time t_c as follows:

$$t_c = \exp (R_n \mu_1 + \sigma_1) \quad (5)$$

The circulation of fluid elements between the bulk zone and the impeller zone suggested that the feed be added intermittently to the fermentor according to the Monte Carlo method. The circulation of fluid elements between all three zones, therefore, can be simulated by feeding the nutrients into the recycle loop, according to the Monte Carlo method. The intermittent supply of nutrients into the loop further reduces the maximum probability of exposure to the feed zone, P , by a factor β given by

$$\beta = t_p / \bar{t}_c \quad (6)$$

The resulting experimental implementation of the three-zone mixing model is schematically shown in Figure 3.5. From equations (4) and (6), this experimental

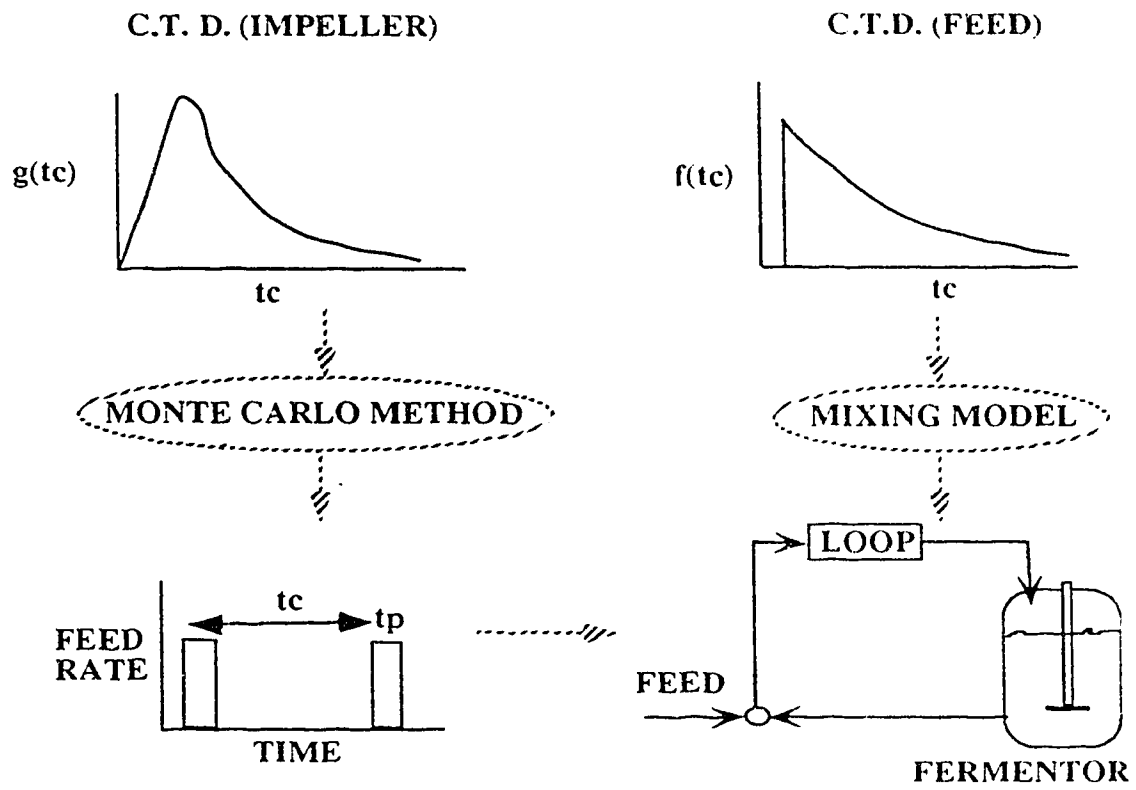


Figure 3.5 Experimental simulation of feed zone effects.

system simulates the maximum probability of exposure to the feed zone, P , given by

$$P = (\alpha\beta) (P)_{\max} \quad (7)$$

and the interval of exposure to the feed zone, t_{lag} , is given by equation (3). An exact estimate of volume of the feed zone was not available, therefore, a single flow-cell volume was selected as a reference cell in using the 'network-of-zones' model to estimate bounds on P and t_{lag} . The volume of this reference flow-cell, 0.5% of total fermentor volume, was the smallest possible cell volume according to the 'network-of-zones' model. The feed zone effect was evaluated over a range of volumes by carrying out several experiments for suitable ranges of recirculation rate, Q_r , and recycle loop volume, V_p . The bounds on Q_r and V_p , given by equations (2) and (3) and the estimates of $(P)_{\max}$ and $(t_{\text{lag}})_{\min}$, were used to guide the selection of these ranges of design parameters. The estimates of these experimental parameters are given in materials and methods section.

MATERIALS AND METHODS

Microorganisms and Medium

Two strains of *S.cerevisiae*, NCYC 1018, and ATCC 32167, were used. Both strains were maintained on YD (Yeast extract, and Dextrose) slants for long term storage. The strains were streaked on MYPD plates (Malt Extract, Yeast Extract, Peptone, and Dextrose) every two weeks, and a single colony was used to inoculate the shake flask. Fermentations using a streak from the plate rather than a single colony for inoculation gave similar results. The NCYC 1018 strain was grown on a complex medium, and the composition used for medium in shake flask, and fermentor was described in Chapter 2.

Experiments with defined medium were performed using the ATCC 32167 strain of *S. cerevisiae* as the strain NCYC 1018 did not grow well on the defined medium. Representative fed-batch experiments with ATCC 32167 were performed on the complex medium and the results were similar to those obtained for the strain NCYC 1018. The composition of the medium in the shake flask was as follows: Glucose, 15 g/L; Yeast Extract, 7 g/L; NH_4Cl , 2.5 g/L; KH_2PO_4 , 1.0 g/L; $\text{MgSO}_4 \cdot 7\text{H}_2\text{O}$, 0.3 g/L; $\text{CaCl}_2 \cdot 2\text{H}_2\text{O}$, 0.1 g/L. The defined medium used for fermentation was based on the 'D' medium (Fiechter *et al.*, 1987). The detailed compositions of the media for the start-up culture, feed for chemostat culture, and feed for exponentially fed-batch culture are described in Table 3.1. RO water was used for preparation of all media.

Equipment

A 2 L New Brunswick Multigen fermentor was equipped with a system for computer monitoring and control. A silicone tube (Masterflex) of 3.1mm ID was used as the recycle loop. The fermentor off-gas was analysed for O_2 , CO_2 , and N_2 ,

TABLE 3.1 Composition of media used in fermentations with *S.cerevisiae* ATCC 32167. Stock solution of chlorides, sulfates, and vitamins were prepared. The final concentrations of various components in the media were in same proportion with respect to glucose as given in 'D' medium by Fiechter *et al.* (1987).

Component	Units	Start-Up	Chemostat	Fed-batch
Glucose	g/L	2.5	5.0	100.0
(NH ₄) ₂ SO ₄	g/L	0.5	1.0	0.0
(NH ₄) ₂ HPO ₄	g/L	0.16	0.32	6.4
Chlorides	mL/L	2.5	5.0	40.0
Sulfates	mL/L	2.5	5.0	40.0
Vitamins	mL/L	0.5	1.0	20.0

by a Dycor quadrupole gas analyser (Model M200BEF, Ametek Thermox Instrument Division, USA) during fermentation experiments with defined medium. No off-gas analyses were performed for fermentation experiments where complex medium was used for growth. The gas composition data was collected and stored on a VAX computer system every two minutes. A peristaltic pump (Cole Parmer) was used for the recirculation of broth between fermentor, and recycle loop. Sensors for pH (Phoenix autoclavable double reference electrode), temperature (Omega), and dissolved oxygen (Ingold autoclavable DO probe) were connected to a microcomputer via an OPTO-22 data-acquisition system. The values for pH, DO, and temperature were recorded every 20 s on the microcomputer. A Tylan Mass flow controller system and a peristaltic pump (Pharmacia P1: 0.6–500 mL/h) were used to control the flow rate of air and nutrients to the fermentor respectively.

Cultures and Assay

For experiments with complex medium, the inoculum (50 mL) was grown in a 250 mL shake flask to exponential phase for 24 h at 30°C, and 250 rpm. The fermentation was carried out with a 2% (v/v) inoculum, and initial volume of broth 1L at 30°C, 500 rpm, and air flow rate of 1 L/min. The dissolved oxygen never fell below 30% for all experiments with the complex medium. The pH was controlled between 4.5 and 4.8 by using 2N NaOH, and 2N HCl. The foam was controlled using 2% (w/v) antifoam (SAG 471, Union Carbide). The feeding to fermentor in all experiments was started at the end of 11 hours of the batch run, which corresponds to a biomass level of 2.0 ± 0.1 g/L, and a glucose level of 0.1 g/L. At this stage, the culture was presumably switching from a respiro-fermentative mode of growth on glucose to a fully respiration mode of growth on ethanol (Kappeli and Sonnleitner, 1986). The feed was supplied at a rate of 13.5 mL/h of complex medium in all continuous fed-batch experiments. This strategy of constant feed rate using

complex medium maintained aerobic growth of the culture and was consistent with the feeding strategy used in Chapter 2. A 5 mL sample from the fermentor was taken every two hours.

The protocol used for experiments with defined medium was as follows. The inoculum (100 mL) was grown in a shake flask (500 mL) to exponential phase for 24 h at 30°C, and 250 rpm. The fermentation was carried out with a 5% (v/v) inoculum and initial volume of 1L of start-up medium at 30°C, 900 rpm, and 1.5 L/min of air supply. These conditions ensured that the dissolved oxygen was always maintained above 20% in all experiments with defined medium. The pH was controlled at 4.9±0.1 by using 2N NaOH, and 2N HCl during batch, and chemostat operation. The chemostat was started after 3 h of batch fermentation. The feed rate to the chemostat was increased, in two equal steps, from 160 mL/h to 200 mL/h within 4 h. All the fed-batch experiments were consistently started from a steady state culture achieved after about 18 h of chemostat operation at a dilution rate of 0.2 h⁻¹. An exponentially increasing feeding strategy was based on the following equation (Lim *et al.*, 1977),

$$Q(t) = \frac{\mu V_c X_o}{Y_{x/s} S_{in}} e^{\mu t} \quad (8)$$

where, the initial conditions used were: biomass, X_o , of 2.25 g/L, fermentor volume, V_o , of 1L. The glucose concentration in the feed (S_{in}) was 100 g/L. The parameters were growth rate, μ , of 0.16 h⁻¹, and biomass yield on substrate, $Y_{x/s}$, of 0.45. The pH was controlled between 4.7 and 5.0 during the fed-batch run by using 2N NH₄OH. This use of NH₄OH also maintained adequate supply of nitrogen for growth during fed-batch fermentations. A 5 mL sample from the fermentor was taken every 1.5 h during the fed-batch experiments with defined medium.

The samples were filtered using 0.45 μm Sartorius cellulose nitrate filters. The biomass was measured by absorbance at 620 nm using a spectrophotometer (Spectronic 21). The dry weight was obtained by drying the filtrate using a microwave oven for 10 min. A correlation between absorbance and dry weight was obtained at various times during a fed-batch run. Glucose in the supernatant was analysed using a YSI Glucose Analyser (model 27). Ethanol and maltose were analysed by enzyme kits (Boehringer Mannheim) with a lower limit of 0.01 g/L, and a precision of ± 0.002 g/L. Acetic acid, and ethanol in samples for experiments with complete medium were measured within 5% precision using a Spectra Physics GC equipped with 80/120 carbopack B/6.6% carbowax 20M column, and a flame ionization detector.

Design of Recycle Experiments

The feed zone effect was evaluated by comparing the performance of two types of experiments: (1) 'continuous' experiments, where feed was continuously supplied into the fermentor, while the broth recirculated through the recycle loop, and (2) 'Monte Carlo' experiments, where the feed was intermittently supplied into the recycle loop, according to a Monte Carlo method (Chapter 2). These two types of experiments simulated the performance of a large fed-batch fermenter under perfect, and poor mixing conditions, respectively. The broth was recirculated in continuous experiments to ensure that any effect due to oxygen limitation in the loop was common to both types of experiments. The gas hold-up in the loop was approximately 15% of total loop volume.

For Monte Carlo experiments, the feed into the recycle loop was switched on and off based on a Monte Carlo algorithm and a log-normal CTD (Chapter 2). For a duration of feeding (t_p) of 5 s, the feed was supplied into the recycle loop at a flow

rate given by

$$Q_{mc} = \frac{\bar{t}_c}{t_p} Q(t) \quad (9)$$

$Q(t)$ was constant at a rate of 13.5 mL/h for experiments with complex medium, while equation (8) was used to calculate the feed rate $Q(t)$ for experiments with defined medium. The feed supply was switched off for a period of $(t_c - t_p)$ where t_c varied from 8 s to 44 s. This range of t_c was obtained by dividing the area under the log-normal CDF ($\bar{t}_c = 20$ s and $\sigma = 8.9$ s) into 25 sections of equal probability of 0.04 (Chapter 2). A mixing bulb made from glass (Figure 3.6) was used to mix the fresh feed with the culture broth at the entrance of the recycle loop. During a typical Monte Carlo run for 14 h, approximately 2500 cycles of feed-on and off were repeated. The cumulative total volumes of feed added to the continuous and Monte Carlo experiments were equal to within ± 5 mL. The total amount of nutrients added during these two types of fermentations, therefore, was identical because the same volume and composition of feed was used.

For a fermentor content of 1L, the equations (2), (3) and the estimates of $(P)_{max}$ and $(t_{lag})_{min}$ obtained from Figure 3.4, gave a maximum recirculation rate of 6.12 L/h and a minimum loop volume of 8.2 mL. A number of experiments were performed for recirculation rates of 0.0, 0.25, 0.5, 2.0, 3.0, and 6.0 L/h, and recycle loop volume of 15, and 50 mL. This range of design parameters evaluated the feed zone effect for a range of maximum probability of visit to the feed zone, P , from 0 to 4.0×10^{-4} , a range of interval of exposure to the high concentrations in the feed zone, t_{lag} , from 0 to 12 min, and a fractional volume of the feed zone up to 0.05 of total fermentor volume. The liquid volume in the mixing bulb was less than 0.2 mL at any time, due to the venturi effect at the point where the nutrient was dropped into

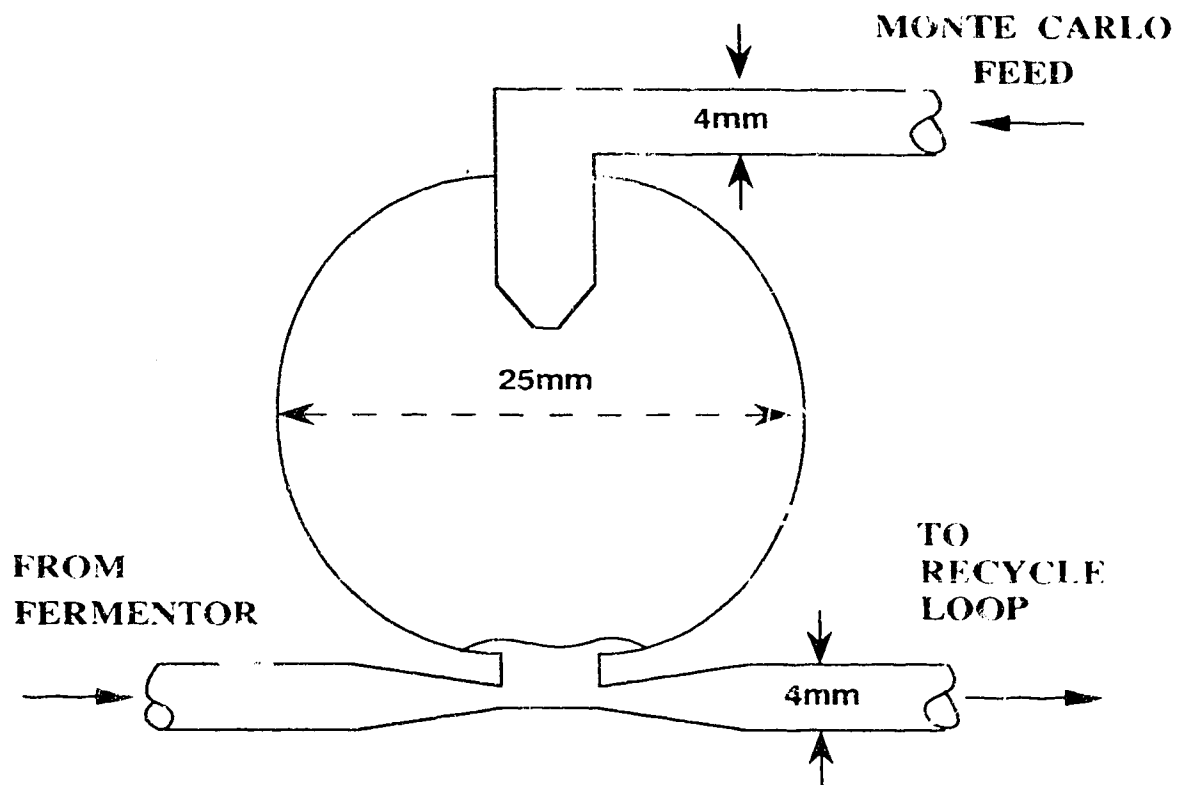


Figure 3.6 A schematic of mixing bulb used to mix fresh feed with the recirculating culture broth.

the incoming culture broth from the fermentor. The residence time of culture in the bulb was less than 3.6 s at the slowest recirculation rate of 0.25 L/h, smaller than the 5 s duration of the feed pulse used in Monte Carlo experiments. The broth leaving the bulb had a glucose concentration of 11 g/L, which is much larger than the 0.5–0.8 g/L required to induce the glucose effect in yeast and cause secretion of ethanol. In continuous fed–batch experiments, the feed was continuously added directly into the fermentor, where the glucose concentration measured at any time was less than 0.3 g/L and the mixing time was less than 5 s.

RESULTS AND DISCUSSION

Fermentations with Complex Media

Two types of fed-batch experiments, continuous and Monte Carlo, were performed using *S.cerevisiae* NCYC 1018. Table 3.2 summarises the initial, and final levels of biomass, ethanol, acetic acid and total amount of carbon consumed from carbon sources for all the fed-batch experiments. The glucose level was maintained below 0.3 g/L during all the fed-batch experiments. The biomass levels at the start of all the fed-batch experiments were 2.0 ± 0.1 g/L, while the final levels varied from 9.1 g/L to 10.0 g/L. Figure 3.7 shows that the profiles of growth for typical Monte Carlo experiments were the same as the continuous fed-batch experiments. Monte Carlo experiments with a range of circulation rates from 0.25 L/h to 6.0 L/h and loop volumes of 15 and 50 mL did not affect the yield of biomass in comparison to the yields obtained from continuous fed-batch experiments (Table 3.2).

The feed zone effect on biomass profiles and yields was not apparent due to utilization of multiple substrates. The total amount of all nutrients added were the same during both continuous and Monte Carlo experiments over 14 h of feeding. The complex medium contained about 0.15 g of maltose for every gram of glucose. Ethanol was also present in the broth at a level up to 3.7 g/L because the fed-batch was started from a batch culture. The feed also contained many amino acids in peptone, which may directly contribute to biosynthesis of macromolecules. Simultaneous uptake of multiple substrates and by-product formation depends on the level of saturation of respiratory capacity of the yeast cells by glucose supply (Kappeli and Sonnleitner, 1986). If the glucose supply over-saturates the respiratory capacity of the yeast cells, then the additional glucose flux will be diverted to produce waste metabolites, such as ethanol, and acetic acid. The diversion of glucose into waste metabolites reduces the yield of biomass. If the

TABLE 3.2 Initial and final levels of biomass, ethanol, and acetic acid for experiments with *S. cerevisiae* NCYC 1018 grown on complex medium.

EXPERIMENT TYPE	RESIDENCE TIME (LOOP) s	LOOP VOLUME mL	FLOW RATE L/h	BIOMASS 0 h g/L	BIOMASS 14 h g/L	ETHANOL 0 h g/L	ETHANOL 14 h g/L	ACETATE 0 h g/L	ACETATE 14 h g/L
Continuous	—	0	0	1.9	8.8	3.4	1.1	0.0	0.0
	27	15	2.0	2.1	9.1	3.1	0.0	0.0	0.0
	720	50	0.25	1.9	9.8	3.4	0.0	0.0	0.5
	360	50	0.5	1.9	9.6	3.3	1.4	0.0	0.0
	60	50	3.0	2.0	9.3	3.7	1.0	0.0	0.0
Monte Carlo	108	15	0.5	1.9	9.3	2.1	1.4	0.0	0.0
	18	15	3.0	1.9	10.0	1.9	0.6	0.0	0.0
	9	15	6.0	2.0	9.4	2.6	1.4	0.0	0.0
	720	50	0.25	2.0	9.2	1.4	0.0	0.0	1.3
	360	50	0.5	2.0	9.0	1.8	1.2	0.0	0.6
	60	50	3.0	1.9	9.4	3.2	1.7	0.0	0.0
	30	50	6.0	2.0	9.7	3.0	1.5	0.0	0.0

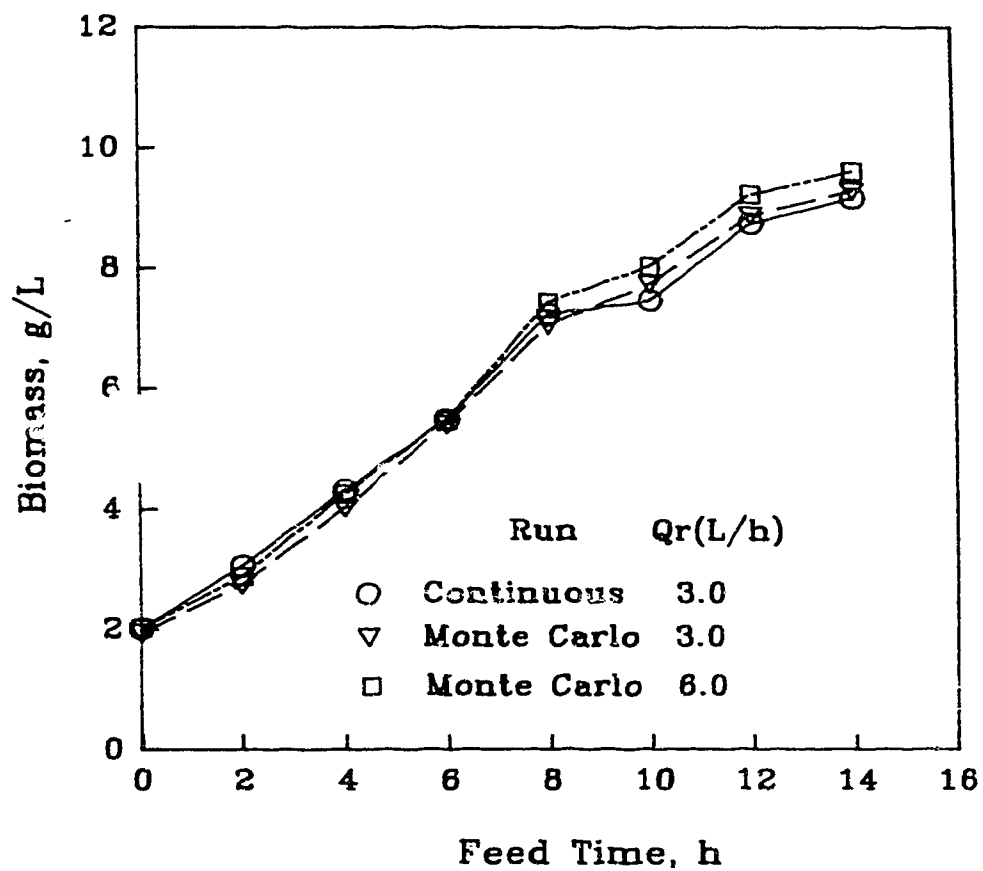


Figure 3.7 A comparison of biomass profiles for experiments with complex medium. A recycle loop of volume (V_p) 50 mL was used.

respiratory capacity is not satisfied by the glucose supply then alternative substrates will be utilized along with glucose (Kappeli and Sonnleitner, 1986). Figure 3.8 compares the theoretical glucose demand by the growing culture with the glucose supply either during continuous feed experiments or during the pulse-on period in Monte Carlo experiments. The theoretical demand for glucose flux for observed growth was estimated by using the following equation,

$$R_g(t) = \left[\frac{\mu(t)}{Y_{x/s}} + m_{x/s} \right] V(t)X(t) \quad (10)$$

where, $Y_{x/s} = 0.34$, estimated from the initial stage of a fed-batch experiment and $m_{x/s} = 0.015 \text{ g/(g DCW-h)}$ (Sweere *et al.*, 1988). The glucose demand rate exceeded the supply rate within the first hour of the continuous fed-batch experiment. Simultaneous utilization of alternative substrates, therefore, was likely. Figure 3.9 compares total amount of glucose, maltose, and ethanol consumed during typical continuous and Monte Carlo experiments. While the total amount of glucose and maltose consumed were similar, the total ethanol consumed during the Monte Carlo experiments was less than half of the amount consumed during the continuous fed-batch experiments. A similar reduction in the total ethanol uptake was observed for other Monte Carlo fed-batch experiments with recirculation rates of 0.5, 3.0 and 6.0 L/h (Table 3.2). The time profile of ethanol uptake in Figure 3.9 showed that the ethanol was not used for about 6 hours during the continuous fed-batch experiment. During the Monte Carlo fed-batch fermentation, additional ethanol was secreted up to about 1 g/L over the initial level before its consumption started.

The feed zone effect on the ethanol uptake under Monte Carlo experiments was similar for experiments with recirculation rates from 0.5 L/h to 6 L/h or

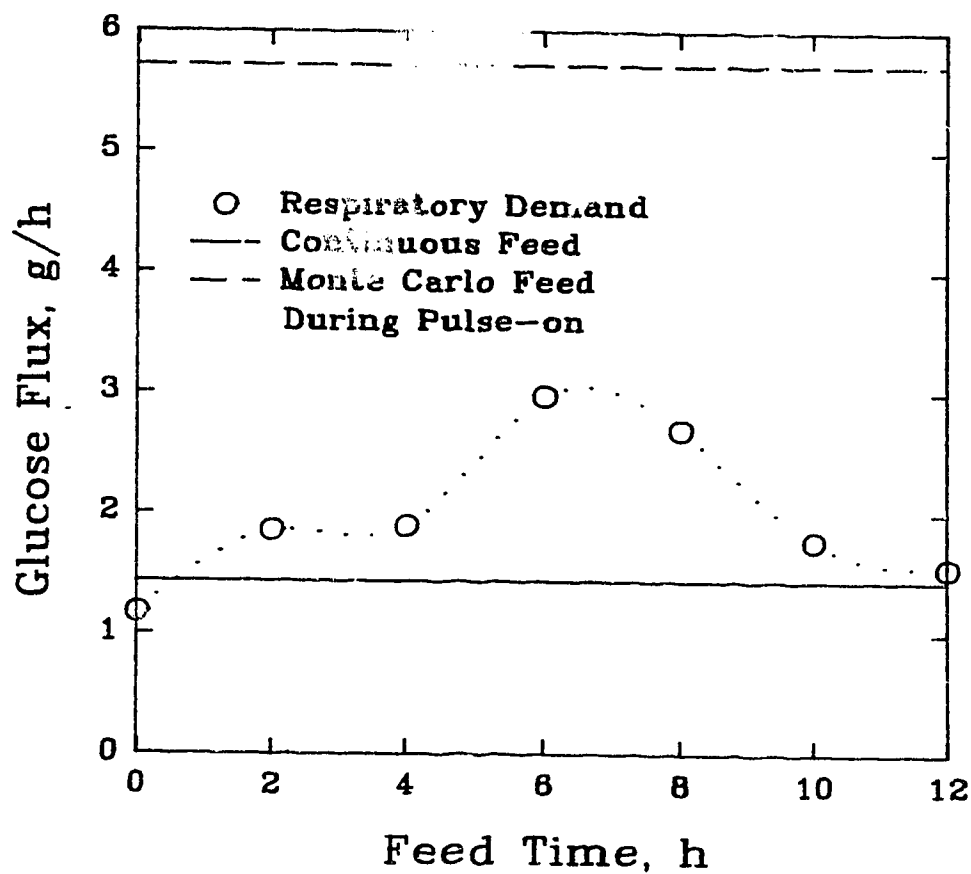


Figure 3.8 Comparison of theoretical demand of glucose equivalent required for observed growth with the glucose supplied during continuous and Monte Carlo experiments with complex medium. The feed rate in Monte Carlo experiments is an instantaneous rate to the recycle loop during the pulse-on period of 5 s.

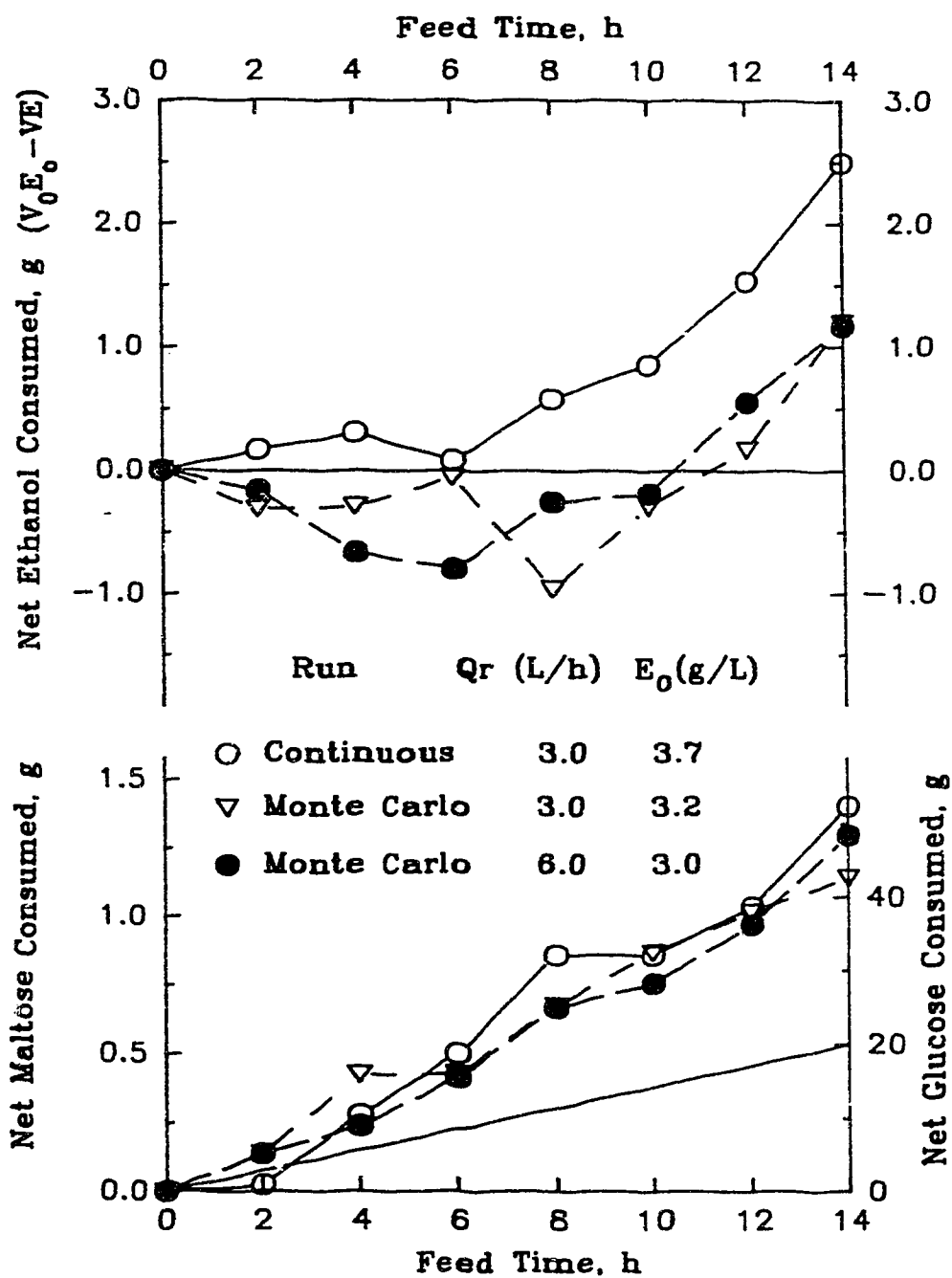


Figure 3.9 Net amount of ethanol (symbols), maltose (symbols), and glucose (line) consumed during experiments with complex medium. A recycle loop of volume (V_p) 50 mL was used.

residence times in the loop from 30 s to 3 min. The acetate levels were below 0.3 g/L for all these experiments. The Monte Carlo experiment with a very low recirculation rate of 0.25 L/h, however, showed significantly different profiles for ethanol and acetate (Figure 3.10). The ethanol uptake was delayed for about 10 h, compared to 2 h delay during the continuous fed-batch experiment. Although the ethanol was completely utilized in both Monte Carlo and continuous fed-batch experiments, acetic acid was secreted up to 1.3 g/L during the last 4 h of the Monte Carlo experiment. The yeast culture had a long residence time of 12 min in the loop when a recirculation rate of 0.25 L/h was used for both continuous and Monte Carlo experiments. No fresh supply of glucose was available to the culture for about 12 min in the loop when the feed was added to the fermentor during continuous fed-batch experiments. This prolonged exposure of culture to starvation conditions in the loop could have caused increased consumption of ethanol over 14 h of fed-batch operation. Dantigny *et al.* (1989) have shown that the incomplete conversion of ethanol to acetic acid takes place during the transition from aerobic growth on glucose to aerobic growth on ethanol. Intermittent supply of fresh feed to the loop during Monte Carlo experiment with a long residence of 12 min in loop could create this transition state and lead to secretion of acetic acid.

Although maltose was being utilized along with glucose and ethanol (Figure 3.9), maltose accumulated in the fermentor from 1 ± 0.01 g/L at the start of feeding to 2.4 ± 0.1 g/L at the end of fermentation for both continuous and Monte Carlo experiments. Higher uptake of ethanol, compared to maltose, indicated that ethanol was preferred over maltose. The accumulation of maltose, and non-zero terminal ethanol concentration values may suggest that some key nutrients were limiting catabolism of maltose and ethanol. The ethanol was, however, completely utilized in experiments with a slow recirculation rate of 0.25 L/h through a 50 mL loop (Figure 3.10), thus eliminating the possibility of other nutrients being limited

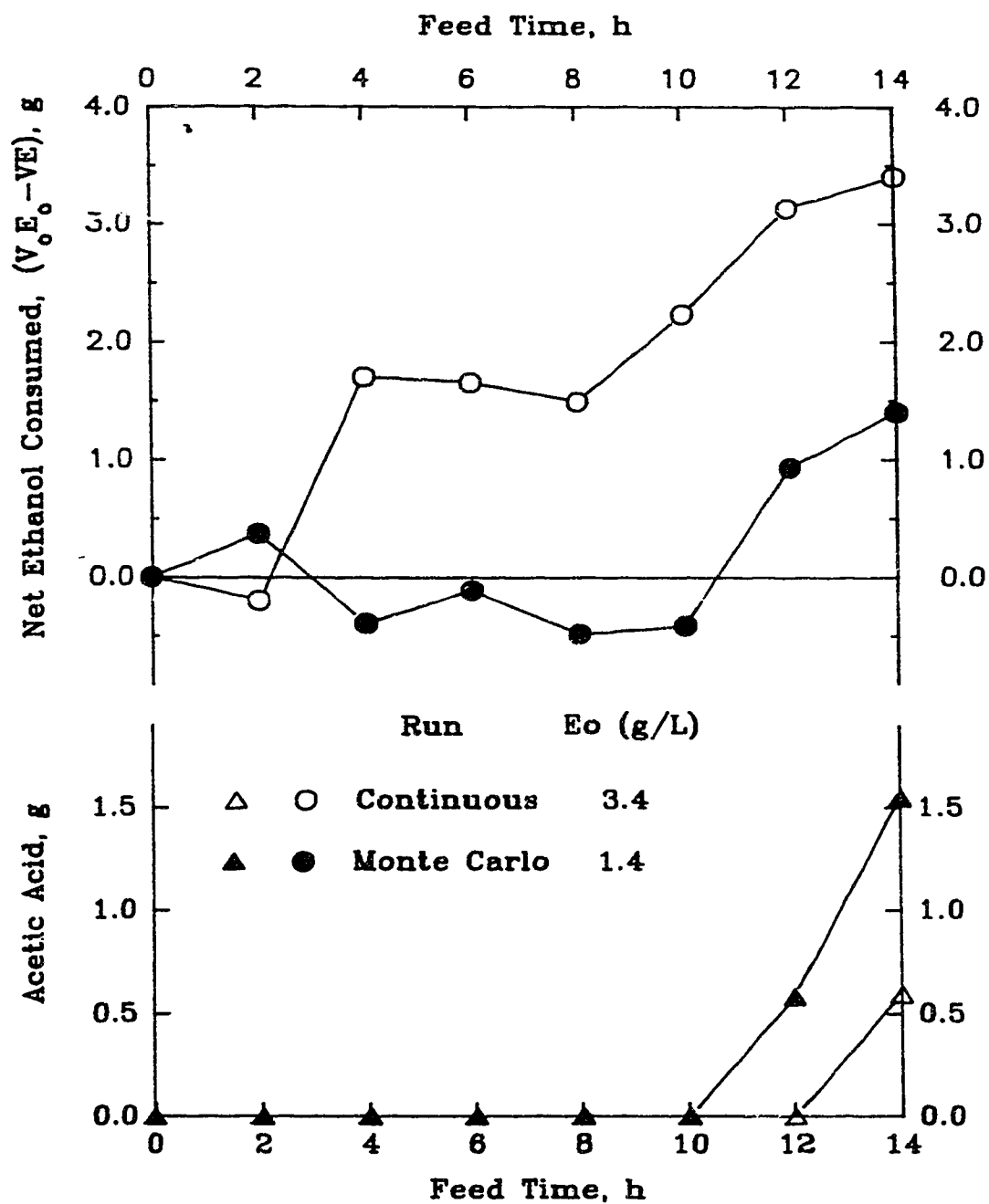


Figure 3.10 Net amount of ethanol consumed (circles), and acetic acid produced (triangles) during experiments with complex medium. A recirculation rate (Q_r) of 0.25 L/h and recycle loop of volume (V_p) 50 mL were used.

for ethanol consumption. The presence of a source of fast energy supply, such as formate or methanol, has been shown to increase the conversion of sugars into biomass (Babel and Muller, 1985). This increase in conversion efficiency of sugars was not observed during both types of fermentations, where maltose accumulated up to 2.4 g/L.

Although similar yields of biomass on glucose and maltose were achieved during Monte Carlo and continuous fed-batch experiments, up to 50% less ethanol was consumed in Monte Carlo fed-batch experiments (Figures 3.7 and 3.9). From Table 3.2, total amount of carbon consumed from glucose, maltose and ethanol for all continuous fed-batch experiments was 9.88 ± 0.64 ($n=4$, 95% confidence) compared to 9.04 ± 0.24 ($n=7$, 95% confidence) for Monte Carlo fed-batch experiments. Thus, a higher apparent yield of biomass on total carbon substrates utilized was observed under fluctuating conditions during Monte Carlo experiments. A significant amount of ethanol was also secreted during the initial 6 h of the Monte Carlo experiment. According to Figure 3.8, the instantaneous glucose supply was much higher than the respiratory demand for glucose, when the feed was switched on during the Monte Carlo experiments. The instantaneous higher supply of glucose could easily saturate the respiratory capacity of a fraction of yeast culture in the recycle loop and cause secretion of ethanol and a drop in the biomass yield. Consider for example, experiments with a recycle loop volume of 50 mL, and recirculation rate of 3 L/h. About 25% of the loop content, or 1.25% of total yeast culture, was exposed to conditions favorable for 'glucose effect' for about 60 s in the loop. The impact of this 'glucose effect' experienced by a small fraction of culture on overall biomass yield would be negligible. When the feed was switched off in Monte Carlo experiments, no fresh glucose was supplied to the yeast culture in the recycle loop as well as the fermentor on time average basis. The possibility of slow-down of growth under this glucose limited condition would be avoided due to the uptake of

alternative carbon sources, including maltose and ethanol.

Fermentations with Defined Media

Baker's yeast is normally produced in large fermentors by supplying molasses at a feed rate increasing with time according to a predetermined strategy (Rosen, 1987). In previous studies (Fowler and Dunlop, 1989; Hansford and Humphrey, 1966; Heinzle *et al.*, 1985; Sweere *et al.*, 1988), defined-medium feeds were used to predict the effects of nutrient fluctuations on the productivity of a large fermentor. Fed-batch experiments with an exponentially-increasing feeding of glucose were performed in present study to check the validity of predictions made from defined medium fermentation experiments about the feed zone effect in large-scale fermentations employing complex medium. In addition to fed-batch experiments with continuous and Monte Carlo feeding, an experiment with periodic feeding with a constant pulse-off time of 15 s was also conducted. The periodic feeding of glucose was used to test whether the distribution of circulation times rather than a mean circulation time is critical for prediction of the feed zone effect.

Figure 3.11 shows the profiles of biomass and ethanol for experiments with the three types of feeding strategies. The protocol of exponentially feeding to the yeast culture was successful in maintaining an aerobic exponential growth of yeast on glucose for about 12 h of feeding time, and controlling glucose and ethanol levels close to zero. Table 3.3 shows the levels of biomass and ethanol after 12 h for fed-batch experiments under different conditions. Although no significant secretion of ethanol was observed, the final biomass level was consistently higher by 10% in Monte Carlo experiments compared to continuous experiments. This magnitude of increase in Monte Carlo experiments was, however, the same for experiments with recirculation rates of 3 L/h and 0.5 L/h.

No significant difference in the ethanol profiles was observed for Monte Carlo

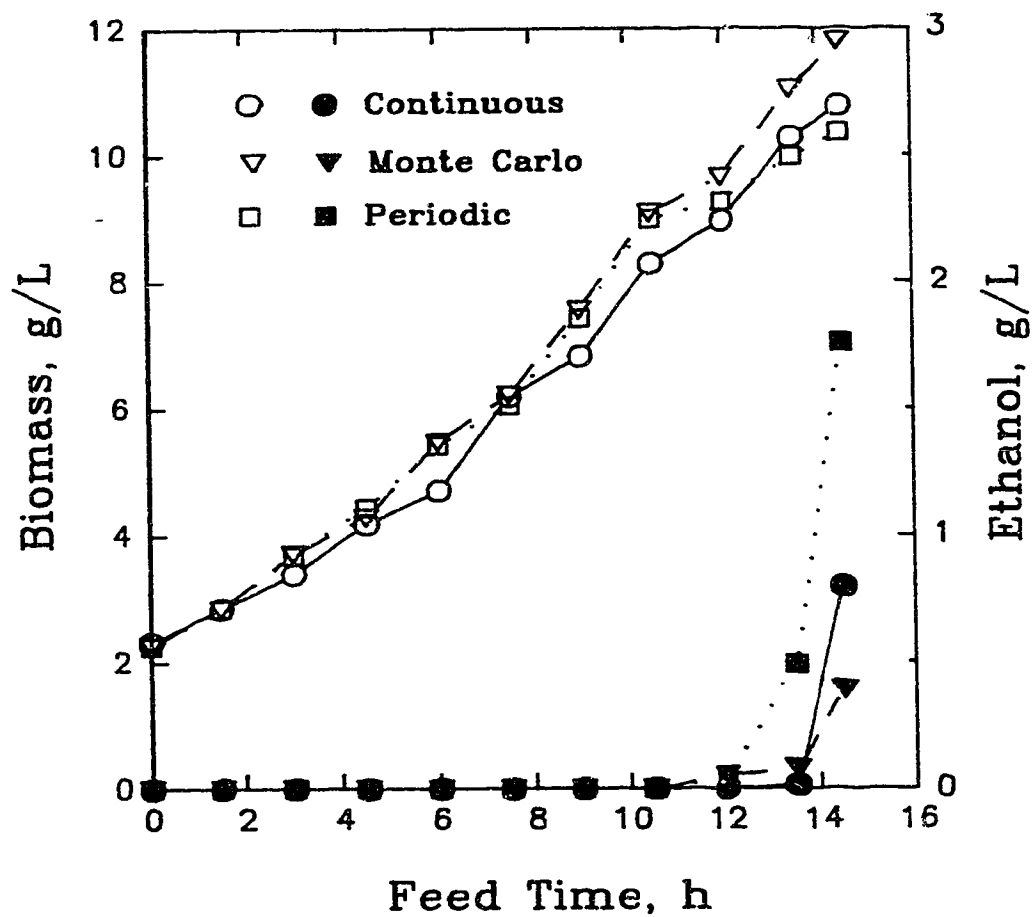


Figure 3.11 Comparison of biomass (open symbols), and ethanol (closed symbols) produced during experiments with defined medium.

TABLE 3.3 Final levels of biomass, and ethanol for experiments with *S. cerevisiae* ATCC 32167 grown on defined media.

Experiment Type	Residence Time—Loop s	Loop Volume L/h	Flow Rate mL	Biomass At 12h g/L	Ethanol At 12h g/L
Continuous	—	0	0	9.0	0
Continuous	—	0	0	9.0	0.06
Continuous	360	50	0.5	9.1	0
Monte Carlo	—	0	0	9.7	0.05
Monte Carlo	—	0	0	10.2	0.07
Monte Carlo	360	50	0.5	10.0	0.06
Monte Carlo	60	50	3.0	9.9	0.05
Periodic	—	0	0	9.2	0.03

experiments compared to continuous fed-batch experiments. The fed-batch experiment with periodic feeding, however, produced ethanol up to 1.7 g/L within the last 2.5 h of the experiment. Usually, the production-scale fed-batch fermentation of yeast culture is carried out for 10 to 14 h before growth begins to slow down due to accumulation of inhibitory products and aged cells. Any effects due to concentration gradients, therefore, are amplified only towards the end of the run. Sweere *et al.* (1988) evaluated the effects of glucose fluctuations by using two fermenters with recirculation of broth between them. This two-fermentor system simulated the effect of periodic fluctuations of glucose levels for different recirculation rates. Their experiment with a broth recirculation time of 36 s showed a reduction of 10% in the overall biomass yield, and ethanol accumulation up to 1.7 g/L during the last hour. In the present study, the significant difference in terminal yield of biomass, and ethanol in the Monte Carlo experiment compared to the experiment with a periodic feeding proves that a strategy based on periodic fluctuation in the fermentor can produce misleading results concerning the feed zone effect. The previous chapter also showed the limitations of periodic feeding strategy in simulating large scale conditions for complex-medium fermentation.

Implications for large-scale fermentations

Production-scale fermentations usually utilize feed of complex media to enhance productivity. The drop in observed yield of baker's yeast in large-scale fermentation compared to bench-scale fermentation is attributed to the spatial gradients in the levels of dissolved oxygen and nutrients (Bajpai and Reuss, 1982). The effects of these concentration gradients can be predicted by simultaneously varying the concentrations of complex substrates as well as dissolved oxygen in the bench-scale fermentation system. The experimental methodology presented here can be easily used to simultaneously vary both oxygen and nutrient levels. The

fluctuations in dissolved oxygen according to the Monte Carlo method lead to a significant drop in yield of biomass (Namdev *et al.*, 1991). The present study evaluated the effects of nutrient gradients, and the dissolved oxygen was kept above the limiting value. No significant feed zone effect on biomass was observed under these conditions for complex medium fermentations. The baker's yeast production in large fermentors, therefore, is expected to be more sensitive to fluctuations in dissolved oxygen levels than to the feed zone effect. The levels of by-products such as ethanol, and acetic acid were influenced by the feed zone effects, although this effect on metabolite levels did not translate into a measurable effect on biomass yield. Other properties of yeast culture such as protein content or bread rising quality could be a better measure of sensitivity of culture to feed zone effects.

Previous studies used chemostat cultures of baker's yeast grown on defined media to determine the effect of glucose fluctuations on biomass yield (Fowler and Dunlop, 1989; Hansford and Humphrey, 1966; Heinzle *et al.*, 1981; Heinzle *et al.*, 1985). Poor mixing at the feeding port decreased the biomass yield due to onset of the 'glucose effect' (Fowler and Dunlop, 1989; Hansford and Humphrey, 1966). Heinzle *et al.* (1985) carried out chemostat experiments wherein poor mixing was simulated by pulses of glucose every 10 s. They observed the expected trend of reduced biomass yield and higher ethanol secretion for glucose-pulse experiments compared to continuous-feed experiments when the dilution rate was decreased from 0.35 h^{-1} to 0.1 h^{-1} . Unexpectedly, 20% higher biomass was obtained at a dilution rate of 0.3 h^{-1} , when the pulse experiments were started from an aerobic culture established at a dilution rate of 0.2 h^{-1} . In the present study, glucose pulse feeding in Monte Carlo experiments gave a similar increase in biomass yields of 10%, compared to continuous feeding of defined medium. These Monte Carlo fed-batch experiments were also started from an aerobic chemostat culture initially established at a dilution rate of 0.2 h^{-1} .

In the present study, the results from experiments with a defined medium compared to a complex medium showed opposite effects on both the final biomass levels and the profile of ethanol levels. This comparison demonstrates that a fed-batch fermentation system grown on a representative complex medium should be used in laboratory experiments to evaluate the feed zone effects. The design parameters for bench-scale experiments, such as feeding pattern, recirculation rate and recycle loop volume, should be based on the mixing quality of large fermentors. Circulation time distributions obtained for a large fermentor, are useful in obtaining suitable ranges for these design parameters.

CONCLUSIONS

1. The experiments with complex medium showed that the feed zone effect on overall biomass yield was negligible for a reasonable range of recirculation rates and recycle loop volumes.
2. The profile of ethanol with time showed a greater sensitivity to the feed zone effect compared to the biomass profile in complex-medium fed-batch fermentations. Acetic acid production was observed when a long residence time of 12 min in the loop was used.
3. Chemostat experiments with defined medium should be used only with caution to evaluate the feed zone effect in a production-scale fermentor fed with complex nutrients.

REFERENCES

- Anderson, C., LeGrys, G.A., Solomons, G.L. Concepts in the design of large-scale fermentors for viscous culture broths. *The Chemical Engineer*. 1982, February, 43–49.
- Babel, W., Muller, R.H. The influence of carbon catabolism on the auxiliary substrate effect. *Acta Biotechnol.* 1985, 5, 333–338.
- Bajpai, R.K., Reuss, M. Coupling of mixing and microbial kinetics for evaluating the performance of bioreactors. *Can. J. Chem. Eng.* 1982, 60, 384–392.
- Brodkey, R.S. Fundamentals of turbulent motion, mixing, and kinetics. *Chem. Eng. Commun.*, 1981, 8, 1–23.
- Brooks, J.D. and Meers, J.L. The effect of discontinuous methanol addition on the growth of a carbon-limited culture of *Pseudomonas* sp.. *J. Gen. Microbiol.*, 1973, 77, 513–519
- Bryant, J. Characterization of mixing in fermenters. *Adv. Biochem. Eng.*, 1977, 5, 101–123.
- Contesse, G., Crepin, Gros, F. Transcription of lactose operon in *E. coli*. In *The Lactose Operon*. J.R. Beckwith, and D. Zisper. Eds.; Cold Spring Harbor Laboratory: New York. 1970, pp 111–142.
- Dantigny, P., Ninow, J.L, Marc, I., Engasser, J.M. Representation of changes in the metabolic patterns of baker's yeast from measurements of extracellular pyruvate, acetate, acetaldehyde and ethanol. *Biotechnol. Lett.* 1989, 11(7), 515–520.
- Einsele, A. Scaling of bioreactors. *Proc. Biochem.*, 1978, July, 13–14.
- Einsele, A., Ristroph, D.L., Humphrey, A.E. Mixing times and glucose uptake measured with a flurometer. *Biotechnol. Bioeng.*, 1978, 20, 1487–1492.
- Fasano, J.B., Penney, W.R. Cut reaction by-products by proper feed blending.

- Chem. Eng. Progr.* **1991**, *87*(12), 46–52.
- Fiechter, A., Kappeli, O., Meussdoerffer, F. *The Yeasts*, A.H. Rose and J.S. Harrison (Ed.), Academic Press: London., **1987**, *2*, pp. 99–128.
- Fowler, J.D. and Dunlop, E.H. Effects of reactant heterogeneity and mixing on catabolite repression in cultures of *Saccharomyces cerevisiae*. *Biotechnol. Bioeng.*, **1989**, *33*, 1039–1046.
- Hansford, G.S., Humphrey, A.E. The effect of equipment scale and degree of mixing on continuous fermentation yield at low dilution rates. *Biotechnol. Bioeng.*, **1966**, *8*, 85–96.
- Heinzle, E., Nishizawa, Y., Dunn, I.J., Bourne, J.R. Dynamic and steady-state effects of cyclic feeding of oxygen and glucose in an ethanol-producing yeast culture. *Ann. N.Y. Acad. Sci.*, **1981**, *369*, 159–166.
- Heinzle, E., Moes, J., Dunn, I.J. The influence of cyclic feeding on a continuous baker's yeast culture. *Biotechnol. Lett.* **1985**, *7*(4), 235–240.
- Kappeli, O. and Sonnleitner, B. Regulation of sugar metabolism in *Saccharomyces* type yeast: Experimental and conceptual considerations. *CRC Crit. Rev. in Biotechnol.*, **1986**, *4*(3), 299–325.
- Khang, S.J., Levenspiel, O. New scale-up and design method for stirred agitated batch mixing vessels. *Chem. Eng. Sci.*, **1976**, *31*, 569–577.
- Knysh, P., Mann, R. Utility of networks of interconnected backmixed zones to represent mixing in a closed stirred vessel. *The Institution of Chemical Engineers*, Symposium Series No. 89: Fluid Mixing II., **1984**, 127–145.
- Levenspiel, O. *Chemical reaction engineering*. p.296, 2nd edition. Wiley–Interscience, New York , **1972**, pp 127–145.
- Lilly, M.D. In *Bioactive metabolite products 2, Development and Production*, L.J. Nisbet and D.J. Winstanley, Eds.; Academic Press: London, **1983**, pp 78–89.
- Lim, H.C., Chen, B.J., Creagan, C.C. An analysis of extended and exponentially

- fed-batch cultures. *Biotechnol. Bioeng.* 1977, 19, 425-433.
- Mann, R., Mavros, P.P., and Middleton, J.C. A structured stochastic flow model for interpreting flow-follower data from a stirred vessel. *Trans. Instn. Chem. Eng.*, 1981, 59, 271-278.
- Manning, F.S., Wolf, D., Keairns, D.L. Model simulation of stirred tank reactors. *AIChE J.*, 1965, 11, 723-727.
- Mou, D.-G. In *Antibiotics containing the β -lactam structure* Part I. A.L. Demain and N.A. Solomon, Eds.; Springer-Verlag:Berlin. 1983, pp 255-284.
- Namdev, P.K., Yegneswaran, P.K., Thompson, B.G., Gray, M.R. Experimental simulation of large-scale bioreactor environments using a Monte Carlo method. *Can. J. Chem. Eng.* 1991, 69, 513-519.
- Petrik, M., Kappeli, O., Fiechter, A. An expanded concept for the glucose effect in the yeast *Saccharomyces uvarum*: Involvement of short- and long-term regulation. *J. Gen. Microbiol.*, 1983, 129, 43-49.
- Reuss, M., Brammer, U. Influence of substrate distribution on productivities in computer controlled baker's yeast production. *Proc. IFAC Modelling and Control of Biotechnological Processes*, Noordwijkerhout, 1985, 145-150.
- Roberts, J.A.E., Slater, N.K.H. Simulation of a methylotroph's behaviour in an imperfectly mixed fermentor. *Intl. Conf. Bioreactor Fluid Dynamics*, Cambridge, UK, 1986, paper 19, 257-267.
- Roels, J.A. Mathematical models and the design of bioreactors. *J. Chem. Tech. Biotechnol.*, 1982, 32, 59-72.
- Rosen, K. In *Yeast Biotechnology*. D.R. Berry, I. Russel, G.G. Stewart, Eds.; Allen & Unwin:London, 1987. p.471-500 .
- Senior, P.J., Windass, J. The ICI single cell protein process. *Biotechnol. Lett.* 1980, 2, 205-210.
- Sittig, W. The present state of fermentation reactors. *J. Chem. Tech. Biotechnol.*

1982, 32, 47–58.

Sweere, A.P.J., Matla, Y.A., Zandvliet, J., Luyben, K.Ch.A.M., Kossen, N.W.F.

Experimental simulation of glucose fluctuations: The influence of continually changing glucose concentrations on the fed–batch baker's yeast fermentation.

Appl. Microbiol. Biotechnol., 1988, 28, 219–224

Zabriskie, D.W., Arcuri, E.J. Factors influencing productivity of fermentations

employing recombinant microorganisms. *Enzyme Microbiol. Technol.* 1986, 8, 706–717.

CHAPTER 4

EFFECTS OF GLUCOSE FLUCTUATIONS ON SYNCHRONY IN FED-BATCH FERMENTATION OF SACCHAROMYCES CEREVISIAE

INTRODUCTION

Spontaneous generation of autonomous oscillations of variables, such as biomass, dissolved oxygen, pH, CO₂ fraction in off-gas, flow cytometry measurements, and NADH fluorescence have been observed in chemostat culture of the budding yeast, *Saccharomyces cerevisiae* (Kuenzi and Fiechter, 1969; Myenburg *et al.*, 1973; Meyer and Beyeler, 1984; Parulekar *et al.*, 1986; Scheper and Schugerl, 1986; Porro *et al.*, 1988; Strassle *et al.*, 1989). These oscillations were shown to be due to the tendency of budding yeast to self-synchronize under perfectly controlled and uniform conditions in a chemostat culture when the dilution rate was below a critical level. If a yeast population is divided into two categories, single cells and budded cells, then all the cells in a fully synchronised population will alternate between these two types of cells. The oscillatory behavior of budding yeast has been considered to be a severe problem in process analysis and control of the chemostat operation (Meyer and Beyeler, 1984; Parulekar *et al.*, 1986; Porro *et al.*, 1988). Growing a synchronous culture of yeast in chemostat culture has been useful in determining the metabolic events associated with various phases of the cell-cycle of a yeast cell (Kuenzi and Fiechter, 1969; Strassle *et al.*, 1988; Munch *et al.*, 1991).

Oscillations in a chemostat culture, which are not caused by imperfect control of culture conditions, could occur due to certain feedback interactions (Harrison and

Topiwala, 1974). These interactions could be either between cells and environment parameters or between linked intracellular reactions. The autonomous oscillations in an aerobic glucose-limited chemostat culture of budding yeast were linked to secretion of ethanol in the budding-cell phase and subsequent utilisation of the ethanol in the single-cell phase (Kuenzi and Fiechter, 1969; Porro *et al.* 1988). Secretion and uptake of ethanol depended on the levels of glucose and dissolved oxygen in the fermentor. The oscillations in chemostat culture were temporarily eliminated when a pulse of glucose or ethanol was added (Parulekar *et al.*, 1986; Martegani *et al.*, 1990). Too high or too low dissolved oxygen levels, or a high steady state glucose level also resulted in a stationary steady state.

Batch and fed-batch fermentations, not continuous fermentation, are used for commercial production of baker's yeast, chemicals and recombinant proteins from *S.cerevisiae*. The quality of baker's yeast, indicated by its fermentative activity and storage capability, is better when the fraction of the population in the budding-cell phase is lower (Reed, 1982). For example, during production of baker's yeast the supply of molasses is reduced at the end of fermentation to obtain a reduced fraction of budded cells. The optimal on-off type control policy for growth rate produced a final product with higher fermentative activity compared to an exponential fed-batch fermentation (Takamatsu *et al.*, 1985). Growth under this optimal control strategy was shown to be equivalent to a synchronously dividing culture. Operational strategies to produce synchrony in fed-batch fermentation, therefore, could be useful in obtaining better and more consistent quality of final product. Pseudo-steady state attained in a fed-batch fermentation under certain conditions has been shown to be equivalent to a chemostat (Yamane *et al.*, 1977; Lim *et al.*, 1977). Thus, it may be possible to establish synchronously dividing culture in fed-batch fermentation.

Partially synchronised populations have been produced in batch (Wiemken *et*

al., 1970) and in fed-batch fermentation (Alberghina *et al.*, 1991). As cells grew in the fermentor to high biomass level, the synchronisation became less pronounced and finally disappeared. The oscillation in budded fraction during the fed-batch fermentation was attributed to the synchronisation of a sub-population caused by on-off control of nutrients used to achieve high cell density. Performance of a large-scale fed-batch fermentation depends on the degree of heterogeneity of the population and contents of the fermentor. Poor mixing in large fermentors causes the formation of gradients in the concentrations of glucose and dissolved oxygen (Anderson *et al.*, 1982). Frequent exposure of yeast cells to different concentrations during their circulation in the fermentor was experimentally simulated using a Monte Carlo method and a circulation time distribution in Chapter 2. These effects of environmental conditions on the cells and the transient nature of fed-batch may lead to difficulty in the establishment of synchrony in fed-batch fermentation.

The objective of this chapter was to evaluate the effect of fluctuations in glucose concentration due to poor mixing on the synchronously dividing culture of *S.cerevisiae* in fed-batch fermentations. Fed-batch fermentation with an exponentially increasing feed supply was started from a synchronous culture of *S.cerevisiae* established in a chemostat. Glucose fluctuations were simulated by intermittently supplying feed to the fermentor. The mixing effects were evaluated by comparing the performance of continuously-fed with intermittently-fed fed-batch fermentations.

MATERIALS AND METHODS

Microorganisms and Medium

S.cerevisiae ATCC 32167 was stored, cultured and grown on a 'D' defined medium as described in materials and methods section of Chapter 3.

Equipment

The details of fermentation equipment, monitoring and control system are described in materials and methods section of Chapter 3.

Cultures and Assay

The inoculum (100 mL) was grown in a shake flask (500 mL) to exponential phase for 24 h at 30°C, and 250 rpm. The fermentation was carried out with a 5% (v/v) inoculum and initial content of 1L of start-up medium at 30°C, 900 rpm, and 1.5 L/min of air supply. These conditions ensured that the dissolved oxygen was always maintained above 20% in all experiments. The pH was controlled at 4.9 ± 0.1 by using 2N NaOH and 2N HCl during batch and chemostat operation. The chemostat was started after 3 hours of batch fermentation. The feed rate was increased, in two equal steps, from 160 mL/h to 200 mL/h within 4 hours to give a final dilution rate of 0.2 h^{-1} . A partially synchronised culture was established after 12 h of chemostat operation which also produced periodic oscillations in CO_2 fraction of off-gas. All fed-batch experiments were consistently started from a partially synchronised culture after about 21h of chemostat operation at a dilution rate of 0.2 h^{-1} . The feed was switched on during the rising period of cycle of CO_2 fraction in off-gas. An exponentially increasing feeding strategy was based on the

following equation (Lim *et al.*, 1977),

$$F(t) = \frac{\mu V_o X_o^T}{Y_{xgo} G_{in}} e^{\mu t} \quad (1)$$

where, the initial conditions used were: biomass, X_o^T , of 2.25 g/L, glucose, fermentor volume, V_o , of 1L, glucose concentration in the feed, G_{in} , of 100 g/L. The parameters were growth rate, μ , of 0.16 h⁻¹, and biomass yield on substrate, Y_{xgo} , of 0.45. The pH was controlled between 4.7 and 5.0 during the fed-batch run by using 2N NH₄OH. A 5 mL sample from the fermentor was taken frequently during chemostat operation and every 1.5 h during the fed-batch experiments.

The samples were immediately filtered using 0.45µm Sartorius cellulose nitrate filters. The biomass was measured by absorbance at 620nm using a spectrophotometer (Spectronic 21). The dry weight was obtained by drying the filtrate using a microwave oven for 10 minutes. A correlation between absorbance and dry weight was obtained at various times during a fed-batch run (Appendix A). Glucose in the supernatant was analyzed using a YSI Glucose Analyzer (model 27). Ethanol was analyzed with an enzyme kit (Boehringer Mannheim) with a lower limit of 0.01g/L, and a precision of ±0.002 g/L. The number of single cells and budded cells was counted by fixing cells with 10% formaldehyde in saline and using a hemocytometer (Pringle and Mor, 1975). From 350 to 500 cells were counted for each sample in duplicate. The budded fraction was calculated by taking the ratio of the total number of budded cells to the total number of cells, and was reproducible within ± 2.5%.

Design Of Cyclic Experiments

The effect of glucose fluctuations on synchrony was evaluated by comparing

the performance of two types of experiments: (1) 'continuous' experiments, where feed was continuously added to the fermentor according to an exponentially increasing feeding strategy, and (2) 'Monte Carlo' experiments, where the feed was intermittently supplied to the fermentor, according to a Monte Carlo method described in Chapter 2. These two types of experiments simulated the performance of a large fed-batch fermenter under perfect and poor mixing conditions respectively. A fed-batch fermentation with periodic feeding with constant period of 15 s was also carried to evaluate the effect of distribution of circulation times. The total volume of feed added to all fed-batch experiments were equal to within ± 5 mL.

RESULTS AND DISCUSSION

Characterisation of oscillations

Chemostat experiments at two dilution rates (D) of 0.1 h^{-1} and 0.2 h^{-1} were carried out. Steady oscillations of CO_2 fraction in off-gas, dissolved oxygen (DO) and biomass were established after 15h of chemostat operation at a dilution rate of 0.2 h^{-1} and after 30 h at 0.1 h^{-1} . Data from repeated experiments are given in Appendix D. Typical cycles of CO_2 fraction and dissolved oxygen are shown in Figure 4.1. The non-harmonic oscillations of these on-line measurements were due to synchrony of a sub-population. If we divide the yeast population into two phases, single-cell phase and budding-cell phase, then the fraction of the population in the budding-cell phase with time indicates the degree of synchrony in the chemostat. The ratio of number of budded cells to total number of cells or budded fraction (BF) measured for a complete cycle of CO_2 is shown in Figure 4.2. The cycle of budded fraction was in phase with the CO_2 -cycle for both dilution rates. Oscillations in the CO_2 fraction were, therefore, used to indicate the degree of synchrony.

Oscillations in the budded fraction from 0 to 1 would indicate complete synchrony of the yeast population. Due to the asymmetric division of a yeast cell, the daughter cell always takes more time to bud than the mother cell. Also some older daughter cells are undistinguishable from mother cells, while some older mother cells bud less frequently than their younger counterparts. Only a sub-population of the chemostat is, therefore, synchronised and the rest of the population remains heterogeneous. When the synchronised sub-population was in the budding-cell phase, the budded fraction increased and reached a maximum level (BF_{max}). The period of the budding-cell phase of the synchronised sub-population (t_b) coincided with the peaks in the CO_2 -cycle (Figures 4.1 and 4.2). The minimum value of the budded fraction (BF_{min}) was due to the background asynchronous

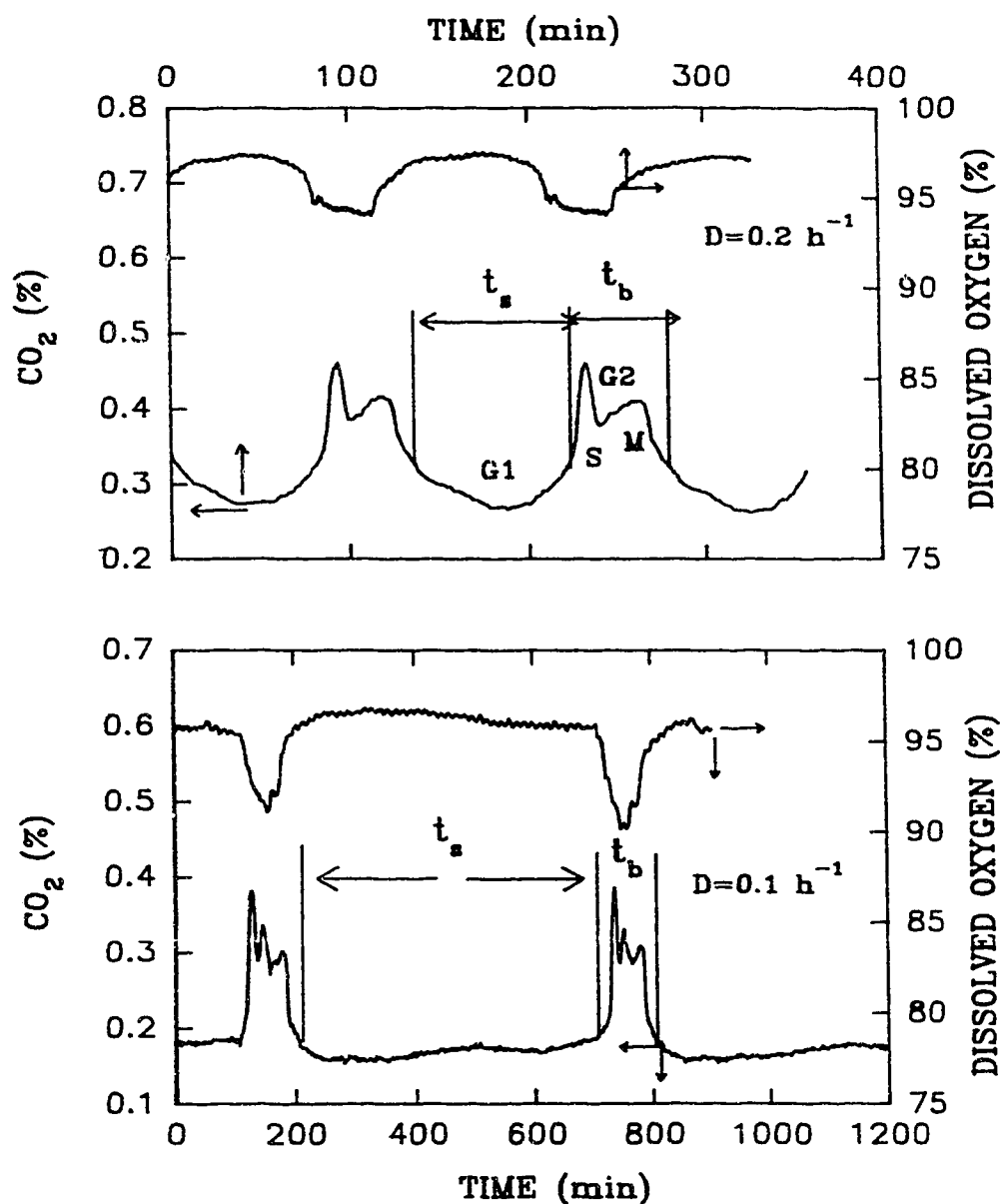


FIGURE 4.1 Effect of dilution rate on oscillations of dissolved oxygen and CO_2 fraction in off-gas. t_s represents the period for the single-cell phase and t_b represents the period for the budding-cell phase. G1, S, G2 and M represent the four phases of the cell-cycle of yeast.

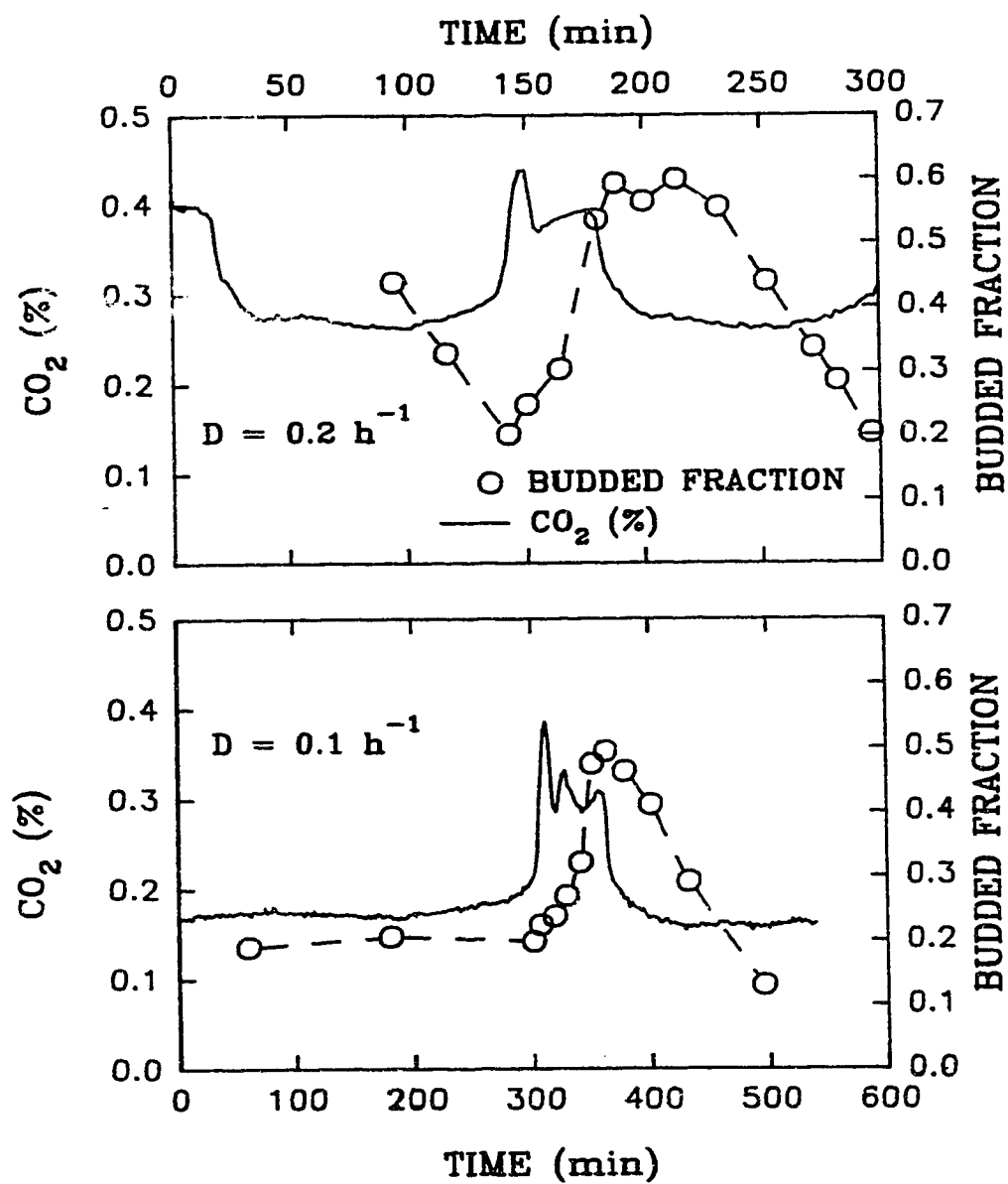


FIGURE 4.2 Correlation between budded fraction of yeast population and CO₂ fraction in off-gas during chemostat operation.

population, and therefore indicated the single-cell phase of the synchronised sub-population. The single-cell phase, t_s , corresponded to the interval of constant low levels of CO_2 in Figures 4.1 and 4.2.

The operating conditions, type of strain, feed composition and biomass level all affect the degree of synchrony. A synchrony index was used by Munch *et al.* (1991) to quantify the degree of synchrony but this index failed to directly relate the effect of dilution rate on the degree of synchrony and was very sensitive to small variations in BF_{\min} . The fraction of the population synchronised, y_s , would vary with time due to dilution between budding events. The value of y_s , therefore, was a function of maximum and minimum budded fraction, cycle time (t_c) and dilution rate (D). The maximum and minimum fractions of the cells synchronised ($y_{s,\max}$ and $y_{s,\min}$) were calculated from the Equations (6) and (7), which are derived in Appendix D.

Effects of Dilution Rates

A long period of 9.8 h for CO_2 -cycles was observed for a dilution rate at 0.1 h^{-1} compared to 2.7 h at 0.2 h^{-1} . Strassle *et al.* (1989) observed a similar drop in the periods of cycles for a range of dilution rates from 0.1 h^{-1} to 0.24 h^{-1} . The interval of budding-cell phase, t_b , was about 1 h and independent of dilution rates. The interval of single-cell phase, t_s , however, varied with dilution rate. The duration of single-cell phase was 1.7 h at a dilution rate of 0.2 h^{-1} compared to 8.5 h at 0.1 h^{-1} . Once budding started, the interval for the budding-cell phase was independent of growth conditions consistent with cell-cycle theory and previous studies (Barford and Hall, 1976; Porro *et al.*, 1988). The maximum fraction of synchronised population ($y_{s,\max}$) was calculated to be about 0.48 for both dilution rates. The minimum fraction of synchronised sub-population ($y_{s,\min}$) was 0.26 at a dilution rate of 0.1 h^{-1} compared to 0.35 at 0.2 h^{-1} . This difference in $y_{s,\min}$ values

was due to more wash-out of synchronous cells at the dilution rate of 0.1 h^{-1} .

Flow-cytometry studies showed that the initiation of budding coincides with the initiation of DNA replication and the separation of buds coincides with the end of nuclear division (Scheper and Schugerl, 1986). The cell-cycle of a yeast cell consist of four phases: G1 phase which separates nuclear division from initiation of DNA synthesis; S phase corresponding to the DNA synthesis; G2 phase which separates S phase from M phase; and M phase, where division of the nuclei occurs. Barford and Hall (1976) performed studies on the effect of growth rate on various phases of the cell-cycle. They showed that the S and M phases occurred in a constant time of about 1h, thus equivalent to the budding-cell phase. The duration of the G1 phase varied from 5 min to 4.7 h, as growth rate of *S.cerevisiae* was varied from 0.45 h^{-1} to 0.096 h^{-1} , thus equivalent to the single-cell phase. The duration of G2 phase also increased from 22 min to 60 min for the same drop in growth rate. This correlation between four phases of the cell-cycle and the budding state of cells was used in the present study to associate the cell-cycle phases with a CO_2 -cycle as shown in the Figure 4.1. Not only did the periods of the CO_2 -cycles vary with dilution rate, but also the number of peaks varied. Two peaks were observed for dilution rate of 0.2 h^{-1} and three for 0.1 h^{-1} . Strassle *et al.* (1989) also observed a similar variation in the number of peaks with dilution rate. The effect of growth conditions on the G2 phase, sandwiched between the S and M phases, may cause this variation in the number of peaks.

Causes of Oscillations

Spontaneous initiation and maintenance of oscillations has been attributed to switching from respiro-fermentative growth on glucose and stored carbohydrates during the budding-cell phase to aerobic growth on glucose and ethanol during the single-cell phase (Kuenzi and Fiechter, 1969; Porro *et al.*, 1988). According to this

mechanism, simultaneous utilisation of glucose and stored carbohydrates saturates the respiratory capacity and leads to excretion of ethanol. The bypass of glucose into ethanol provides a fast supply of ATP needed to complete the budding-cell phase in a constant duration. The self-synchronisation of the culture is induced by acceleration of growth of single cells due to simultaneous uptake of glucose and ethanol. Any perturbations in glucose and dissolved oxygen levels during the single-cell phase will, therefore, affect the degree of synchrony.

In the present study, ethanol accumulated up to 0.015 g/L for a period of 0.5 h when a dilution rate of 0.1 h^{-1} and 5 g/L of glucose in the feed was used. Porro *et al.* (1989) showed that ethanol accumulated up to 0.037 g/L for a period of 2.5 h when a dilution rate of 0.106 h^{-1} and 5 g/L of glucose in the feed was used. Lower levels of ethanol and excretion for a shorter duration in the present study could be due to ethanol consumption by the significant non-synchronised sub-population. Figure 4.1 shows that dissolved oxygen oscillated between 93% and 97% at a dilution rate of 0.2 h^{-1} , and between 91% and 96% at 0.1 h^{-1} . These close to saturation levels of dissolved oxygen were higher than those reported in previous studies where oscillations disappeared when dissolved oxygen was higher than 70–90% (Parulekar *et al.*, 1986; Porro *et al.*, 1989).

Fed-batch Experiments

Fed-batch experiments using glucose feeds were performed to study the effect of transient conditions on the synchrony of *S.cerevisiae*. Figure 4.3 shows the variation of the CO_2 fraction of off-gas during a typical complete fermentation experiment. Fermentations were started from partially synchronised cultures established in chemostat culture at a dilution rate of 0.2 h^{-1} . The chemostat culture was shut-off after three CO_2 -cycles and fed-batch was immediately started during the rising portion of a CO_2 -cycle. The oscillations in CO_2 continued during the

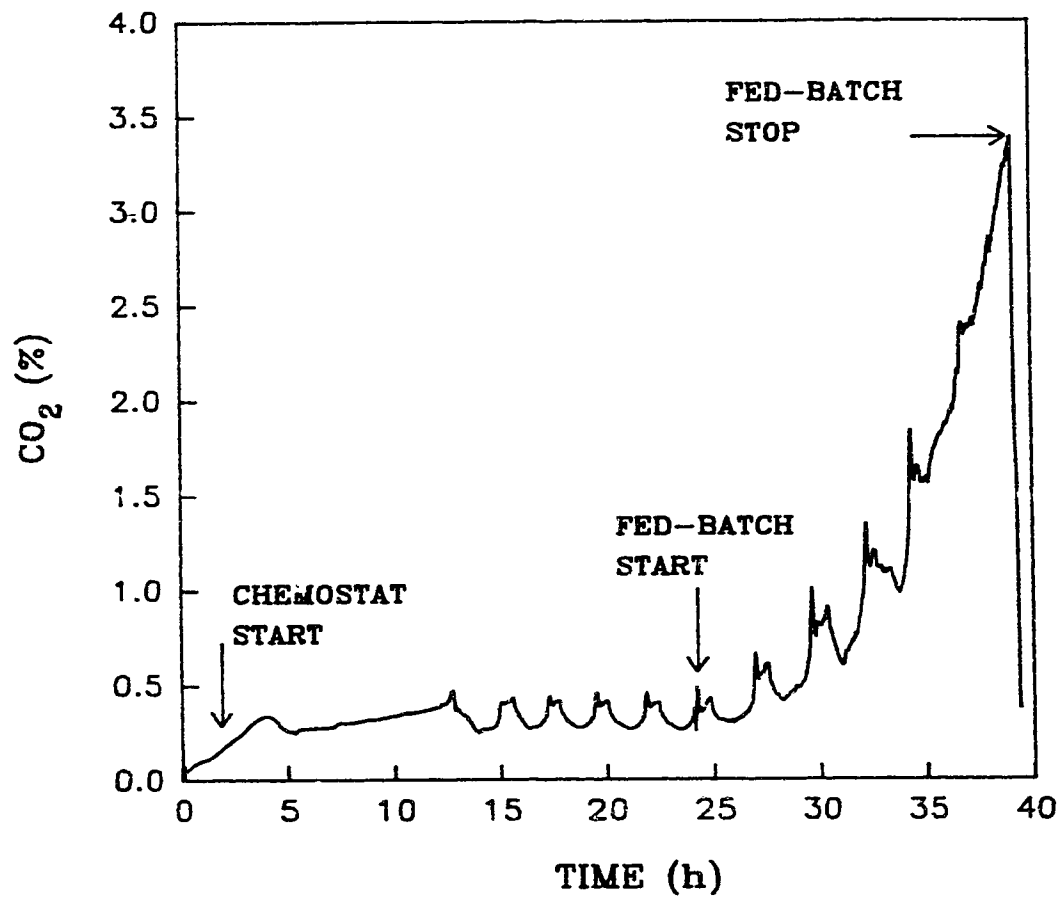


FIGURE 4.3 Profile of CO₂ fraction in off-gas for a complete experiment consisting of batch, chemostat and fed-batch operations.

fed-batch fermentation for about 5 cycles (11 h of feeding) after which they disappeared (Figure 4.3). Similar oscillations in the oxygen fraction of off-gas, and in the dissolved oxygen levels were also observed (Appendix D). Ethanol, biomass and glucose were analysed every 1.5 h. No detectable ethanol was observed in the fermentor for the initial 12 h of feeding duration, after which accumulation of 0.7 g/L in last 2.5 h of feeding was detected. Glucose remained below 0.35 g/L during the fed-batch operation. Biomass accumulation from 2.25 g/L to 10.5 g/L in 14.5 h of fed-batch operation were detected.

The profiles of the budded fraction measured during fed-batch experiments are shown in Figure 4.4. The amplitude of the first cycle of the budded fraction immediately after the start of feeding was larger than the amplitude of a typical cycle observed in chemostat culture. The amplified cycle of the budded fraction was followed by four cycles with reduced amplitudes. About 90% of the population was in the single cell phase at the end of 12 h of feed supply. These variations in the oscillations of budded fraction indicated that the degree of synchrony was affected by the dynamics of fed-batch operation. Equations (6) and (7) of Appendix D, derived for chemostat fermentation, cannot be used to indicate the degree of synchrony in fed-batch fermentation.

The CO₂ fraction in off-gas was due to two contributions, a constant base level from the asynchronous population, and superimposed oscillations due to the synchronous cells. The area under the portion of a cycle with elevated CO₂ levels relative to the area under the curve for base level of CO₂, therefore, can be used as a measure of the fraction of the population synchronised during that CO₂-cycle. The fractional area under the CO₂ oscillations for all the five cycles during fed-batch fermentation in Figure 4.3 varied from 0 to 0.3 with a maximum at the second cycle after the fed-batch operation was started. This variation in CO₂ production by the synchronised sub-population indicated an initial increase in the degree of synchrony

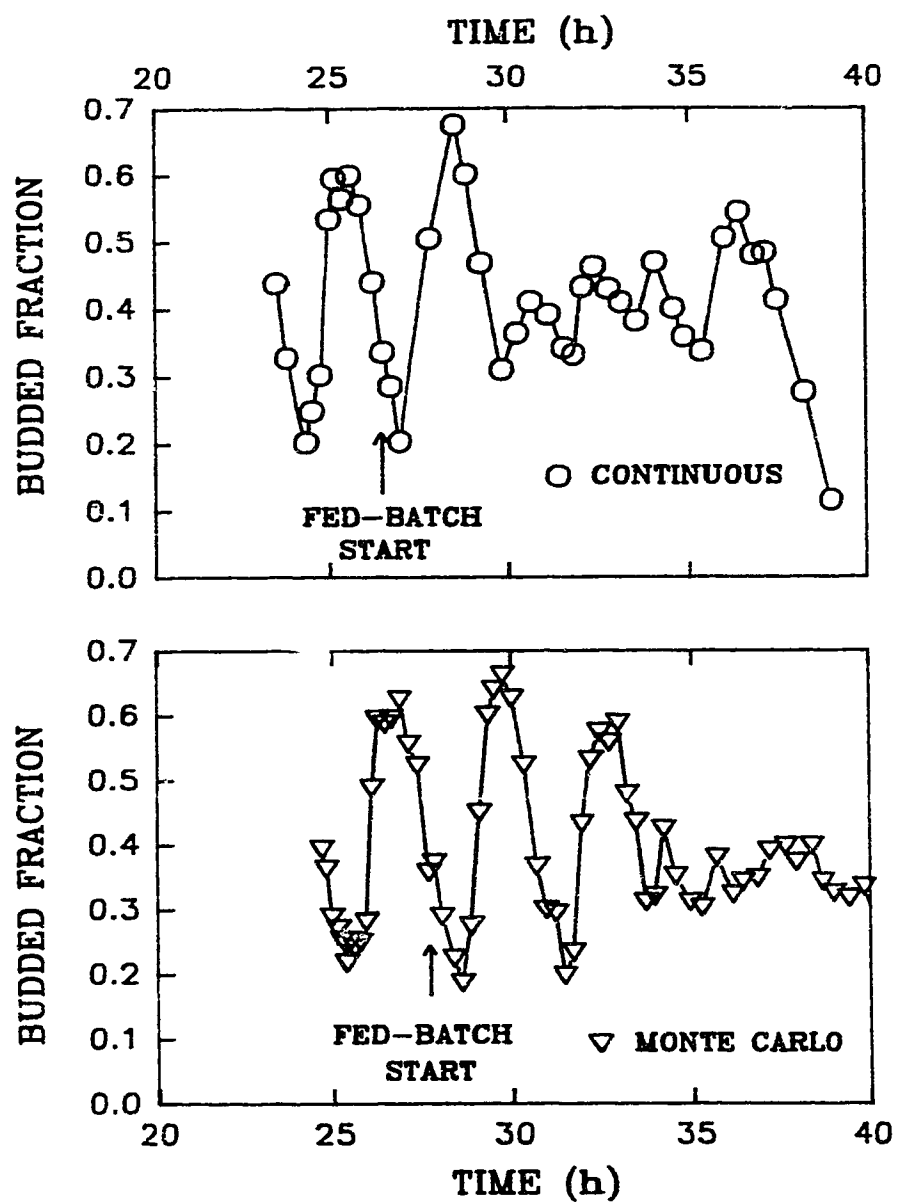


FIGURE 4.4 Comparison of profiles of budded fraction for the continuous fed-batch fermentation and the Monte Carlo fed-batch fermentation.

and a later decrease to extinction. The switch to fed-batch operation also affected the relative size and number of the peaks in a single CO₂-cycle. The second peak of CO₂ during the fed-batch fermentation increased relative to the first peak in the initial three CO₂-cycles, then disappeared in later cycles (Figure 4.3). A third peak appeared between the original two peaks during the third cycle of fed-batch operation. Strassle *et al.* (1989) observed that the form of oscillations switched from cycles with three peaks to two peaks before being spontaneously eliminated in a chemostat due to unknown reasons. Given that changes in dilution rate also changed the number of peaks during each CO₂-cycle (Figure 4.1), the shift from two to three peaks during fed-batch operation can also be attributed to effects on the G2 phase of the cell-cycle.

From Lim *et al.* (1977), the exponential fed-batch fermentation based on Equation (1) would be similar to a constant volume chemostat with dilution rate steadily varying from 0.008 h⁻¹ to 0.052 h⁻¹ in 14 h. A complete elimination of oscillations in chemostat cultures has been observed following step-up (0.2 h⁻¹ to 0.25 h⁻¹) and step-down (0.2 h⁻¹ to 0.05 h⁻¹) in dilution rates while the oscillations returned on the reverse step changes (Strassle *et al.*, 1989). Unlike the disturbance caused by step changes in dilution rate on the synchronised chemostat culture, the exponential fed-batch fermentation produced a smaller variation in 'equivalent' dilution rate. The transient condition introduced by the exponential fed-batch strategy, therefore, would be insufficient to disrupt the synchrony immediately.

Fluctuations in Glucose Supply

The effect of concentration gradients due to poor mixing was simulated by supplying the glucose feed intermittently according to a Monte Carlo method. During Monte Carlo experiments, feed was switched-on for 5 s and switched-off for an interval in the range of 3 s to 39 s. The Monte Carlo fed-batch experiment was

compared with continuously-fed fermentation according to an exponential feeding strategy. In addition to these two types of fed-batch fermentations, a periodic fed-batch fermentation was carried out where feed was added every 15 s for 5 s. The biomass profiles were similar during the first 12 h of feed supply for all three types of experiments. No ethanol was detected while glucose remained below 0.35 g/L for the same period. The biomass and ethanol profiles for these three experiments diverged after 10 h of fed-batch operation. About 10% lower biomass and ethanol accumulations up to 1.7 g/L were observed for periodic and exponential fed-batch experiments during the last 2.5 h of a 14.5 h experiment.

The profiles of CO₂ and dissolved oxygen for all three types of fed-batch experiments are shown in Figures 4.5 and 4.6 respectively. Continuous and Monte Carlo experiments were repeated in triplicate and reproducible results were obtained (Appendix D). The CO₂ and dissolved oxygen cycles were eliminated after the first 5 h of the Monte Carlo experiments, giving instead a chaotic response. Fast fourier-transform analysis showed no dominant frequency in the CO₂ fluctuations during Monte Carlo experiments, implying a chaotic respiratory response of the yeast culture. Minkevich and Neubert (1985) showed that off-gas composition was not affected by pH disturbances for pH below 6. The chaotic response of CO₂ was, therefore, not an artifact of pH fluctuations that could have been caused by Monte Carlo addition of feed to the fermentor. The periodic fed-batch experiments gave prolonged cycles of CO₂ and dissolved oxygen, similar to continuous fed-batch experiments, and in addition gave smaller induced oscillations of shorter period (Figure 4.5).

The first two CO₂-cycles during the Monte Carlo experiment were delayed compared to continuous fed-batch experiments due to a longer duration of the single-cell phase of the synchronised sub-population. Figure 4.4 compares the budded fraction from exponential fed-batch experiments with the Monte Carlo

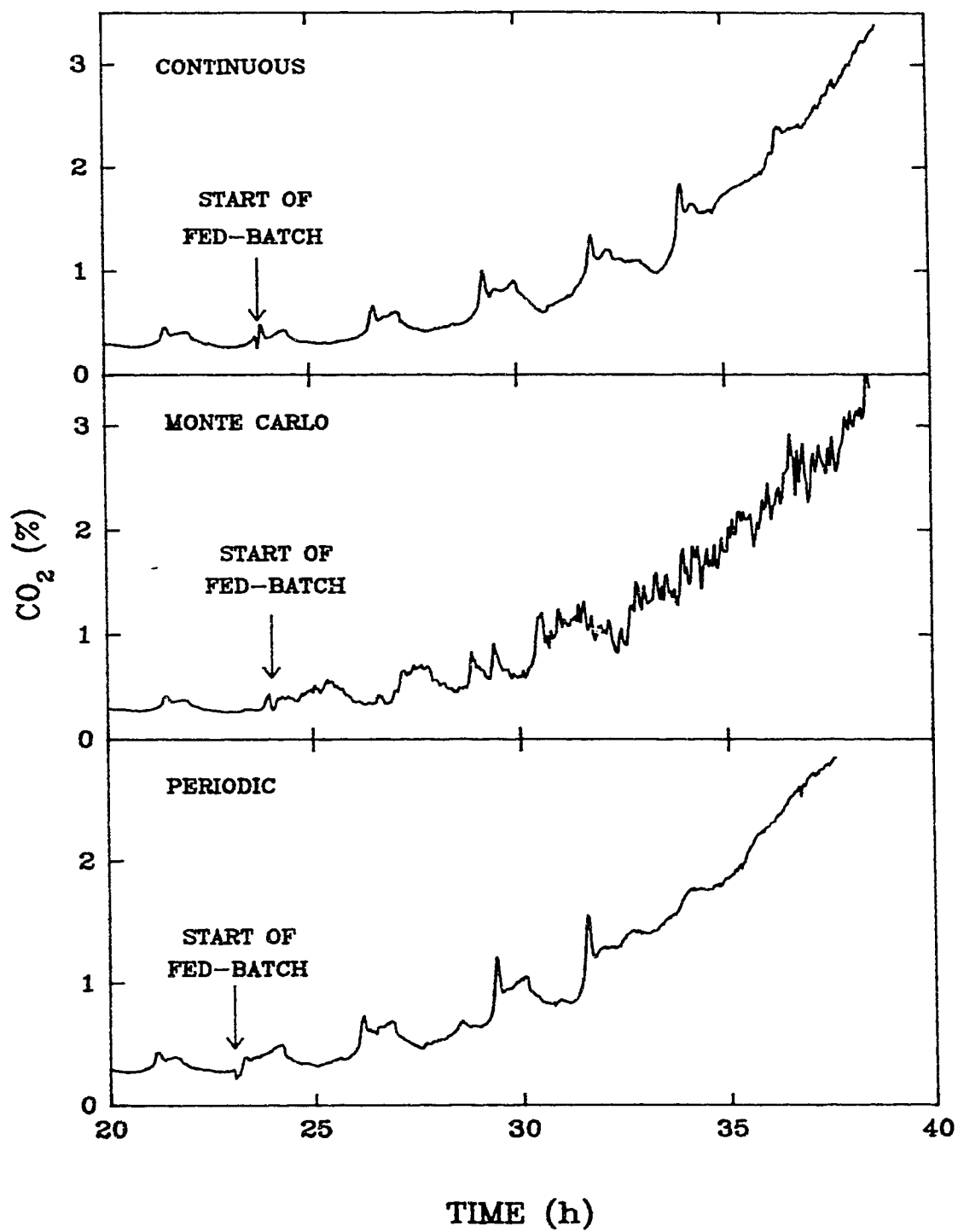


FIGURE 4.5 Comparison of profiles of CO₂ fraction in off-gas for the three types of fed-batch experiments: continuous, Monte Carlo, and periodic.

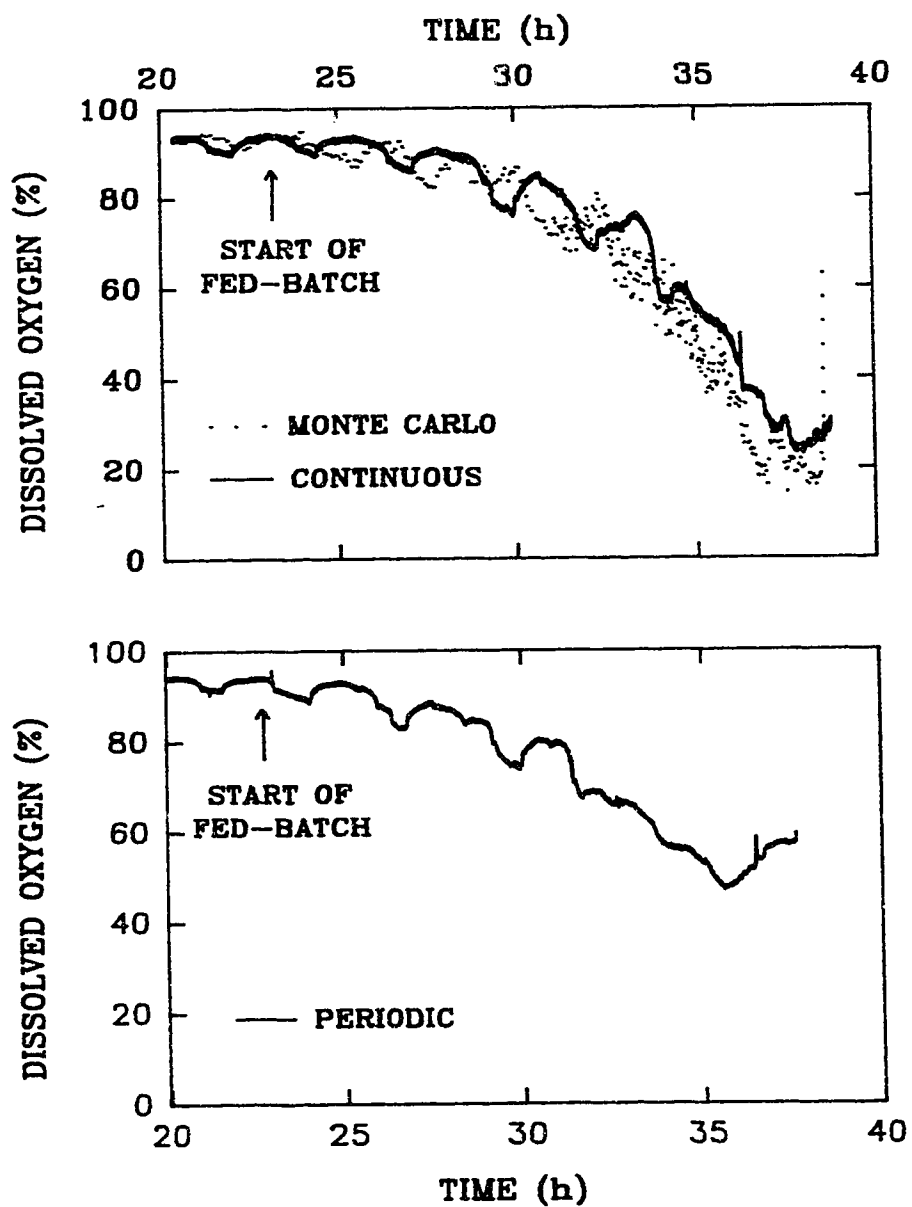


FIGURE 4.6 Comparison of profiles of dissolved oxygen for the three types of fed-batch experiments: continuous, Monte Carlo, and periodic.

experiments. The budded fraction of the second cycle during Monte Carlo experiments showed a delay of about 1 h to attain the maximum level. The second cycle showed a larger amplitude of the budded-fraction cycle compared to the second cycle in the continuous fed-batch experiments. Subsequently, the oscillations in the budded fraction were dampened, with the budded fraction remaining at 0.35. Chaotic fluctuations in CO₂, together with stable budded fraction during Monte Carlo experiment, proved that synchrony was destroyed after the first two cycles. A low budded fraction of 0.1 at the end of 12 h of feeding in continuous fed-batch experiments compared to 0.35 in the Monte Carlo experiments reflected a higher growth rate and a lower fermentative activity at the end of the Monte Carlo experiments.

Implications of Chaotic Response

The mechanism responsible for maintenance of synchrony was affected by short but variable intervals of feed interruption on the order of seconds during the fed-batch fermentation. Regular interruption of the feed supply during the periodic fed-batch experiment not only retained the first four CO₂-cycles, similar to that observed in the continuously-fed fermentation, but also introduced peaks in between two cycles (Figure 4.5). Chemostat studies have indicated the role of ethanol secretion and uptake in the regulation of synchrony (Porro *et al.*, 1988). Although no ethanol was observed for 12h during Monte Carlo experiment, this may have been due to the relatively longer sampling period of 1.5 h used. Alternatively, fast characteristic times of respiratory response indicate the possibility of control of synchrony at the glycolytic level by other factors. For example, the NADH response of yeast cells to glucose pulses has been shown to be in the order of few seconds (Einsele *et al.*, 1978). Mathematical models for spontaneous synchrony of yeast culture in chemostat have been proposed, based on the production and uptake of

ethanol and storage carbohydrates by yeast cells (Heinzle *et al.*, 1982; Strassle *et al.*, 1988). The transient conditions created by continuous, Monte Carlo and periodic fed–batch fermentations would provide a severe test to discriminate between models and to validate the mechanisms for synchrony. This discrimination of models is the objective of the Chapter 5.

Spontaneous synchrony is considered to be a hurdle in the control of steady state in chemostat operation, whereas it is shown to be useful in production of baker's yeast of higher fermentative activity in fed–batch fermentations. Large sparged and stirred fermentors of volume up to 150 m³ are regularly used to grow *S.cerevisiae*. Inherent poor mixing in production vessels creates gradients in both dissolved oxygen and glucose levels. These Monte Carlo experiments using intermittent supply of glucose feeds showed that synchrony cannot be maintained in large–scale fed–batch fermentation. Such mixing effects have even been observed in poorly mixed bench–scale chemostats (Strassle *et al.*, 1988). Alberghina *et al.* (1991) also observed that the partial synchrony of the yeast culture was eliminated by the fast control actions of feed supply used for maintaining ethanol at a low level in high cell density fermentation. The fluctuations in glucose concentration inherent in large–scale production conditions will, therefore, ensure a high degree of heterogeneity in yeast populations.

CONCLUSIONS

1. Monte Carlo fluctuations in glucose supply to the fed-batch culture of *S.cerevisiae* with off-times from 3 s to 39 s produced chaotic response of CO₂ levels in off-gas.
2. Cells with higher fermentative activity were obtained at the end of the exponential fed-batch fermentation than in the Monte Carlo fed-batch fermentation.
3. Synchronous cultures of *S.cerevisiae* in the large-scale fermentors cannot be established due to inherent concentration fluctuations in the fermentor.

REFERENCES

- Alberghina, L., Ranzi, B.M., Porro, D., Martegani, E. Flow cytometry and cell—cycle kinetics in continuous and fed—batch fermentations of budding yeast. *Biotechnol. Progr.* **1991**, *7*, 299—304.
- Anderson, C., LeGrys, G.A., Solomons, G.L., Concepts in the design of large—scale fermenters for viscous culture broths. *The Chem. Engr.* **1982**, February, 43—49.
- Barford, J.P., Hall, R.J. Estimation of cell cycle phases from synchronous cultures of *Saccharomyces cerevisiae*. *Exp. Cell Res.* **1976**, *102*, 276—284.
- Einsele, A., Ristroph, D.L., Humphrey, A.E., Mixing times and glucose uptake measured with a flurometer. *Biotechnol. Bioeng.* **1978**, *20*, 1487—1492.
- Harrison, D.E.F., Topiwala, H.H., Transients and oscillatory states of continuous culture. *Adv. Biochem. Eng.* **1974**, *3*, 167—220.
- Heinzle, E., Dunn, I.J., Furukawa, K., Tanner, R.D. Modelling of sustained oscillations observed in continuous culture of *Saccharomyces cerevisiae*. *Proc. First IFAC Workshop on Modelling and Control of Biotechnological Processes*, **1982**, 57—65.
- Kuenzi, M.T., Fiechter, A. Changes in carbohydrate composition and trehalase activity during the budding cycle of *Saccharomyces cerevisiae*. *Arch. Mikrobiol.* **1969**, *64*, 396—407.
- Lim, H.C., Chen, B.J., Creagan, C.C., An analysis of extended and exponentially fed—batch cultures., *Biotechnol. Bioeng.* **1977**, *19*, 425—433.
- Martegani, E., Porro, D., Ranzi, B.M., Alberghina, L. Involvement of a cell size control of mechanism in the induction and maintenance of oscillations in continuous cultures of budding yeast. *Biotechnol. Bioeng.* **1990**, *36*, 453—459.
- Meyer, C., Beyeler, W. Control strategies for continuous bioprocesses based on

- biological activities. *Biotechnol. Bioeng.* 1984, 26, 916–925.
- Munch, T., Sonnleitner, B., Fiechter, A. In *Biochemical Engineering*; Reuss, M., Chmiel, H., Gilles, E., Knackmuss, H., Ed.; Gustav Fischer: Stuttgart 1991; pp 373–376.
- Myenburger, von H.K. In *Biological and Biochemical Oscillators*; Chance, B., Pye, E.K., Ghosh, T.K., Hess, B., Ed.; Academic Press: New York, 1973, pp 411–417.
- Parulekar, S.J., Semones, G.B., Rolf, M.J., Lievens, J.C., Lim, H.C. Induction and elimination of oscillations in continuous cultures of *Saccharomyces cerevisiae*. *Biotechnol. Bioeng.* 1986, 28, 700–710.
- Porro, D., Martegani, E., Ranzi, B.M., Alberghina, L. Oscillations in continuous cultures of budding yeast: A segregated parameter analysis. *Biotechnol. Bioeng.* 1988, 32, 411–417.
- Pringle, J.R., Mor, J. In *Methods in Cell Biology Vol. XI: Yeast Cells*; Prescott, D.M., Ed.; Academic Press: New York, 1975; pp 131–168.
- Reed, G. In *Prescott & Dunn's Industrial Microbiology*; Reed, G., Ed.; AVI Publishing Company, Inc.: Westport, Connecticut, 1982, pp 593–633.
- Scheper, Th., Schugerl, K. Culture fluorescence studies on aerobic continuous cultures of *Saccharomyces cerevisiae*. *Appl. Microbiol. Biotechnol.* 1986, 23, 440–444.
- Strassle, C., Sonnleitner, B., Fiechter, A. A predictive model for the spontaneous synchronisation of *Saccharomyces cerevisiae* grown in continuous culture. I. Concept. *J. Biotechnol.* 1988, 7, 299–318.
- Strassle, C., Sonnleitner, B., Fiechter, A. A predictive model for the spontaneous synchronisation of *Saccharomyces cerevisiae* grown in continuous culture. II. Experimental verification. *J. Biotechnol.* 1989, 9, 191–208.
- Takamatsu, T., Shioya, S., Chikatani, H. Comparison of simple population models

- in a baker's yeast fed-batch culture. *Chem. Eng. Sci.* **1985**, *40*(3), 499–507.
- Wiemken, A. Matile, P., Moor, H. Vacuolar dynamics in synchronously budding yeast. *Arch. Mikrobiol.* **1970**, *70*, 89–103.
- Yamane, T., Shimizu, S. Fed-batch techniques in microbial processes. *Adv. Biochem. Eng.* **1984**, *30*, 148–194.

CHAPTER 5

MODELLING THE SYNCHRONY OF SACCHAROMYCES CEREVISIAE IN CHEMOSTAT AND FED-BATCH FERMENTATIONS

INTRODUCTION

Saccharomyces cerevisiae or budding yeast is an important eukaryotic microorganism for cell-cycle studies as well as for industrial fermentation processes. Chemostat cultures of *S.cerevisiae* showed a tendency to synchronise when grown in a well mixed and perfectly-controlled laboratory fermentor (Kuenzi and Fiechter, 1969; Parulekar, 1986; Porro *et al.*, 1988; Strassle *et al.*, 1988). The synchrony was reflected by oscillations in many variables, including the budded fraction of the population, biomass, flow cytometry measurements of NADH and cell-size, and CO₂ fraction of off-gas. Various types of mathematical models have been proposed to simulate these autonomous oscillations (MacDonald, 1976; Heinzle *et al.*, 1982; Ivanitskay *et al.*, 1989; Strassle *et al.*, 1988; Cazzador *et al.*, 1990). These models have helped to test the mechanisms responsible for triggering the spontaneous synchronisation by relating the parameters regulating the cell-cycle events to the growth parameters. The models have been also used to suggest the control strategies required to either promote or eliminate synchrony (Meyer and Beyeler, 1984; Takamatsu *et al.*, 1985).

In earlier modelling attempts, the unstructured and non-segregated type models were obtained from various modifications of the simple Monod model, including a delay in the response of growth to the nutrient conditions (MacDonald,

1976), product inhibition (Suzuki *et al.*, 1985), maintenance effects, and variable biomass yields (Ivanitskay *et al.*, 1989). Although these simple models produced limit cycles, no mechanistic models for the spontaneous synchrony were used. Two types of conceptual models have been proposed in the literature to explain the spontaneous synchrony of chemostat culture of *S.cerevisiae*. Kuenzi and Fiechter (1969) suggested that the alteration of the nutrient environment, due to different metabolism in the single-cell and the budding-cell phases of the cell-cycle, led to the establishment of a partial synchrony. In another attempt, the spontaneous synchronisation was attributed to the modulation of threshold size of cells at the time of bud-initiation and bud-separation by the availability of ethanol as a secondary carbon source during the glucose-limited chemostat operation (Martegani *et al.*, 1990).

Heinzle *et al.* (1982) used a non-segregated, structured type model based on a metabolic network involving formation of storage carbohydrates and subsequent conversion into ethanol by an enzyme. Stable harmonic oscillations in biomass, glucose, storage carbohydrates, and enzyme levels were predicted for dilution rates up to 0.125 h^{-1} . Strassle *et al.* (1988, 1989) developed a structured, segregated model with an elaborate metabolic network of reactions. The population was divided into three phases of cells, budded-cell, single mother cell and single daughter cell and each phase was further divided into a number of classes based on the age of the cell. The rates of carbon fluxes of glucose, storage carbohydrates and ethanol for a cell depended on the phase of its cell-cycle. Relaxation-type oscillatory behaviour of many variables, including biomass, storage compounds, ethanol, glucose, CO_2 in off-gas and pH was predicted. A structured, segregated type model was also proposed by Cazzador *et al.* (1990) based on the role of a limiting substrate in modulation of the critical cell size for bud-separation and different biomass yield coefficient for single-cell and budding-cell phases. The model predicted

harmonic-type oscillations in the budded fraction of daughter and mother cells, the total biomass and the limiting substrate concentration. A much simpler unstructured, segregated model by Cazzador (1991) resulted in an analytical equation describing the relaxation-type oscillations in the masses of single-cells and budded-cells. This model segregated the population into the single-cell type and budded-cell type with the control of switching rates between two population by the limiting substrate levels.

On-line measurement of the off-gas compositions, NADH, and dissolved oxygen show fast response to any changes in the state of the fermentation culture. In chemostat culture of *S.cerevisiae*, oscillations in CO₂ fraction of off-gas and NADH were usually observed to be of a mixed-mode type with multiple peaks in each cycle (Strassle *et al.*, 1989; Chapter 4). These non-harmonic type oscillations represent a higher order of instability than the harmonic and relaxation-type oscillations predicted by the previous models (Lyberatos *et al.*, 1985). The profiles of the sensitive indicators, such as CO₂ fraction, were not simulated by any of the above models except by Strassle *et al.* (1988). The structured and segregated model of Strassle *et al.* (1989) predicted amplitudes and frequency of CO₂ oscillations in close agreement with the experiments. The model, however, predicted relaxation type oscillations rather than the experimentally observed non-harmonic oscillations with multiple peaks. Incidentally, this model contained six differential equations for balance of six state variables over all the 97 classes and three differential equations for each class.

Previous studies on the modelling of synchrony have shown that the relationship between the cell-cycle events and the nutrient environment should be considered to model the spontaneous generation of stable oscillations. Similar success, although limited, from the predictions of oscillatory behaviour by a wide range of models necessitates the need for discrimination between the models. Hjortso

and Bailey (1983) used the response of a population balance model to the step-changes in growth rates for a budding yeast population as a test for the validity of the cell-cycle model. Strassle *et al.* (1989) imposed a step change in the dilution rate to evaluate their model. These types of 'transient response' methods were shown to be insufficient in providing a stringent test to discriminate between the kinetic models (Lyberatos *et al.*, 1984).

The response of a culture to the transient conditions in a fed-batch fermentation provides a sensitive and severe test, to discriminate between the models for spontaneous synchrony. Results in Chapter 4 showed the CO₂ oscillations of a synchronously dividing culture in a chemostat continued for five cycles after switching to an exponentially fed-batch operation, then they disappeared. The perturbation in the feed supply according to a Monte Carlo method (Chapter 2) during the fed-batch fermentation promptly disrupted the CO₂ cycles and apparently produced chaotic response. These experimental observations on fed-batch fermentations are useful for testing the current conceptual models on the self-synchronisation property of *S.cerevisiae*.

The objective of this chapter was to evaluate models based on the role of ethanol and storage carbohydrates in the induction and maintenance of synchrony of *S.cerevisiae* during glucose-limited chemostat and fed-batch cultures. The model was used to predict the fate of synchrony under continuously-fed and intermittently-fed fed-batch fermentations.

THE MODEL

Model Concept

A cell of *S.cerevisiae* has two distinct phases during its life-cycle: the single-cell phase and the budding-cell phase. These two phases were characterised to be metabolically distinct based on their mode of uptake and formation of ethanol and storage carbohydrates (Kuenzi and Fiechter, 1969). A model for simulating the spontaneous synchrony in chemostat culture must consider these two distinct phases of the cell-cycle. The complex segregated and structured model of Strassle *et al.* (1990) predicted relaxation-type oscillations similar in the form to that predicted by the simpler non-structured model of Cazzador (1991) with only two sub-populations. Furthermore, three or four non-linear differential equations were shown to be sufficient to predict a higher order of instability for a non-linear kinetic model (Lyberatos *et al.* 1984). The division of the population into two sub-populations with an adequate representation of metabolism for each sub-population, therefore, would be sufficient to model the synchrony.

The two phases of the cell-cycle with the metabolic interaction between them are shown in Figure 5.1. The representation in Figure 5.1 was used to develop the model for synchrony in the present study. The metabolic reaction scheme for each of the two phases followed Strassle *et al.* (1988). The duration of the budding-cell phase was found to be close to 1 h and independent of the nutrient environment (Barford and Hall, 1976). The budded-cells consumed internal glucose or 'storage carbohydrates' to supplement their glucose uptake from the medium, and in the process excreted ethanol. The storage carbohydrates were produced and stored by the single-cells from growth on glucose and ethanol. Synchrony is believed to spontaneously arise due to a positive feedback on the growth of single-cells in the presence of ethanol (Martegani *et al.*, 1990).

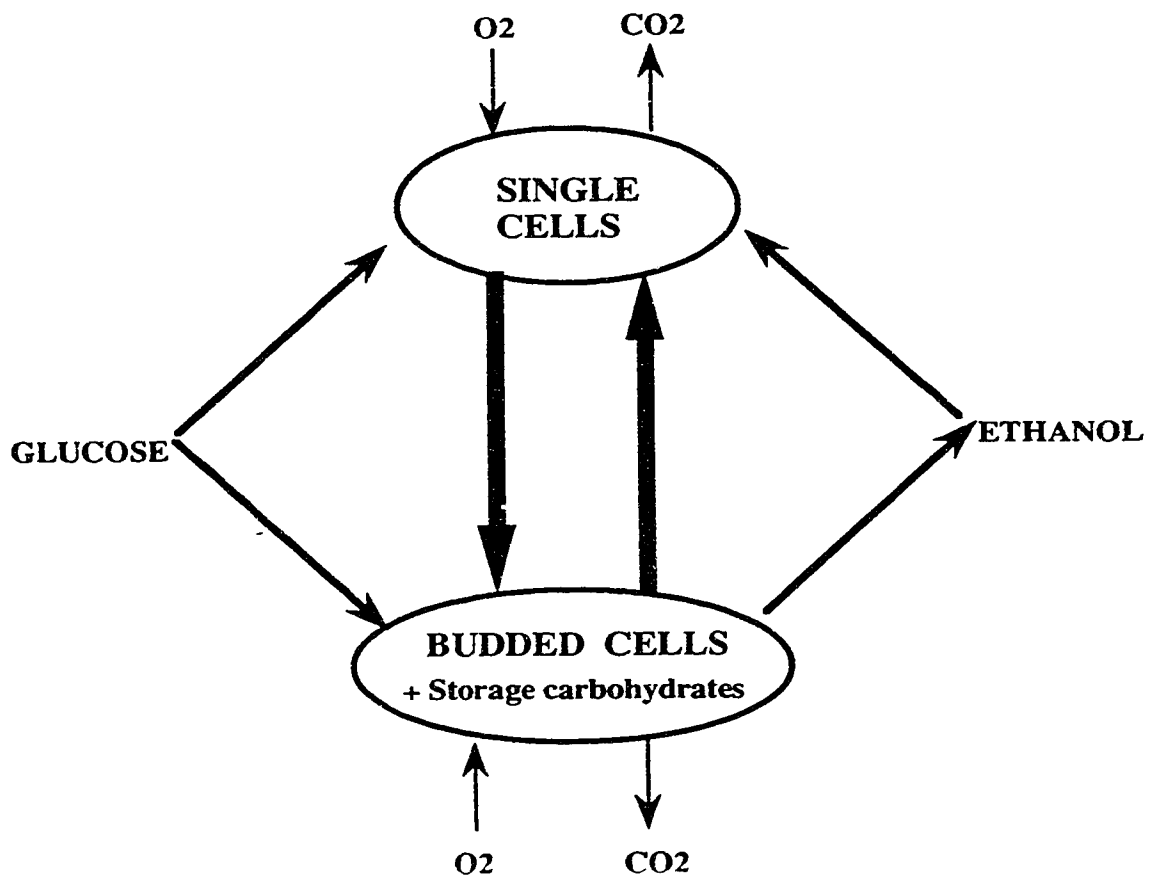


FIGURE 5.1: A cell-cycle model showing the interaction between the cell-cycle events and the nutrient environment.

The segregation of the two phases of cells was modelled in the present study by differentiating between biomass without storage carbohydrates or 'residual biomass', and the storage carbohydrates. The conversion between the single-cell and budding-cell phases was modelled by considering a time delay in the uptake of storage carbohydrates. The resulting structured model is shown in Figure 5.2. According to this model, the rate of uptake of storage carbohydrates depends on the past values of the concentration of storage carbohydrates. Various types of memory functions have been used to weight the past values and thus introducing a delay in chemostat models (MacDonald, 1976; Abulesz and Lyberatos, 1989). A simplest delay, 'pure delay' was selected in the present study whereby the uptake rate of storage carbohydrates at any given time was a function of one concentration of storage carbohydrates in the past. The duration of delay was selected to be equal to the interval of budding-cell phase. This selection of the delay is equivalent to making an assumption that the budded-cells would consume their storage carbohydrates content, which was received from single-cells, at the end of the budding-cell phase.

Metabolic Rates

The kinetic equations for the metabolic reactions (Figure 5.2) followed Strassle *et al.* (1988), and are listed below.

1. Uptake of carbon sources

The specific rate of uptake of glucose, Q_g , depends on the level of glucose in the fermentor, G , as follows,

$$Q_g = Q_{g\text{gm}} \frac{G}{(K_g + G)} \quad (1)$$

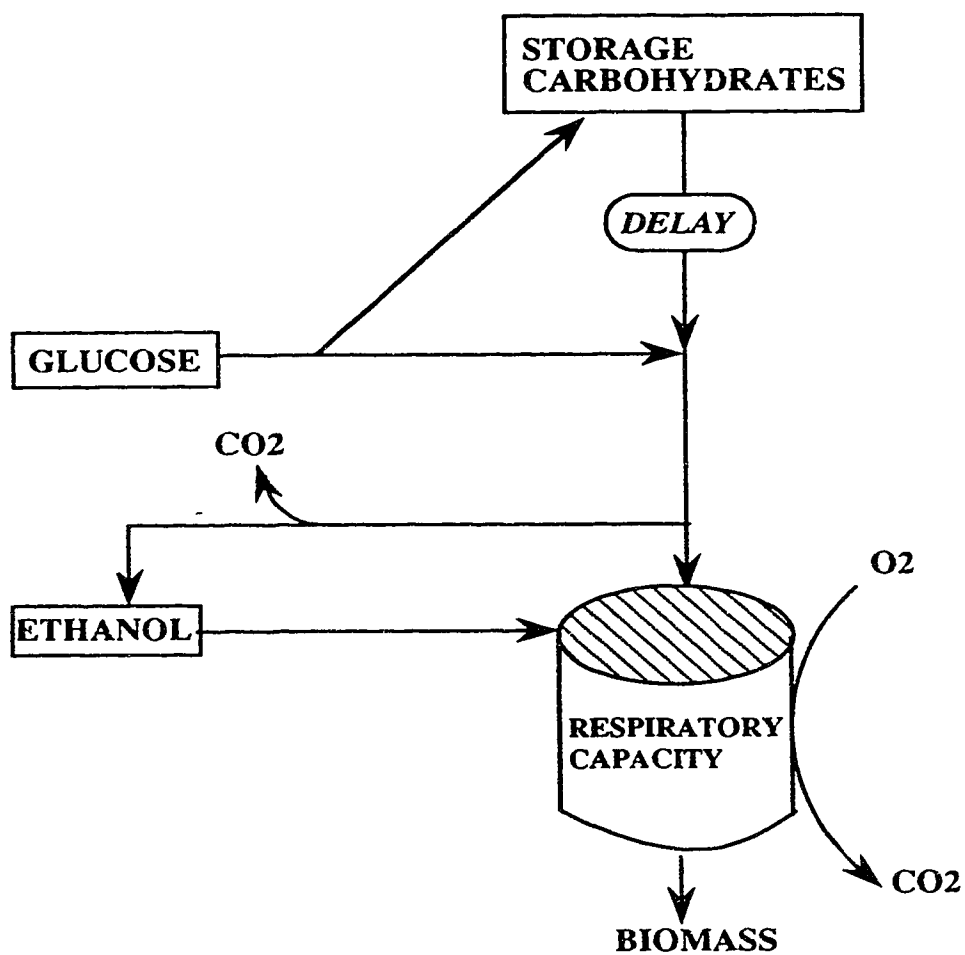


FIGURE 5.2: The metabolic network scheme used to model the synchrony in the chemostat culture of *S.cerevisiae*.

A part of glucose flux, Q_{t1} , was diverted into formation of storage carbohydrates according to the following equation.

$$Q_{t1} = 0.5e^{(K_t \ln h Q_g)} \left[Q_{gtm}/Q_{qo} - Q_g - \sqrt{(Q_{gtm}/Q_{qo} - Q_g)^2 + 4 Q_{gtm} Q_g} \right] \quad (2)$$

According to Equation (2), a higher proportion of the glucose flux was diverted into the formation of storage carbohydrates when the glucose uptake rate was low. This assumption is consistent with growth of yeast cells under poor medium conditions. The degradation of storage carbohydrates contributes to the glucose flux entering the glycolytic pathway (Figure 5.2). The specific rate of conversion of storage carbohydrates depends on a past value of storage carbohydrates content, $T_r(t-\tau)$. The wash out of budded-cells in the chemostat further reduces the storage carbohydrates available to the cells. The expression for the consumption of storage carbohydrates from Strassle *et al.* (1988) was, therefore, modified to give:

$$Q_{t2} = Q_{ggm} \frac{T_r(t-\tau) e^{-(\tau D)} / X}{(K_t + T_r(t-\tau) e^{-(\tau D)}) / X} \quad (3)$$

where X is the residual biomass. The total flux of 'glucose equivalent' entering the glycolytic pathway, Q_{gg} , is given below:

$$Q_{gg} = Q_g + Q_{t1} + Q_{t2} \quad (4)$$

2. Bottleneck Hypothesis

The oxygen concentration in the liquid phase, O_{2L} , controls the respiratory capacity for the oxidative conversion of carbon sources. The maximum flux of the carbon

sources utilised in an oxidative mode, Q_{gcrit} , is given by

$$Q_{\text{gcrit}} = \frac{Q_{\text{o2m}}}{Y_{\text{og}}} \frac{O_2 L}{(K_{O_2} + O_2 L)} \quad (5)$$

The excess of carbon flux through the glycolytic pathway, over and above the respiratory capacity, would be converted to ethanol in a reductive mode at a rate, Q_e , given below,

$$Q_e = - \left\{ \frac{Y_{\text{og}}}{Y_{\text{oe}}} \right\} Q_{\text{gr}} \quad (6)$$

when $Q_{\text{gr}} < 0.0$

The excess of carbon flux, Q_{gr} , is given by

$$Q_{\text{gr}} = Q_{\text{gg}} - Q_{\text{go}} \quad (7)$$

$$Q_{\text{go}} = \max (Q_{\text{gcrit}}, Q_{\text{gg}}) \quad (8)$$

The ethanol would be consumed, however, when the carbon flux through the glycolytic pathway, Q_{gg} , cannot saturate the respiratory capacity. The rate of ethanol uptake is a function of ethanol concentration, E , as follows:

$$Q_e = \frac{Y_{\text{og}}}{Y_{\text{oe}}} (Q_{\text{gcrit}} - Q_{\text{go}}) \frac{E}{(K_e + E)} \quad (9)$$

when $Q_{\text{gr}} = 0.0$

3. Growth

The growth occurs due to the oxidative conversion of all carbon sources and due to the reductive conversion of glucose to ethanol. The specific growth rate of biomass, μ , is given by:

$$\mu = -(Q_{go}Y_{xgo}) + \max(Q_eY_{xgr}, 0.0) - \min(Q_eY_{xe}, 0.0) \quad (10)$$

4. Respiration

Oxygen is used for the oxidative conversion of carbon sources at a rate, OUR, as follows,

$$OUR = X \left[Y_{og} Q_{go} + Y_{oe} \left\{ \min(0.0, Q_e) \right\} \right] \quad (11)$$

Carbon dioxide is produced under the oxidative and reductive mode of uptake of carbon sources according to the following equation:

$$CPR = X \left[Y_{cgo} Q_{go} + \max(Y_{ce1} Q_e, Y_{ce2} Q_e) \right] \quad (12)$$

Fermentor Dynamics

Consider a well-mixed fermentor of liquid volume, V , fed with the fresh feed at a volumetric flow rate, F_{in} , and the inlet concentration of a limiting substrate, such as glucose, G_{in} . The fermentor contents are removed at a volumetric flow rate, F_{out} . Air, of molar density ρ , is fed to the fermentor at a volumetric flow rate, F_{air} . The gas and liquid phases in the fermentor are assumed to be well-mixed. The mass balance equations for the residual biomass, X , glucose, G , ethanol, E , and storage

carbohydrates, T_r across the fermentor are given as follows.

$$\frac{d(VX)}{dt} = F_{in} X_{in} - F_{out} X + \mu (VX) \quad (13)$$

$$\frac{d(VG)}{dt} = F_{in} G_{in} - F_{out} G + Q_g (VX) \quad (14)$$

$$\frac{d(VE)}{dt} = F_{in} E_{in} - F_{out} E + Q_e (VX) \quad (15)$$

$$\frac{d(VT_r)}{dt} = F_{in} T_{rin} - F_{out} T_r + (Q_{t1} + Q_{t2}) (VX) \quad (16)$$

Assuming no variation in the density of the fermentor contents during the fermentation, the overall mass balance around the fermentor gives

$$\frac{dV}{dt} = F_{in} - F_{out} \quad (17)$$

The dynamics of oxygen and carbon dioxide in the gas-phase and the liquid-phase are neglected as they are fast compared to the dynamics of growth and metabolism (Yegneswaran *et al.*, 1990). From the mass balance for oxygen and carbon dioxide in the gas-phase, the gas phase compositions are obtained from the following algebraic equations.

$$O_{2g} = (F_{air} O_{2gin} + OUR/\rho)/F_{air} \quad (18)$$

$$CO_{2g} = (F_{air} CO_{2gin} + CPR/\rho)/F_{air} \quad (19)$$

Under pseudo—steady state conditions, the mass transfer of oxygen from the gas—phase to the liquid—phase equals the oxygen uptake rate due to growth. The concentration of oxygen in the liquid phase is given as follows:

$$O_2L = H_{O_2} * O_{2g} + OUR/k_L a \quad (20)$$

where H_{O_2} is the solubility factor for oxygen and $k_L a$ is the mass transfer coefficient. The relative level of oxygen in the liquid phase with respect to the saturation level, or dissolved oxygen (DO), is calculated as follows.

$$DO = 100 O_2L / (H_{O_2} O_{2gin}) \quad (21)$$

Initial Conditions

Three modes of operation of the fermentor were considered: chemostat operation, fed—batch operation with continuous feed supply, and fed—batch operation with intermittent feed supply. The fresh feed for all modes of operation satisfied the following conditions,

$$X_{in} = 0.0, E_{in} = 0.0, T_{rin} = 0.0 \quad (22)$$

1. Chemostat operation

The following conditions apply for the chemostat mode of operation of the fermentor:

$$F_{in} = F_{out} = F = \text{constant} \quad (23)$$

The dilution rate, D , was defined as follows,

$$D = F/V \quad (24)$$

2. Fed-batch operation

In continuous fed-batch fermentation, the feed was supplied at an exponentially increasing rate to the fermentor according to the following equation,

$$F_{in} = F_{in0} e^{\mu t} \quad (25)$$

No product was removed during the fed-batch fermentation, so that

$$F_{out} = 0.0 \quad (26)$$

For the fed-batch fermentation with intermittent supply of feed, the feed rate during the pulse-on, t_p , was given by

$$F_{mc} = \frac{\bar{t}_c}{t_p} F_{in} \quad (27)$$

where F_{in} was calculated from Equation (25). The pulse-off intervals, t_{off} , were obtained from a log-normal distribution of circulation times with a mean, \bar{t}_c , and a standard deviation, σ using a Monte Carlo method (Chapter 2). A periodic feeding to the fermentor was also considered where the pulse-off period was constant at $(\bar{t}_c - t_p)$.

RESULTS

Chemostat fermentation

The equations for the chemostat, and fed-batch fermentations were integrated using the IMSL subroutine GEAR in FORTRAN-77 on a VAX 8600. The operating conditions for the simulations of fermentors, listed in Table 5.1, followed the experimental conditions in Chapter 4. The past values of 'storage carbohydrates' were stored in a vector to account for the delay present in the differential equation (16). The integration was started by assuming a steady state to be the initial condition. The values of parameters of the model are also listed in Table 5.2. All the parameters followed Strassle *et al.* (1989) except for the parameter K_t and a new parameter, the time delay, $\tau = 1$ h. K_t affects the rate of consumption of storage carbohydrates as given by Equation (3). The value for K_t was adjusted from an initial estimate of 0.2 (Strassle *et al.*, 1989) so that stable oscillations were obtained in a chemostat at a dilution rate of 0.2 h^{-1} and glucose concentration of 5 g/L in the feed. Figure 5.3 shows the harmonic-type oscillations in the CO_2 fraction of off-gas, dissolved oxygen, total biomass, glucose and storage carbohydrates in the chemostat for $K_t=1.425$. Higher values of K_t caused damped oscillations, whereas lower values amplified the oscillations. Parameter values of $K_t = 1.425$ and $\tau = 1$ h were used, therefore, for simulation of chemostat and fed-batch fermentations.

The periods, amplitudes and forms of calculated oscillations from the model were compared with the experiments of Chapter 4. The period of the oscillations in all variables (Figure 5.3) was 3.56 h compared to 2.7 h obtained experimentally for a chemostat at a dilution rate of 0.2 h^{-1} . The CO_2 fraction of off-gas varied from 0.32% to 0.38% compared to 0.27% to 0.42% in experiments. The biomass level varied from 2.52 g/L to 2.6 g/L compared to no detectable variation of biomass at 2.25 g/L. The measurement error associated with the biomass is ± 0.1 g/L which is

TABLE 5.1: Operating conditions used in the simulations following the experiments described in Chapter 4

1. Chemostat		
D	0.2	h^{-1}
F	0.2	L/h
G_{in}	5.0	g/L
V	1.0	L
2. Fed-batch fermentations		
F_{inc}	0.008	L/h
G_{in}	100.0	g/L
\bar{t}_c	20	s
t_p	5	s
μ	0.16	h^{-1}

TABLE 5.2: Model parameters used in the simulations following
Strassle *et al.* (1988).

$\text{CO}_{2\text{gin}}$	0.00033	—
H_{O_2}	1.0416	mmol/L
K_e	0.01	g/L
K_g	0.5	g/L
K_{La}	1000.0	1/h
K_{O_2}	0.001	mmol/L
K_{tinh}	1.0	h g/g
$\text{O}_{2\text{gin}}$	0.20946	—
Q_{ggm}	−3.5	g/(g−h)
Q_{gtm}	0.40	g/(g−h)
$Q_{\text{O}_2\text{m}}$	−7.9	mmol/(g−h)
Q_{qo}	0.98	—
Y_{ce1}	−14.7	mmol/g
Y_{ce2}	21.9	mmol/g
Y_{cgo}	−13.7	mmol/g
Y_{oe}	35.0	mmol/g
Y_{og}	12.8	mmol/g
Y_{xe}	0.72	g/g
Y_{xgo}	0.49	g/g
Y_{xgr}	0.05	g/g
ρ	41.67	mmol/L

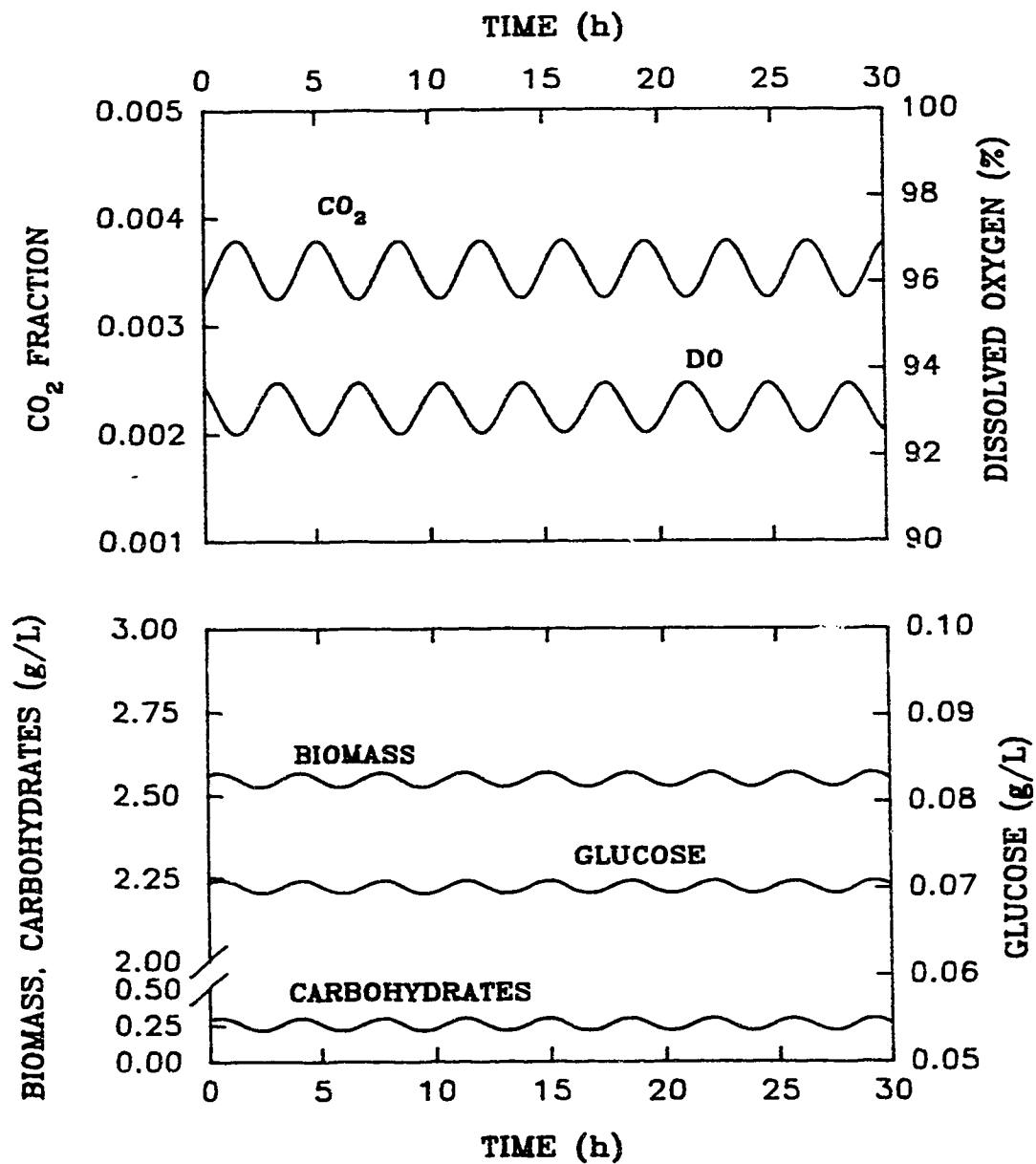


FIGURE 5.3: Prediction of the stable oscillations in chemostat culture of *S. cerevisiae* at a dilution rate of 0.2 h^{-1} and $G_{\text{in}} = 5 \text{ g/L}$.

close to the amplitudes of oscillations in biomass from the model. The glucose concentration also showed a small variation from 0.068 g/L to 0.071 g/L from model, whereas it remained close to 0.05 g/L in experiments. The dissolved oxygen levels oscillated between 95.6% and 97% compared to the experimental observations of 93% to 97%. The ethanol concentrations remained at zero even though all other variables oscillated. Ethanol concentration of 0.015 g/L close to the detectable limit of 0.007 g/L were detected in the experiments for short intervals. The form of oscillations in CO₂ showed harmonic oscillations indicating a lower order of instability compared to the non-harmonic oscillations with multiple peaks observed in experiments.

Simulations with two extremes of segregation of the population were also carried out. A case of zero time delay implied a homogeneous population, whereas considering segregation of single-cell and budding-cell phases (Figure 5.1) and their respective metabolism of storage carbohydrate implied complete segregation of population into two states. Integration of both models over a range of K_t failed to give stable oscillations. These simulations with alternative models suggest that the delay is instrumental in causing stable oscillations, consistent with Lyberatos (1985). Parulekar *et al.* (1986) suggested that high dissolved oxygen levels can eliminate synchrony by increasing the respiratory capacity of the cells. Chemostat operation with the control of dissolved oxygen at 100 % was simulated using the present model. No difference in the oscillatory behaviour was predicted for the fermentation with DO control compared to the fermentation without DO control. Simulations were also carried out at lower dilution rates of 0.15 h⁻¹ and 0.2 h⁻¹. Stable oscillations were predicted when the value of K_t was changed to 1.56 for a dilution rate 0.15 h⁻¹ and 1.65 h for a dilution rate of 0.1 h⁻¹. Tuning of one parameter, K_t , with the dilution rate to obtain oscillations indicate the limitation of

use of a constant delay and effect of explicit use of dilution rate in the degradation kinetics of storage carbohydrates (Equation 3).

Fed–batch fermentations

Simulations of fed–batch fermentations were started from a chemostat culture where stable oscillations were established at a dilution rate of 0.2 h^{-1} . The feeding strategy for the continuous fed–batch fermentations followed an exponentially increasing rate profile according to Equation (25) with the operating conditions given in Table 5.1. The duration of pulse–on during fed–batch fermentations with intermittent feed supply was 5s. The duration of pulse–off varied from 3 s to 39 s according to a Monte Carlo method for the Monte Carlo fed–batch fermentation and was constant at 15 s for the periodic fed–batch fermentation (Chapter 2). These conditions for the feeding strategy were the same as that used in the experimental study of Chapter 4. Simulations for fed–batch fermentations were performed by integrating the five differential equations (Equations (13) to (17)) and using the remaining algebraic relationships. The differential equations were solved every 30 s for the continuous fed–batch fermentation and every 1 s for fermentations with intermittent feeding.

Figure 5.4 shows the profiles of biomass, storage carbohydrates, CO_2 fraction in the off–gas, and dissolved oxygen. The oscillations in the CO_2 fraction and dissolved oxygen continued during fed–batch fermentation with increasing amplitudes. This prediction was contrary to the experimental observations where the amplitudes of CO_2 cycles initially increased then disappeared completely. The storage carbohydrates also showed oscillations during the fed–batch fermentation. No significant oscillations appeared in the biomass corresponding to the oscillations in the storage carbohydrates consistent with the internal conversion of storage carbohydrates (Kuenzi and Fiechter, 1969) and experiments (Chapter 4).

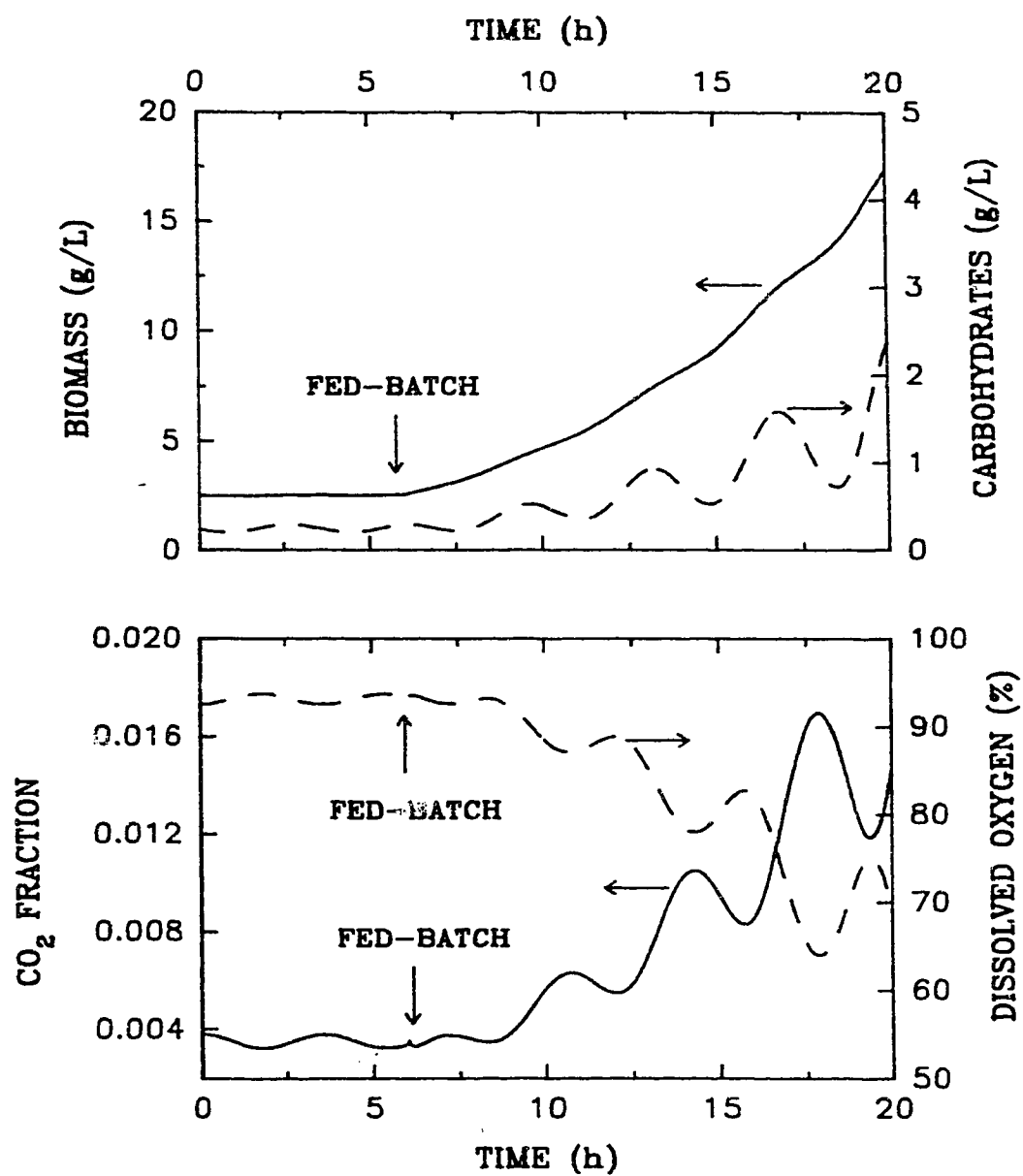


FIGURE 5.4: Prediction for the continuous fed-batch fermentation at an exponentially increasing rate, $F_{in} = 8 \exp(0.16t)$ with $G_{in} = 100 \text{ g/L}$.

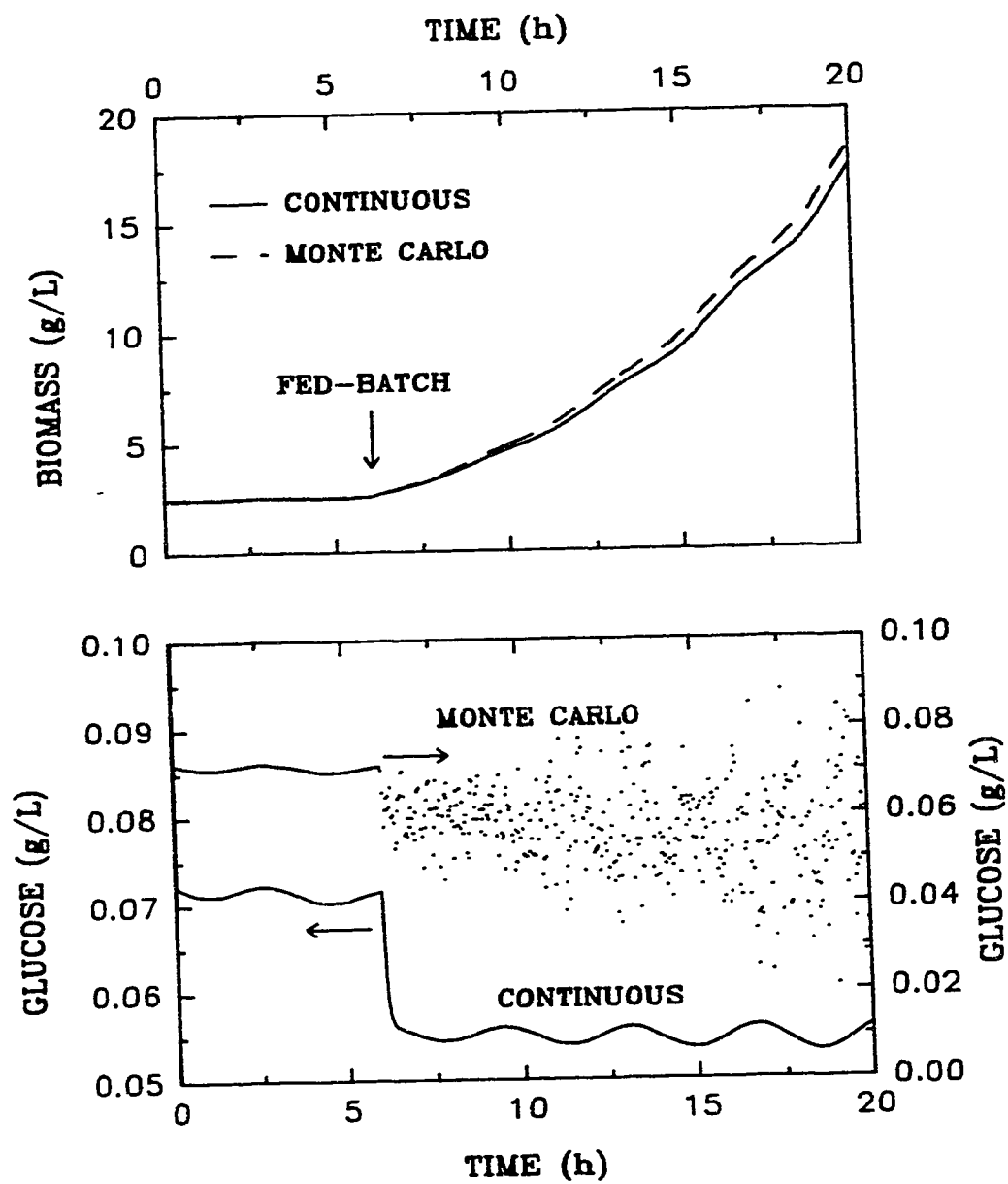


FIGURE 5.5: Comparison of model predictions for Monte Carlo fed-batch fermentation with continuous fed-batch fermentation.

Figure 5.5 compares the profiles of biomass and glucose for Monte Carlo fed-batch fermentation with continuous fed-batch fermentation. The biomass level at the end of the Monte Carlo fermentation was higher by 1 g/L compared to the continuous fed-batch fermentation. The small increase in the biomass for Monte Carlo fed-batch fermentation was consistent with the experiments (Chapter 4). The comparison of glucose profiles showed large and random fluctuations during the Monte Carlo fermentation compared to small and harmonic oscillations in the continuous fed-batch fermentation. No ethanol was predicted from simulations of all types of fed-batch fermentations, whereas the ethanol accumulated up to 0.4 g/L for Monte Carlo fermentation and up to 1.2 g/L in periodic fermentation during the last 2.5 h of fed-batch fermentation. The high glucose levels in the fermentor towards the end of Monte Carlo fermentations from simulation were not sufficient to saturate the respiratory capacity. Alternatively, the decrease in the growth rate towards the end of fed-batch fermentation due to accumulation of 'inhibitory compounds' could lead to imbalance between substrate demand and substrate supply in experiments.

The profiles of dissolved oxygen and CO₂ fraction in off-gas for the Monte Carlo fermentation are shown in Figure 5.6. The CO₂ and DO profiles showed fast and random fluctuations superimposed on the oscillatory pattern predicted for the continuously fed-batch fermentation. The model did predict the fast fluctuations in the CO₂ fraction in agreement with the experiments, however, indicating the partial success of the model under transient conditions. The experimental study showed that the use of a range of off-times in the Monte Carlo fed-batch fermentation produced a significantly different result compared to the use of a constant off-time in the periodic fed-batch fermentation. Periodic fed-batch fermentation produced no effect on final biomass yields, and retained the CO₂ cycles similar to the continuous fed-batch fermentation. Figures 5.7 and 5.8 show the prediction of the

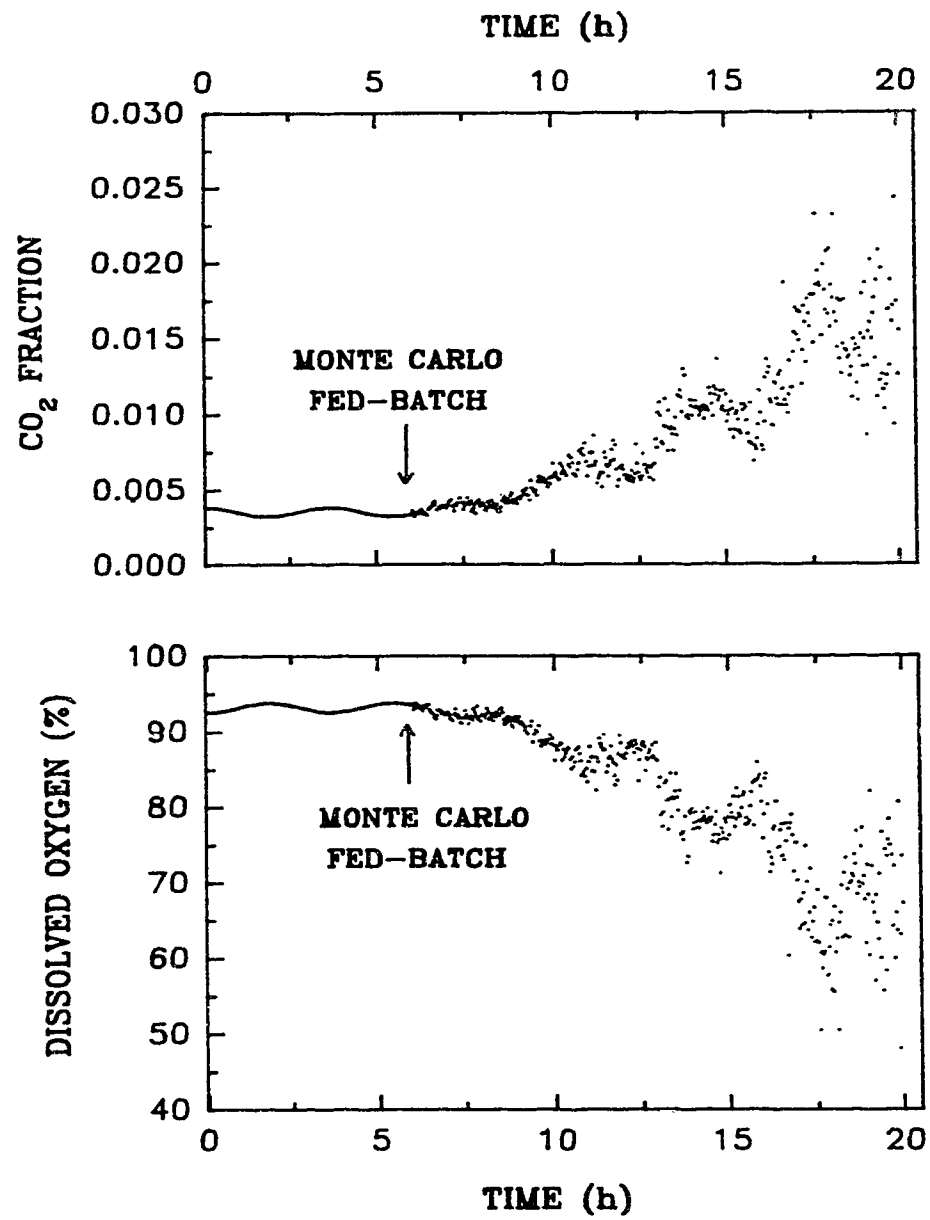


FIGURE 5.6: Prediction for the Monte Carlo fed-batch fermentation.

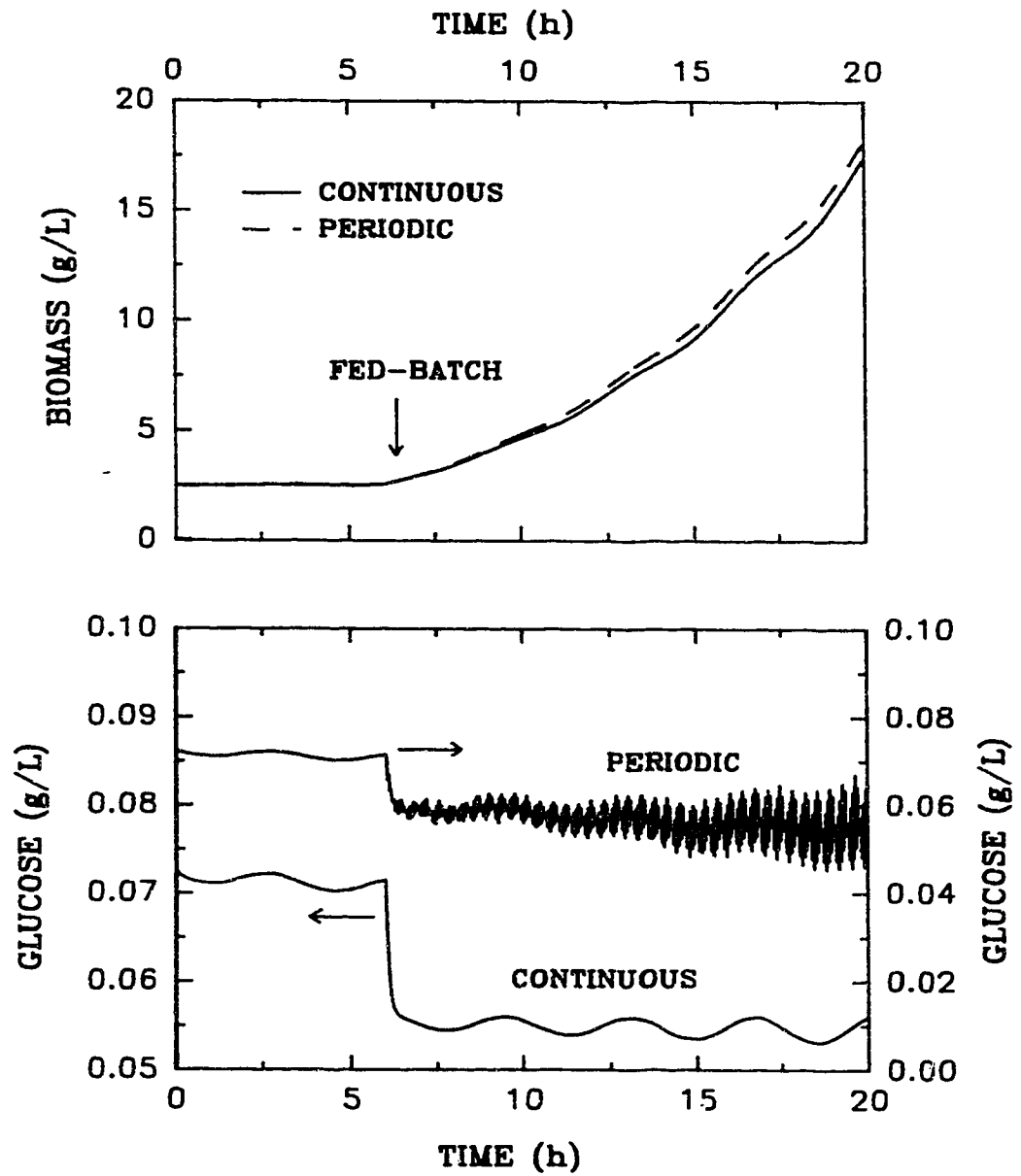


FIGURE 5.7: Comparison of model predictions for periodic fed-batch fermentation with the Monte Carlo fed-batch fermentation.

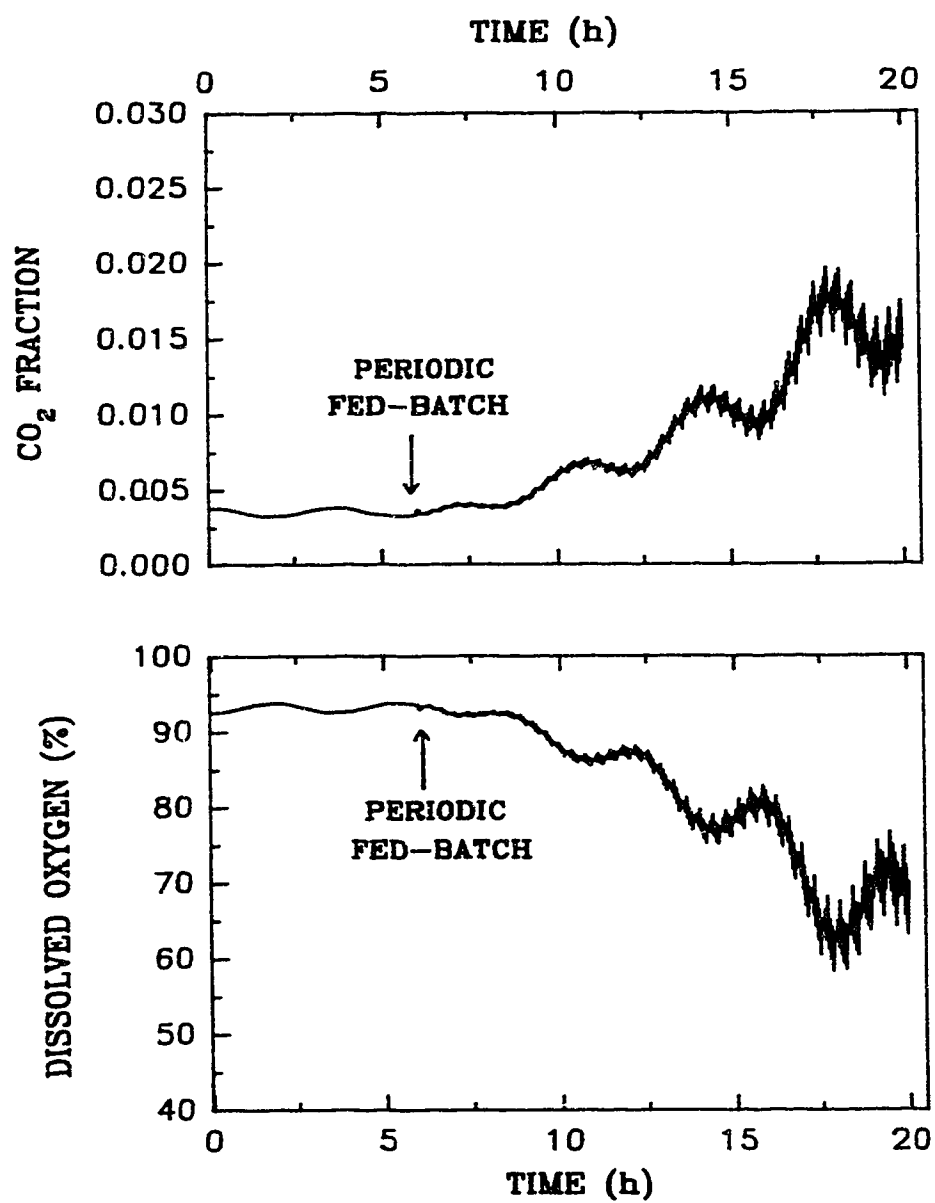


FIGURE 5.8: Predictions for the Periodic fed-batch fermentation.

model for the periodic fed–batch fermentation. The glucose, CO₂ and DO profiles show smaller and uniform fluctuations compared to the Monte Carlo fed–batch fermentation. No new peaks in CO₂ were predicted as observed in the periodic fed–batch fermentation experiment. The model predicted an increase of 1 g/L in biomass for periodic fed–batch fermentation compared to the continuously–fed fermentation (Figure 5.7), in contrast with no effect on the final biomass yield in experiments. The insensitivity of the model to a constant off–time of 15 s compared to a range of off–times of 3 s to 39 s in fed–batch fermentations indicate the need to identify mechanisms of characteristic times of less than a minute required for synchrony.

DISCUSSION

Previous studies have suggested the role of ethanol and storage carbohydrates in generating the spontaneous synchronisation in chemostat culture (Kuenzi and Fiechter, 1969; Martegani *et al.*, 1990). The present simulations for a chemostat predicted oscillatory behaviour for all variables except for ethanol which remained at zero concentration. Ethanol levels in the range of 0.015 g/L to 0.050 g/L have been detected for short intervals in chemostats for operating conditions consistent with the conditions used in the present simulation (Porro *et al.*, 1986; Chapter 4). The contribution of such a small level of ethanol in accelerating the growth of single-cells would be unlikely to have any effect on the generation of synchrony. The oscillations in storage carbohydrates reflect the repeated cycles of formation and degradation of storage carbohydrates as cells cycled between single-cell phase and budding-cell phase. These variations in formation and degradation of storage carbohydrate, however, were not adequate to predict non-harmonic oscillations in CO₂.

The model was tested under the transient conditions introduced by the three modes of fed-batch fermentation. Comparison of simulations for fed-batch fermentations with the experimental observations in Chapter 4 showed that the model was partially successful. The oscillatory behaviour in the continuous fed-batch fermentation, and the fast fluctuations in CO₂ fraction in the Monte Carlo fed-batch fermentation were simulated. The model, however, failed to predict the eventual elimination of synchrony in fed-batch fermentation and the presence of multiple peaks in the CO₂ oscillations.

The limited success of the present model could be due to the over-simplification of the population structure and the selection of values for certain parameters involved in carbohydrate and ethanol metabolism, including K_t ,

K_{tinh} and K_e . In the chemostat experiments, a significant fraction of the population has been shown to be non-synchronous as complete synchrony was never achieved (Kuenzi and Fiechter, 1969, Porro *et al.*, 1988; Chapter 4). The role of the non-synchronous sub-population in dampening the oscillations was not explicitly considered in the model. The absence of ethanol oscillations from model predictions and disruption of oscillations by small and random fluctuations in glucose level point to the need for a better understanding of the mechanism for inducing the synchrony.

Lyberatos (1985) showed the existence of stable steady states and harmonic oscillations, when one feedback parameter was varied for a chemical reaction system with a delay. In the present study, the parameter, K_t , for uptake of storage carbohydrates was varied from 0.2 to 1.5. The variation in other parameters relevant to kinetics of formation of storage carbohydrates were not considered. Use of a second time delay to the model could produce non-harmonic oscillations including cycles with multiple peaks (Lyberatos, 1985). The oscillatory behaviour of chemical reactions for the catalytic oxidation of carbon monoxide (Lynch and Wanke, 1984) was strikingly similar to the non-harmonic oscillations in CO_2 observed in chemostat experiments (Chapter 4). Lynch *et al.* (1986) showed that a model consisting of six ordinary differential equations based on the mechanisms for oxidation was capable of reproducing their experimental results. The challenge in the context of synchrony of yeast cultures is to formulate such a non-linear model from known characteristics of yeast growth and metabolism.

CONCLUSIONS

1. A simple model based a metabolic reaction network with delay in degradation of storage carbohydrates predicted stable harmonic-type oscillations in all variables except ethanol.
2. The model predicted fast and random fluctuations in CO_2 fraction of off-gas and dissolved oxygen when the feed was supplied intermittently according to a Monte Carlo method in the fed-batch fermentation.
3. The model failed to predict the non-harmonic type oscillations in the CO_2 fraction of off-gas during chemostat operation and the elimination of CO_2 cycles towards the end of the fed-batch fermentation.

REFERENCES

- Abulesz, E.M., Lyberatos, G. Periodic operation of a continuous culture of baker's yeast. *Biotechnol. Bioeng.* **1989**, *34*, 741–749.
- Barford, J.P., Hall, R.J. Estimation of cell cycle phases from synchronous cultures of *Saccharomyces cerevisiae*. *Exp. Cell Res.* **1976**, *102*, 276–284.
- Cazzador, L., Mariani, L., Martegani, E., Alberghina, L. Structured segregated models and analysis of self-oscillating yeast continuous cultures. *Bioproc. Eng.* **1990**, *5*, 175–180.
- Cazzador, L. Analysis of oscillations in yeast continuous cultures by a new simplified model. *Bul. Math. Biol.* **1991**, *53*(5), 685–700.
- Heinzle, E., Dunn, I.J., Furukawa, K., Tanner, R.D. Modelling of sustained oscillations observed in continuous culture of *Saccharomyces cerevisiae*. *Proc. First IFAC Workshop on Modelling and Control of Biotechnological Processes*, **1982**, 57–65.
- Hjortso, M.A., Bailey, J.E. Transient responses of budding yeast populations. *Math. Biosci.* **1983**, *63*, 121–148.
- Ivanitskay, J.G., Petrikevich, S.B., Bazykin, A.D. Oscillations in continuous cultures of microorganisms: Criteria of utility of mathematical models. *Biotechnol. Bioeng.* **1989**, *33*, 1162–1166.
- Kuenzi, M.T., Fiechter, A. Changes in carbohydrate composition and trehalase activity during the budding cycle of *Saccharomyces cerevisiae*. *Arch. Mikrobiol.* **1969**, *64*, 396–407.
- Lyberatos, G., Kuszta, B., Bailey, J.E. Discrimination and identification of dynamic catalytic reaction models via introduction of feedback. *Chem. Eng. Sci.* **1984**, *39*(4), 739–750.
- Lyberatos, G. The effect of delay on the feedback identification of chemical

- reacting systems. *Chem. Eng. Sci.* **1985**, *40*(11), 2160–2162.
- Lynch, D.T., Wanke, S.E. Oscillations during CO oxidation over supported metal catalysts. II. Effects of reactor operating conditions on oscillatory behaviour for a (Pt–Pd)/Al₂O₃ catalyst. *J. of Catal.* **1984**, *88*, 345–354.
- Lynch, D.T., Emig, G., Wanke, S.E. Oscillations during CO oxidation over supported metal catalysts. III. Mathematical modelling of the observed phenomena. *J. Catal.* **1986**, *97*, 456–468.
- MacDonald, N. Time delay in simple chemostat models. *Biotechnol. Bioeng.* **1976**, *18*, 805–812.
- Martegani, E., Porro, D., Ranzi, B.M., Alberghina, L. Involvement of a cell size control of mechanism in the induction and maintenance of oscillations in continuous cultures of budding yeast. *Biotechnol. Bioeng.* **1990**, *36*, 453–459.
- Meyer, C., Beyeler, W. Control strategies for continuous bioprocesses based on biological activities. *Biotechnol. Bioeng.* **1984**, *26*, 916–925.
- Parulekar, S.J., Semones, G.B., Rolf, M.J., Lievens, J.C., Lim, H.C. Induction and elimination of oscillations in continuous cultures of *Saccharomyces cerevisiae*. *Biotechnol. Bioeng.* **1986**, *28*, 700–710.
- Porro, D., Martegani, E., Ranzi, B.M., Alberghina, L. Oscillations in continuous cultures of budding yeast: A segregated parameter analysis. *Biotechnol. Bioeng.* **1988**, *32*, 411–417.
- Strassle, C., Sonnleitner, B., Fiechter, A. A predictive model for the spontaneous synchronisation of *Saccharomyces cerevisiae* grown in continuous culture. I. Concept. *J. Biotechnol.* **1988**, *7*, 299–318.
- Strassle, C., Sonnleitner, B., Fiechter, A. A predictive model for the spontaneous synchronisation of *Saccharomyces cerevisiae* grown in continuous culture. II. Experimental verification. *J. Biotechnol.* **1989**, *9*, 191–208.
- Suzuki, S., Shimizu, K., Matsubara, M. On the parameter–space classification of

- the dynamic behaviour of a continuous microbial flow reactor. *Chem. Eng. Commun.* **1985**, *33*, 325–335.
- Takamatsu, T., Shioya, S., Chikatani, H. Comparison of simple population models in a baker's yeast fed–batch culture. *Chem. Eng. Sci.* **1985**, *40*(3), 499–507.
- Yegneswaran, P.K., Thompson, B.G., Gray, M.R. Kinetics of CO₂ hydration in fermentors: pH and pressure effects. *Biotechnol. Bioeng.* **1990**, *36*, 92–96.

CHAPTER 6

CONCLUSIONS AND RECOMMENDATIONS

Conclusions and Implications

A major difficulty in reproducing a laboratory-scale fed-batch fermentation on the production-scale is the establishment of a nutrient-rich zone close to the feeding point due to incomplete mixing, along with a range of concentrations in the bulk fluid in a production-scale fermentor. In this thesis, a rational strategy was developed to simulate these nutrient fluctuations in a laboratory-scale fermentor by using circulation time distributions, CTD, from production fermentors. The strategy was simple to implement as it involved additions of feed pulses to a fermentor. A Monte Carlo method simulated a given CTD by controlling the feed pulses. This method provided the flexibility to use any given CTD of production vessels. Also, the simultaneous fluctuation of the two critical variables, dissolved oxygen and nutrient concentrations would be possible.

In fed-batch fermentation for the baker's yeast production, the fluctuations in glucose concentration could play an important role in determining the biomass quality and byproduct formation. Comparison of continuously-fed fermentation with Monte Carlo fermentation showed a higher state of metabolic activity of the yeast culture under conditions of fluctuating nutrient levels. The effect of a nutrient-rich 'feed-zone' close to the feeding point was simulated by using a fermentor and a plug-flow loop with recirculation of broth between them. A CTD for the feed-zone was adequate to calculate a range of volumes of the recycle loop and recirculation flow rates. The levels of byproducts, including ethanol and acetic acid, showed a greater degree of sensitivity to the feed-zone effect compared to the

final biomass levels, especially for a long residence time of 12 min in the loop. Experiments with a defined medium gave results in contrast to the above results from experiments with the complex media. This difference indicated that the presence of alternative carbon and nitrogen sources in complex media could play an important role in controlling the extent of 'glucose effect' on the final levels of biomass.

Chemostat experiments with a defined medium showed spontaneous generation of synchrony and stable, non-harmonic oscillations in various measurements including CO₂ fraction of off-gas and dissolved oxygen, DO. The cycles of CO₂ correlated very well with the phases of the cell-cycle, and were used as a measure of the degree of synchrony. Fed-batch fermentation, with an exponentially increasing supply of the feed showed continuation of CO₂ and DO oscillations for five cycles. A chaotic response in CO₂ and DO was obtained, however, when short fluctuations in glucose feed with off-times from 3 s to 39 s were imposed on the fed-batch culture. A higher budded-fraction of cells of 0.3 was obtained at the end of this Monte Carlo fermentation compared to 0.1 at the end of the continuous fed-batch fermentation, consistent with the biomass levels. A synchronous culture of baker's yeast, therefore, cannot be established in a production-scale fermentor due to inherent concentration fluctuations in the fermentor.

The interaction among cells through excretion and uptake of ethanol is usually speculated to cause synchrony in the culture. A simple structured-type model with a delay in degradation of storage carbohydrates predicted stable harmonic oscillations in all variables except ethanol. The CO₂ profiles of a synchronously dividing culture under the fed-batch fermentations with continuous and intermittent supply of feed were used to test the model. The model predicted fast and random fluctuations in CO₂ and DO during Monte Carlo fermentation,

consistent with experiments but failed to predict dampening of the oscillations in continuous fed-batch fermentations. These simulation results, coupled with experimental measurements, suggested that ethanol need not be the cause of synchrony.

Fed-batch experiments with periodic feeding gave different results compared to Monte Carlo experiments with both defined and complex media. This comparison indicated that the distribution of circulation times and not the mixing time should be used to characterise the bulk circulation patterns or macromixing in the production fermentor. Any strategy that could affect the long tail of the circulation time distribution, therefore, would be useful in achieving a desirable performance in the production vessel.

Limitations and Recommendations

Macromixing, as characterised by a CTD, was assumed to be the rate limiting step in the transport of nutrients from the feeding point into the microenvironment of a cell. Assuming macromixing or complete segregation in the bulk of the vessel would predict a limit on the final performance of the production fermentor. In baker's yeast production, as in many other fermentations, high concentrations of nutrients cause a drop in the yield of product, whereas low availability of a nutrient prompts cells to use alternative sources. The Monte Carlo fermentation would, therefore, predict a lower limit of the possible yield.

The Monte Carlo experiments with feed added to a recycle loop were designed by assuming a certain range of size of the feed-zone. The degree of turbulence at the point of feed addition would control the size of the feed-zone. The micromixing would also affect the concentration gradients in the microenvironment or the vicinity of a cell. The characterisation of length- and time-scales of micromixing and its effect on the fermentation would complement the present study. These

bench-scale studies on effect of macro- and micro-mixing would be directly useful for scale-up if the operating conditions for the production fermentor could be related to the mixing parameters, including the CTD for macromixing and the length- and time-scales for micromixing.

A single impeller system was assumed implicitly in the development of the Monte Carlo strategy. Production fermentors, however, often employ multiple impeller system, which increases the number of micromixed regions. The Monte Carlo method could be extended by including a switching probability between the adjacent impeller zones and providing different proportion of the fresh feed to these zones. The Monte Carlo method is not limited to evaluating the effect of concentration gradients in stirred tanks. Similar methods could be developed to evaluate the effects of gradients in other variables, for example, shear rates during mammalian cell cultivation in a bioreactor. The challenge in the context of variables other than concentrations would be to characterise distributions of those variables in the bioreactor.

The success of a model for synchrony of yeast culture depends on its ability to predict the stable, non-harmonic oscillations in CO_2 during chemostat operation and the observed responses during the various fed-batch fermentations, including a chaotic response in CO_2 during Monte Carlo fermentation. The challenge in conforming to these tests lies in developing a cell-cycle model that would give a kinetic model with sufficient non-linearity, and not in using a model with a large number of differential equations. The random or 'chaotic' response of CO_2 indicated that the small fluctuations in environment directly interfered with that interaction among cells which produced synchrony or 'order' in the yeast population. More insight into control of the cell-cycle event would be required to propose the mechanism for synchrony, and subsequently to develop a model based on the metabolic control processes.

APPENDIX A

CALIBRATION EQUATIONS FOR BIOMASS

Procedure: Optical density of sample was measured after suitable dilution with RO water such that $OD_{620} < 0.4$. The samples were filtered with filters (0.45 μm) and dried in microwave oven for 10 min.

Table A.1 Dry cell weight vs optical density for *S.cerevisiae*, NCYC 1018 grown on complex medium during fed–batch fermentation

DCW (g/L) = 0.82 (OD_{620}) $r^2=0.976$	for $0 \leq t < 6$ h and $2.5 \leq OD_{620} < 6.5$
DCW (g/L) = 0.76 (OD_{620}) $r^2=0.983$	for $6 \leq t < 10$ h and $6.5 \leq OD_{620} < 10.0$
DCW (g/L) = 0.68 (OD_{620}) $r^2=0.968$	for $10 \leq t < 14$ h and $10.0 \leq OD_{620} < 14.0$
DCW (g/L) = 0.64 (OD_{620}) $r^2=0.99$	for $t \geq 14$ h and $OD_{620} \geq 14.0$

Table A.2. Dry cell weight vs optical density for *S.cerevisiae*, ATCC 32167 grown on defined medium during fed–batch fermentation.

DCW (g/L) = 0.86 (OD ₆₂₀) r ² =0.99	for 0 ≤ t < 5 h and 2.0 ≤ OD ₆₂₀ < 6.0
DCW (g/L) = 0.76 (OD ₆₂₀) r ² =0.981	for 5 ≤ t < 12 h and 6.0 ≤ OD ₆₂₀ < 13.0
DCW (g/L) = 0.74 (OD ₆₂₀) r ² =0.975	for t ≥ 12 h and OD ₆₂₀ ≥ 13.0

APPENDIX B

DATA FROM REPEATED EXPERIMENTS FOR FED-BATCH FERMENTATIONS WITH COMPLEX MEDIUM

(For Chapter 2)

- TABLE B.1 DCW and ethanol data for continuous fed-batch fermentations with *S.cerevisiae* NCYC 1018, grown on complex medium.
- TABLE B.2 DCW and ethanol data for Monte Carlo fed-batch fermentations with *S.cerevisiae* NCYC 1018, grown on complex medium.
- TABLE B.3 DCW and ethanol data for Periodic fed-batch fermentations with *S.cerevisiae* NCYC 1018, grown on complex medium.
- FIGURE B.1 Comparison of RQ profiles for continuous fed-batch with Monte Carlo fed-batch fermentations with *S.cerevisiae*, NCYC 1018 grown on complex medium.
- FIGURE B.2 Comparison of DO profiles for continuous fed-batch with Monte Carlo fed-batch fermentations with *S.cerevisiae*, NCYC 1018 grown on complex medium.

TABLE B.1
Continuous Fed-batch Experiments
S.cerevisiae NCYC 1018

RUN 1			RUN 2		
FEED TIME (h)	DCW (g/L)	ETHANOL (g/L)	FEED TIME (h)	DCW (g/L)	ETHANOL (g/L)
0.0	1.9	3.9	0.0	1.8	3.8
6.0	5.0	4.0	3.0	2.8	4.5
10.0	6.3	2.7	6.0	4.7	4.2
13.0	8.9	1.1	9.0	7.3	3.1
15.0	9.6	0.1	12.0	8.6	1.9
			15.0	9.5	0.5

RUN 3		
FEED TIME (h)	DCW (g/L)	ETHANOL (g/L)
0.0	1.8	3.8
3.0	2.5	4.3
6.0	4.6	4.4
9.0	7.3	2.6
12.0	8.4	1.6
15.0	9.7	0.1

TABLE B.2
 Monte Carlo Fed-batch Experiments
S.cerevisiae NCYC 1018

RUN 1			RUN 2		
FEED TIME (h)	DCW (g/L)	ETHANOL (g/L)	FEED TIME (h)	DCW (g/L)	ETHANOL (g/L)
0.0	1.9	3.9	0.0	1.8	3.6
3.0	3.0	4.4	3.5	3.4	4.7
6.0	5.1	4.4	6.0	5.2	4.6
9.0	7.7	3.5	9.0	7.7	3.4
12.0	9.1	2.0	12.0	9.1	2.1
15.0	10.4	0.1	15.0	10.3	0.4
18.0	11.4	0.1			

RUN 3		
FEED TIME (h)	DCW (g/L)	ETHANOL (g/L)
0.0	1.9	3.7
3.0	3.2	4.1
6.0	5.3	3.9
10.0	7.8	2.3
18.0	11.4	0.1

TABLE B.3
Periodic Fed-batch Experiments
S.cerevisiae NCYC 1018

RUN 1			RUN 2		
FEED TIME (h)	DCW (g/L)	ETHANOL (g/L)	FEED TIME (h)	DCW (g/L)	ETHANOL (g/L)
0.0	1.9	4.0	0.0	1.7	4.0
3.0	3.0	4.2	3.0	2.8	4.4
6.0	4.9	4.1	6.0	4.4	4.3
9.0	7.0	3.1	9.0	7.2	3.6
12.0	8.4	1.7	12.0	8.3	2.1
15.0	9.2	0.1	15.0	9.3	0.1

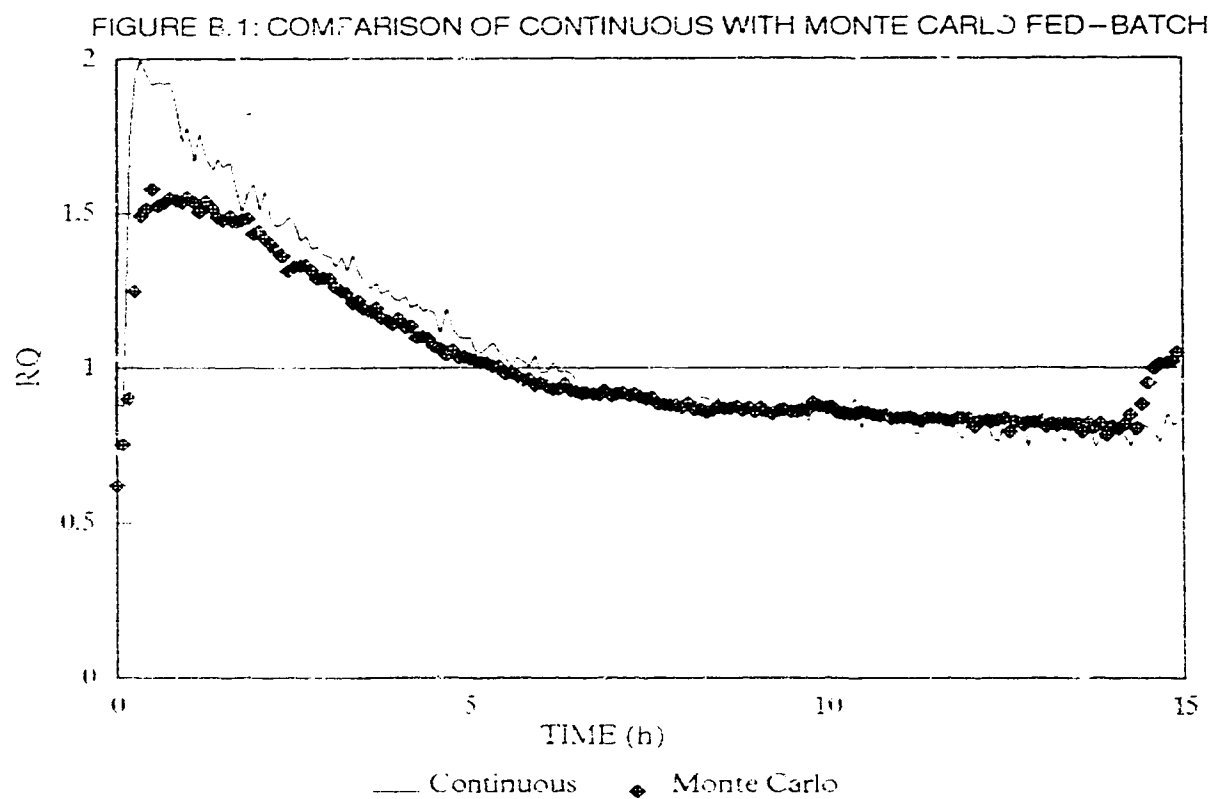


FIGURE B.1 Comparison of RQ profiles for continuous fed-batch with Monte Carlo fed-batch fermentations with *S.cerevisiae*, NCYC 1018 grown on complex medium.

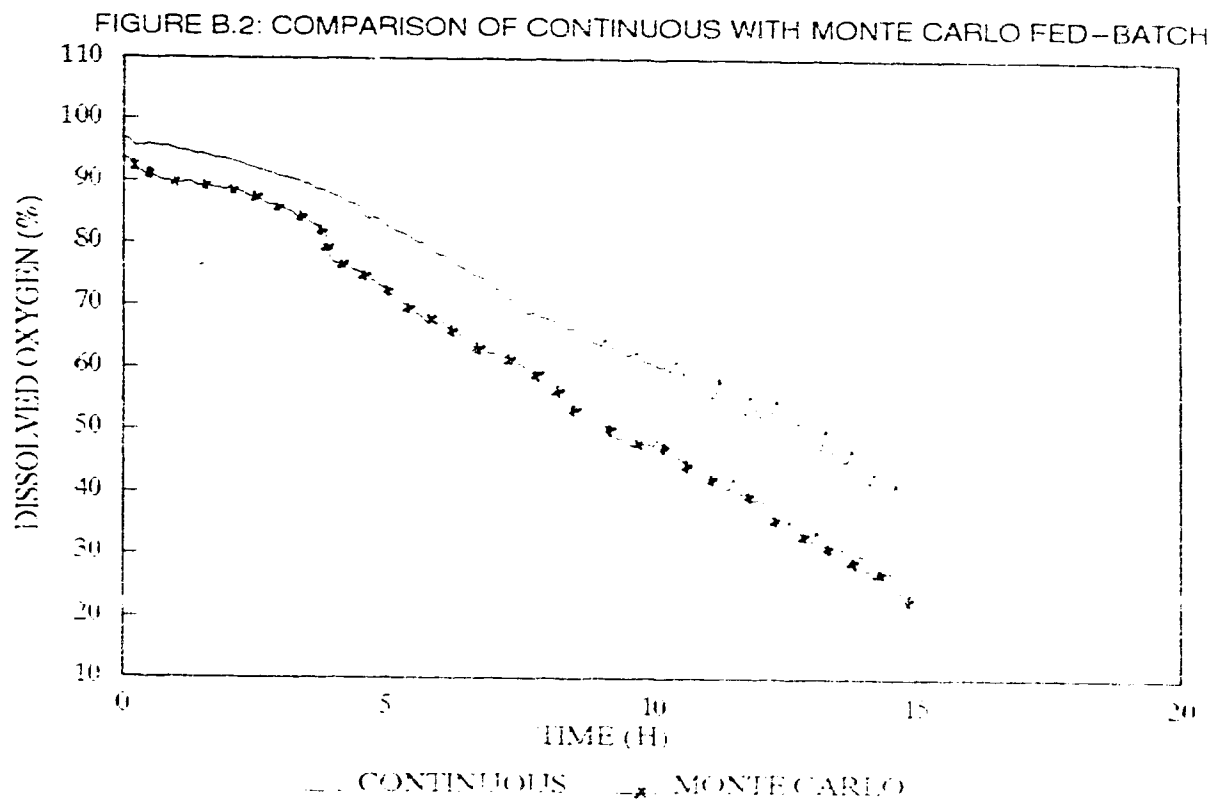


FIGURE B.2 Comparison of DO profiles for continuous fed-batch with Monte Carlo fed-batch fermentations with *S.cerevisiae*, NCYC 1018 grown on complex medium.

APPENDIX C

CTD CALCULATION AND DATA FROM REPEATED EXPERIMENTS FOR FED-BATCH FERMENTATIONS WITH COMPLEX AND DEFINED MEDIA (for Chapter 3)

C.1 CTD CALCULATIONS

FIGURE C.1.1 An algorithm to calculate a CTD for a reference zone using the 'Network-of-Zones' stochastic model.

FIGURE C.1.2 A CTD calculated with respect to the impeller zone

C.2 Biomass, ethanol and acetate data for complex-medium fermentations with *S.cerevisiae*, NCYC 1018.

TABLE C.2.1 Continuous fed-batch fermentations.

TABLE C.2.2 Monte Carlo fed-batch fermentations.

C.3 Biomass and ethanol data for defined-media fermentations with *S.cerevisiae*, ATCC 32167.

TABLE C.3.1 Continuous fed-batch fermentations.

TABLE C.3.2 Monte Carlo fed-batch fermentations.

TABLE C.3.3 Periodic fed-batch fermentations.

FIGURE C.3.1 Reproducibility of the biomass profiles for continuous and Monte Carlo fed-batch fermentations.

C.4 Experimental results from complex-media fermentations with *S.cerevisiae*, ATCC 32167.

TABLE C.4.1 Biomass and ethanol data for continuous and Monte Carlo fed-batch fermentations.

FIGURE C.4.1 Comparison of OUR profiles of continuous with Monte Carlo fed-batch fermentations.

FIGURE C.4.2 Comparison of DO profiles of continuous with Monte Carlo fed-batch fermentations.

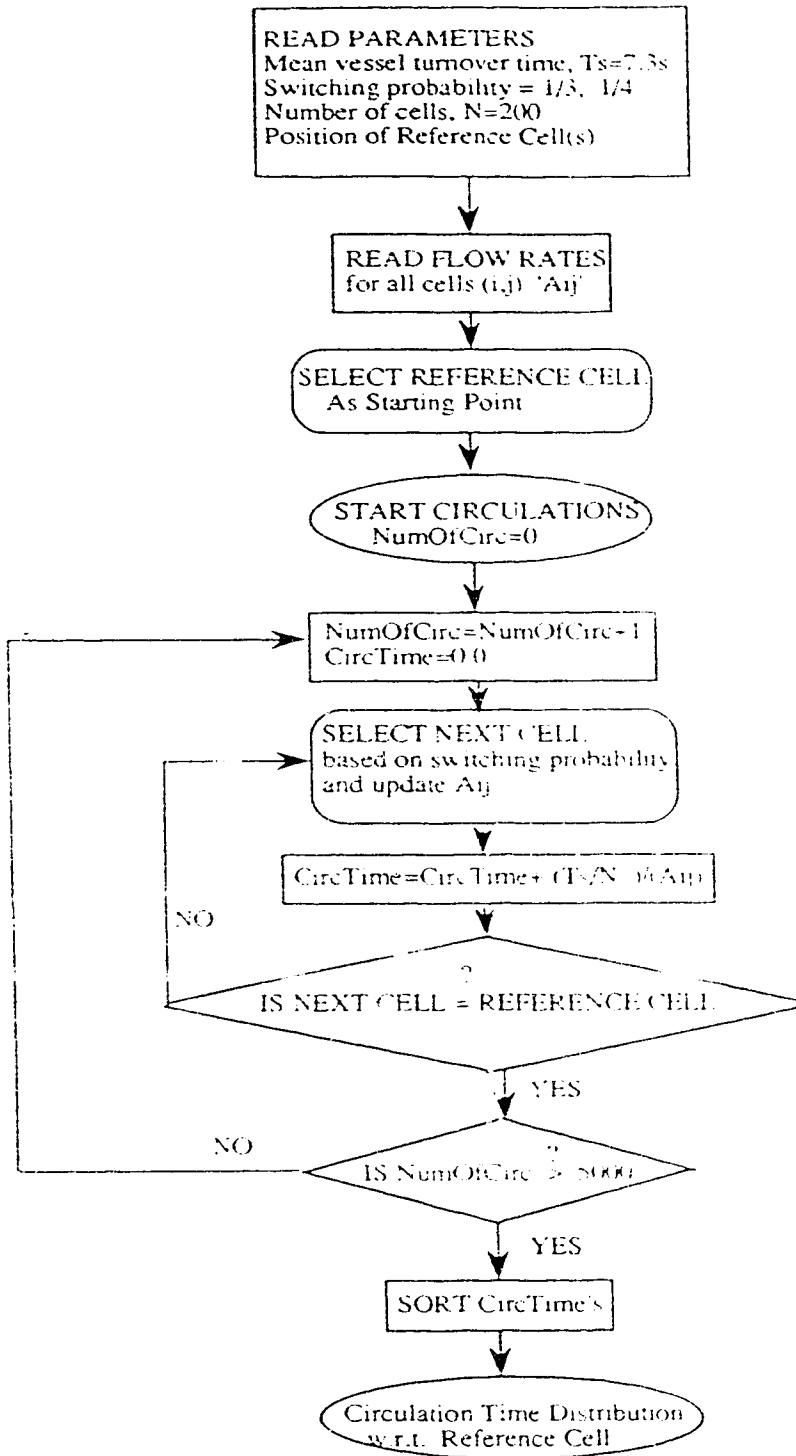


FIGURE C.1.1 An algorithm to calculate CTD for a reference zone using 'Network-of-Zones' stochastic model.

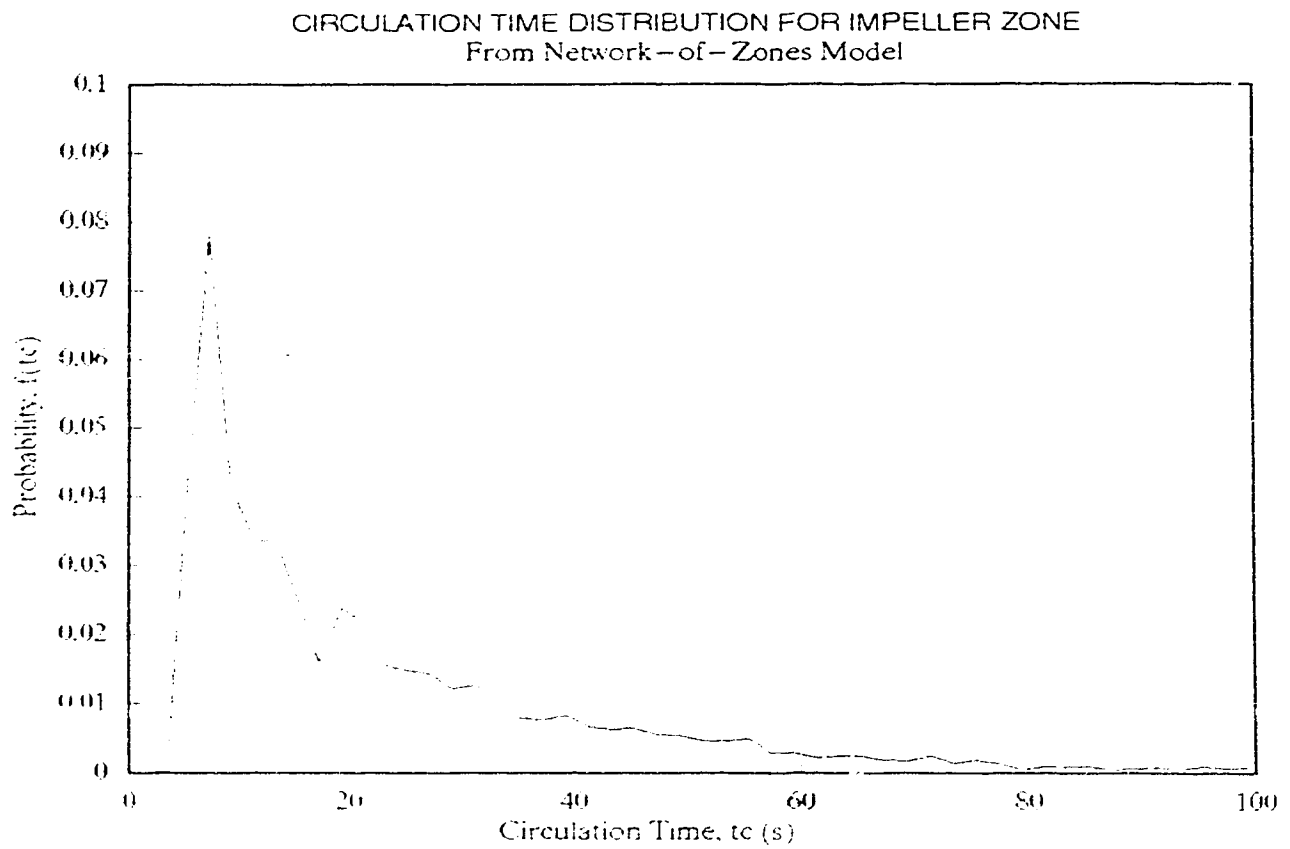


FIGURE C.1.2: A CTD calculated with respect to the impeller zone

TABLE C.2.1
Continuous Fed-batch Experiments
S.cerevisiae NCYC 1018

Vp=0mL, Qr=0L/h				Vp=15mL, Qr=2.0L/h		
FEED TIME (h)	DCW (g/L)	ETHANOL (g/L)	ACETATE (g/L)	DCW (g/L)	ETHANOL (g/L)	ACETATE (g/L)
0	1.9	3.4	0.0	2.2	3.1	0.0
2	2.8	4.0	0.0	3.1	2.5	0.0
4	4.2	3.5	0.0	4.9	2.1	0.0
6	5.3	3.5	0.0	5.8	1.8	0.0
8	6.9	3.2	0.0	7.4	1.7	0.0
10	7.2	2.5	0.0	7.7	1.7	0.0
12	8.2	1.9	0.0	8.9	0.5	0.0
14	8.8	1.1	0.0	9.1	0.0	0.0

Vp=50mL, Qr=0.25L/h				Vp=50mL, Qr=0.5L/h		
FEED TIME (h)	DCW (g/L)	ETHANOL (g/L)	ACETATE (g/L)	DCW (g/L)	ETHANOL (g/L)	ACETATE (g/L)
0	1.9	3.8	0.0	1.9	3.4	0.0
2	2.8	3.7	0.0	2.8	3.9	0.0
4	4.4	1.8	0.0	4.3	4.0	0.0
6	5.5	1.8	0.0	5.6	3.3	0.0
8	7.6	1.9	0.0	7.7	3.2	0.0
10	7.9	1.2	0.0	7.9	2.9	0.0
12	9.0	0.4	0.0	9.0	2.2	0.0
14	9.8	0	0.0	9.6	1.4	0.0

Vp=50mL, Qr=3.0L/h			
FEED TIME (h)	DCW (g/L)	ETHANOL (g/L)	ACETATE (g/L)
0	2	3.7	0.0
2	3.1	3.4	0.0
4	4.3	3.2	0.0
6	5.5	3.3	0.0
8	7.2	2.8	0.0
10	7.5	2.5	0.0
12	8.7	1.8	0.0
14	9.3	1.0	0.5

TABLE C.2.2
Monte Carlo Fed-batch Experiments
S.cerevisiae NCYC 1018

FEED TIME (h)	Vp=15mL, Qr=0.5L/h			Vp=15mL, Qr=3.0L/h		
	DCW (g/L)	ETHANOL (g/L)	ACETATE (g/L)	DCW (g/L)	ETHANOL (g/L)	ACETATE (g/L)
0	1.9	2.1	0.0	1.9	1.9	0.0
2	2.8	3.2	0.0	2.8	1.8	0.0
4	4.2	3.1	0.0	4.3	2.6	0.0
6	5.7	2.1	0.0	5.7	3.0	0.0
8	7.5		0.0	7.6	1.8	0.0
10	7.8	1.2	0.0	8.2	0.9	0.0
12	9.0	1.8	0.0	9.4	0.9	0.0
14	9.5	1.4	0.4	10.0	0.6	0.0

FEED TIME (h)	Vp=15mL, Qr=6.0L/h			Vp=50mL, Qr=0.25L/h		
	DCW (g/L)	ETHANOL (g/L)	ACETATE (g/L)	DCW (g/L)	ETHANOL (g/L)	ACETATE (g/L)
0	2.0	2.6	0.0	2.0	1.1	0.0
2	2.9	2.6	0.0	2.9	1.7	0.0
4	4.2	4.0	0.0	4.4	1.4	0.0
6	5.4	2.3	0.0	5.7	1.4	0.0
8	7.1	2.0	0.0	6.6	1.7	0.0
10	7.5	2.3	0.0	7.6	1.6	0.0
12	8.8	2.2	0.0	8.7	0.4	0.8
14	9.4	1.4	0.0	9.2	0.0	1.3

FEED TIME (h)	Vp=50mL, Qr=0.5L/h			Vp=50mL, Qr=6.0L/h		
	DCW (g/L)	ETHANOL (g/L)	ACETATE (g/L)	DCW (g/L)	ETHANOL (g/L)	ACETATE (g/L)
0	2.0	1.8	0.0	2	3.0	0.0
2	2.8	2.0	0.0	2.9	3.0	0.0
4	4.1	2.2	0.0	4.1	3.4	0.0
6	5.4	2.6	0.0	5.5	3.5	0.0
8	7.0	2.2	0.0	7.4	2.9	0.0
10	7.5	1.9	0.0	8.0	2.8	0.0
12	8.7	1.7	0.3	9.2	2.1	0.0
14	9.0	1.2	0.6	9.7	1.5	0.0

TABLE C.3.1
Continuous Fed-batch Experiments
S.cerevisiae ATCC 22167

Vp=0mL, Qr=0L/h			Vp=0mL, Qr=0L/h		
FEED TIME (h)	DCW (g/L)	ETHANOL (g/L)	FEED TIME (h)	DCW (g/L)	ETHANOL (g/L)
0.0	2.3	0.0	0.0	2.3	0.0
1.5	2.8	0.0	1.5	2.7	0.0
3.0	3.4	0.0	3.0	3.2	0.0
4.5	4.2	0.0	4.5	4.3	0.0
6.0	4.7	0.0	6.0	4.8	0.0
7.5	6.2	0.0	7.5	5.8	0.0
9.0	6.8	0.0	9.0	6.4	0.0
10.5	8.3	0.0	10.5	8.1	0.03
12.0	9.0	0.0	12.0	9.0	0.07
13.5	10.3	0.01	13.5	-	-
14.5	10.8	0.79	14.5	-	-

Vp=50mL, Qr=0.5L/h		
FEED TIME (h)	DCW (g/L)	ETHANOL (g/L)
0.0	2.1	0.0
1.5	3.0	0.0
3.0	4.0	0.0
4.5	4.4	0.0
6.0	5.3	0.0
7.5	6.2	0.0
9.0	7.1	0.0
10.5	8.7	0.0
12.0	9.1	0.0
13.5	-	0.0
14.5	10.7	0.15

TABLE C.3.2
Monte Carlo Fed-batch Experiments
S.cerevisiae ATCC 32167

Vp=0mL, Qr=0.0L/h			Vp=0mL, Qr=0.0L/h		
FEED TIME (h)	DCW (g/L)	ETHANOL (g/L)	FEED TIME (h)	DCW (g/L)	ETHANOL (g/L)
0.0	2.3	0.0	0.0	2.4	0.0
1.5	2.8	0.0	1.5	2.7	0.0
3.0	3.9	0.0	3.0	3.7	0.0
4.5	4.3	0.0	4.5	4.5	0.0
6.0	5.5	0.0	6.0	5.6	0.0
7.5	6.2	0.0	7.5	6.3	0.0
9.0	7.6	0.0	9.0	7.8	0.0
10.5	9.1	0.0	10.5	9.1	0.0
12.0	9.7	0.0	12.0	10.2	0.07
13.5	11.0	0.0	13.5	-	-
14.5	11.8	0.2	14.5	-	-

Vp=50mL, Qr=0.5L/h			Vp=50mL, Qr=3.0L/h		
FEED TIME (h)	DCW (g/L)	ETHANOL (g/L)	FEED TIME (h)	DCW (g/L)	ETHANOL (g/L)
0.0	2.4	0.0	0.0	2.3	0.0
1.5	2.9	0.0	1.5	2.8	0.0
3.0	3.8	0.0	3.0	3.9	0.0
4.5	4.5	0.0	4.5	4.5	0.0
6.0	5.6	0.0	6.0	5.8	0.0
7.5	6.7	0.0	7.5	7.0	0.0
9.0	8.0	0.0	9.0	8.2	0.0
10.5	9.6	0.0	10.5	9.6	0.02
12.0	10.0	0.06	12.0	9.9	0.05
13.5	11.1	0.11	13.5	11.0	0.12
14.5	11.0	0.73	14.5	11.2	0.65

TABLE C.3.3
 Periodic Fed-batch Experiment
S.cerevisiae ATCC 32167

$V_p=50\text{mL}$, $Q_r=0.5\text{L/h}$

FEED TIME (h)	DCW (g/L)	ETHANOL (g/L)
0.0	2.2	0.0
1.5	2.8	0.0
3.0	3.7	0.0
4.5	4.4	0.0
6.0	5.4	0.0
7.5	6.0	0.0
9.0	7.4	0.0
10.5	9.0	0.0
12.0	9.3	0.03
13.5	10.0	0.49
14.5	10.4	1.76

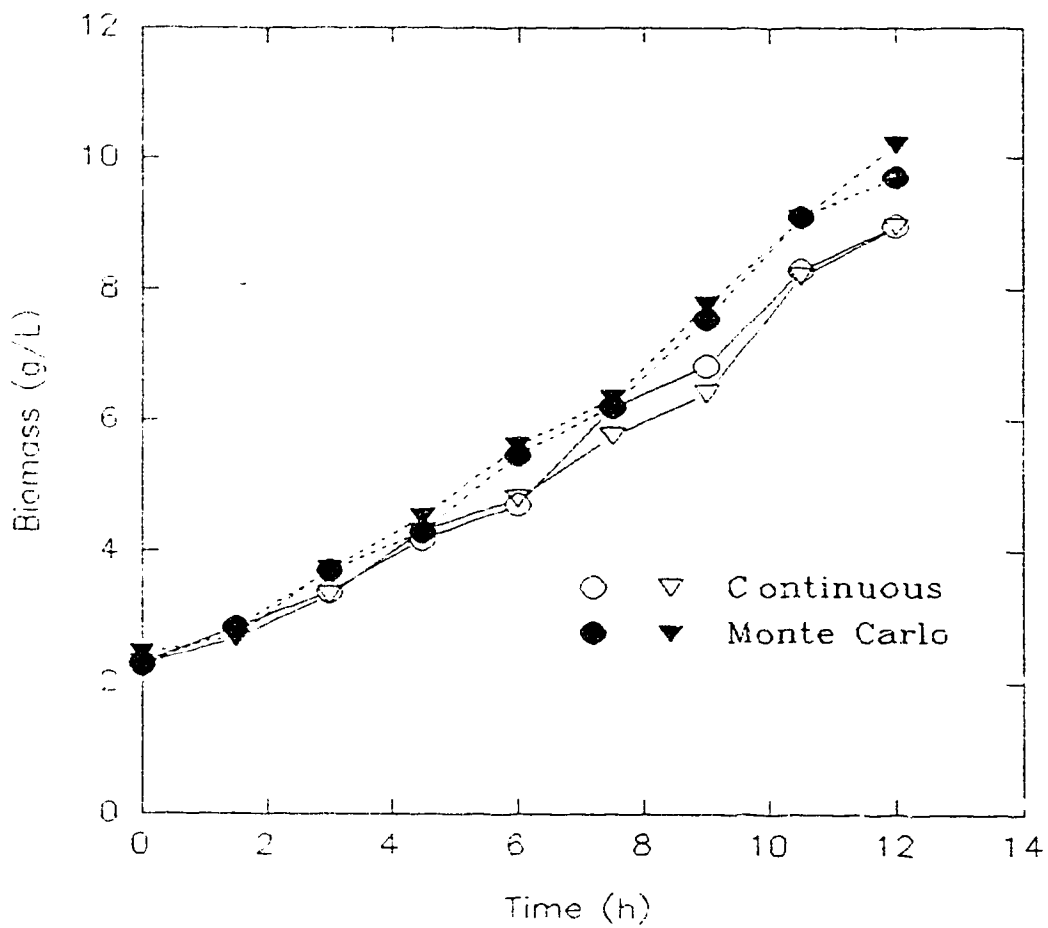


FIGURE C.3.1 Reproducibility of biomass profiles for continuous and Monte Carlo fed-batch fermentations with *S.cerevisiae* NCYC 1016, grown on a Complex medium.

TABLE C.4.1
Fed-batch Experiments with
S.cerevisiae ATCC 32167, Complex Feed

(1) Continuous			(2) Monte Carlo		
Vp=50mL, Qr=0.5L/h			Vp=50mL, Qr=0.5L/h		
FEED TIME (h)	DCW (g/L)	ETHANOL (g/L)	FEED TIME (h)	DCW (g/L)	ETHANOL (g/L)
0	1.8	3.5	0	1.7	3.7
2	3.1	3.6	2	2.8	4.1
4	5	2.9	4	4.6	4.1
6	7	1.8	6.12	6.1	2.9
8	9.3	0.7	8	8.1	2.1
10	11.8	0	10	10.5	1.6
14	13.7	0.1	14.2	14.1	0.1

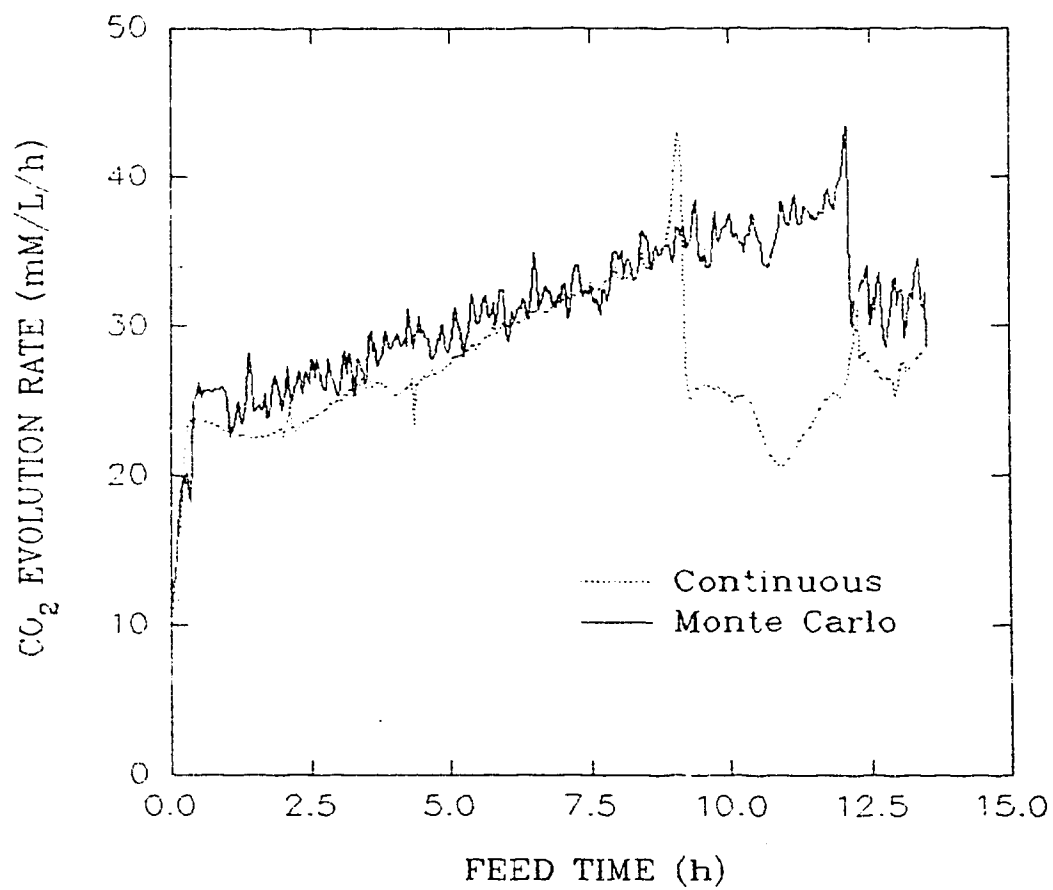


FIGURE C.4.1 Comparison of CER profiles for fermentations of *S.cerevisiae* ATCC 32167 grown on a complex medium.

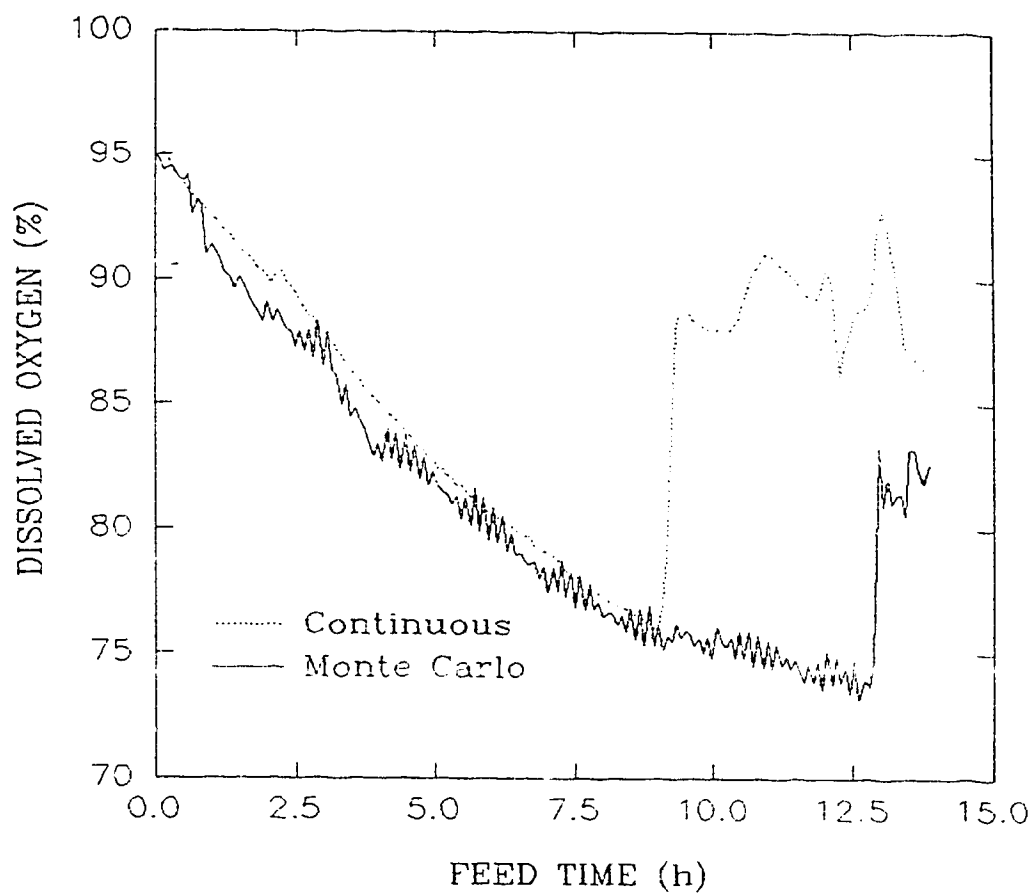


FIGURE C.4.2 Comparison of DO profiles for fermentations of *S. cerevisiae* ATCC 32167 grown on a complex medium.

APPENDIX D

CALCULATION OF SYNCHRONY FRACTION AND DATA FROM REPEATED EXPERIMENTS FOR FED-BATCH FERMENTATIONS WITH DEFINED MEDIUM (For Chapter 4)

1. Estimation of fraction of synchronised sub-population in a chemostat

The population of yeast cells in the chemostat is assumed to consist of two sub-populations: a synchronised sub-population with number of cells N_s and a heterogeneous sub-population with number of cells N_h . The heterogeneous population will have a constant budded fraction (ψ) and constant number of cells (N_h) during a constant volume chemostat operation. The synchronised sub-population will have a minimum budded fraction of 0 and a maximum budded fraction of 1. The synchronised sub-population will wash out between the successive cell divisions according to the following equation,

$$dN_s/dt = -D N_s \quad (1)$$

The number of cells in synchronised population (N_s) will be maximum (N_{smax}) immediately after the cell division and will be at its lowest level (N_{smin}) just before the next cell division. The interval of a cell-cycle for the synchronised sub-population is equal to the interval of a CO_2 cycle (T_c). From Equation (1), we obtain a relationship between these extreme levels of synchronised sub-population as follows,

$$N_{smin} = N_{smax} \exp(-DT_c) \quad (2)$$

The observed minimum budded fraction (BF_{min}) is given by

$$BF_{min} = N_h \psi / (N_h + N_{smax}) \quad (3)$$

and the observed maximum budded fraction (BF_{\max}) is given by

$$BF_{\max} = (N_h\psi + N_{s\min}) / (N_h + N_{s\min}) \quad (4)$$

The fraction of synchronised population is defined as

$$y_s(t) = N_s(t) / (N_s(t) + N_h) \quad (5)$$

On eliminating N_s , N_h , and ψ from Equations (2)–(5), we obtain extreme values for y_s as follows:

$$y_{s\min} = (BF_{\max} - BF_{\min}) / [1 + BF_{\min}(\exp(DT_c) - 1)] \quad (6)$$

$$y_{s\max} = \exp(DT_c)(BF_{\max} - BF_{\min}) / [1 + BF_{\max}(\exp(DT_c) - 1)] \quad (7)$$

The fraction of synchronised population can be calculated from measured values of minimum and maximum budded fraction, dilution rate and period of CO_2 cycles by using Equations (6) and (7).

2. Tables

- D.1 Budded fraction data for chemostat ($D=0.2 \text{ h}^{-1}$) to continuous fed-batch fermentation.
- D.2 Budded fraction data for chemostat ($D=0.2 \text{ h}^{-1}$) to Monte Carlo fed-batch fermentation.
- D.3 Budded fraction data for chemostat at $D=0.1 \text{ h}^{-1}$.

3. Figures

- D.1 Reproducibility of CO_2 profiles for chemostat fermentations at $D=0.2 \text{ h}^{-1}$.
- D.2 CO_2 -cycles during chemostat fermentations ($D=0.2 \text{ h}^{-1}$) as a measure of synchrony.
- D.3 Profile of Dissolved oxygen during a chemostat at $D=0.2 \text{ h}^{-1}$.
- D.4 Profile of pH during a chemostat at $D=0.2 \text{ h}^{-1}$.
- D.5 Profile of CO_2 during a continuous fed-batch fermentation.
- D.6 Profile of CO_2 during a Monte Carlo fed-batch fermentation.
- D.7 Profile of O_2 during a batch-chemostat-continuous fed-batch fermentation.
- D.8 Profile of O_2 during a batch-chemostat-Monte Carlo fed-batch fermentation.
- D.9 Profile of pH during a batch-chemostat-continuous fed-batch fermentation.
- D.10 Profile of pH during a batch-chemostat-Monte Carlo fed-batch fermentation.
- D.11 Cell number density in chemostat-continuous fed-batch fermentation.
- D.12 Cell number density in chemostat-Monte Carlo fed-batch fermentation.

Table D.1 Budded fraction data for chemostat ($D=0.2 \text{ h}^{-1}$) to continuous fed-batch fermentation.

NUMBER OF CELLS ON SLIDE						
SAMPLE NUMBER	TIME (h)	SINGLE CELLS	BUDDED CELLS	TOTAL CELLS	BUDDED FRACTION	TOTAL million/mL
INOCULUM	0.00	185	261	446	0.59	2 BATCH START
1	2.00	171	436	607	0.72	14
2	7.00	180	400	580	0.69	13
3	11.08	162	268	430	0.62	75
4	23.50	331	258	589	0.44	147 CHEMOSTAT START
5	23.80	411	200	611	0.33	153
6	24.33	482	122	604	0.20	151
7	24.48	481	159	640	0.25	160
8	24.72	473	205	678	0.30	170
9	24.98	312	357	669	0.53	167
10	25.12	250	367	617	0.59	154
11	25.32	266	344	610	0.56	153
12	25.55	215	323	539	0.60	162
13	25.83	216	269	485	0.55	146
14	26.18	288	226	514	0.44	154
15	26.45	364	184	548	0.34	164
16	26.67	371	148	519	0.29	156
17	26.93	568	145	713	0.20	178 FED-BATCH START
18	27.80	325	331	656	0.50	164
19	28.50	221	459	680	0.68	170
20	28.83	321	483	804	0.60	201
21	29.23	465	409	874	0.47	219
22	29.80	716	321	1037	0.31	259
23	30.22	644	368	1012	0.36	253
24	30.60	819	570	1389	0.41	347
25	31.07	524	337	861	0.39	301
26	31.50	561	291	852	0.34	298
27	31.78	540	268	808	0.33	323
28	32.05	437	333	770	0.43	347
29	32.35	430	370	800	0.46	360
30	32.75	474	356	830	0.43	374
31	33.08	549	381	930	0.41	419
32	33.51	319	197	516	0.38	473
33	34.03	283	250	533	0.47	489
34	34.53	308	206	514	0.40	471
35	34.83	376	210	586	0.36	537
36	35.35	386	196	582	0.34	534
37	36.00	307	314	621	0.51	569
38	36.40	313	374	687	0.54	630
39	36.82	320	296	616	0.48	565
40	37.13	332	311	643	0.48	590
41	37.47	406	286	692	0.41	634
42	38.22	566	216	782	0.28	717
43	39.00	736	96	832	0.12	763 FED-BATCH STOP

Table D.2 Budded fraction data for chemostat ($D=0.2 \text{ h}^{-1}$) to Monte Carlo fed-batch fermentation.

NUMBER OF CELLS ON SLIDE						
SAMPLE NUMBER	TIME (h)	SINGLE CELLS	BUDDED CELLS	TOTAL CELLS	BUDDED FRACTION	TOTAL million/mL
10	24.68	343	223	566	0.39	113
11	24.82	360	205	565	0.36	113
12	24.97	383	155	538	0.29	108
13	25.13	404	150	554	0.27	111
14	25.25	413	140	553	0.25	111
15	25.37	521	145	666	0.22	133
16	25.47	452	153	605	0.25	121
17	25.58	502	159	661	0.24	132
18	25.75	465	155	620	0.25	124
19	25.92	491	192	683	0.28	137
20	26.08	333	318	651	0.49	130
21	26.25	232	340	572	0.59	114
22	26.45	254	361	615	0.59	123
23	26.63	224	329	553	0.59	111
24	26.87	200	332	532	0.62	106
25	27.12	296	370	666	0.56	133
26	27.37	323	353	676	0.52	169
27	27.67	461	256	717	0.36	179
28	27.82	483	286	769	0.37	192

(Cont.)TABLE D.2: BUDDED FRACTION DATA FOR CHEMOSTAT AT $D=0.2$ (1/h)
AND MONTE CARLO FED-BATCH FERMENTATION

NUMBER OF CELLS ON SLIDE							REMARK
SAMPLE NUMBER	TIME (h)	SINGLE CELLS	BUDDED CELLS	TOTAL CELLS	BUDDED FRACTION	TOTAL million/mL	
29	28.03	626	254	880	0.29	220	FED-BATCH START
30	28.37	592	171	763	0.22	191	
31	28.60	774	177	951	0.19	238	
32	28.85	607	230	837	0.27	209	
33	29.08	496	406	902	0.45	226	
34	29.33	314	471	785	0.60	196	
35	29.50	339	602	941	0.64	235	
36	29.75	256	502	758	0.66	227	
37	30.00	300	502	802	0.63	241	
38	30.33	427	468	895	0.52	269	
39	30.67	575	332	907	0.37	272	
40	30.92	632	269	901	0.30	270	
41	31.17	718	298	1016	0.29	305	
42	31.42	680	167	847	0.20	296	
43	31.67	646	197	843	0.23	295	
44	31.92	510	388	898	0.43	314	
45	32.17	465	526	991	0.53	347	
46	32.42	407	549	956	0.57	335	
47	32.67	332	419	751	0.56	338	
48	32.92	317	452	769	0.59	346	
49	33.17	448	410	858	0.48	386	
50	33.42	501	385	886	0.43	399	
51	33.67	593	267	860	0.31	387	
52	33.92	670	315	985	0.32	443	
53	34.17	363	267	630	0.42	473	
54	34.50	481	260	741	0.35	556	
55	34.92	428	192	620	0.31	465	
56	35.25	462	200	662	0.30	497	
57	35.67	444	272	716	0.38	537	
58	36.13	492	234	726	0.32	545	
59	36.42	446	232	678	0.34	622	
60	36.83	510	272	782	0.35	717	
61	37.17	437	280	717	0.39	657	
62	37.62	483	319	802	0.40	735	
63	37.92	473	281	754	0.37	691	
64	38.35	451	298	749	0.40	687	
65	38.67	500	260	760	0.34	697	
66	38.99	498	239	737	0.32	676	
67	39.42	564	261	825	0.32	756	
68	39.83	617	310	927	0.33	850	
69	40.17	697	265	962	0.28	882	

FED-BATCH STOP

Table D.3 Budded fraction data for chemostat at $D=0.1 \text{ h}^{-1}$.

SAMPLE NUMBER	TIME (min)	NUMBER OF CELLS ON SLIDE			BUDDED FRACTION	TOTAL million/mL	REMARK
		SINGLE CELLS	BUDDED CELLS	TOTAL CELLS			
1	0	364	85	449	0.19	180	Cycle Start
2	120	382	99	481	0.21	192	
3	240	344	85	429	0.20	172	
4	246	401	116	517	0.22	207	
5	258	357	111	468	0.24	187	
6	268	318	117	435	0.27	174	
7	280	287	136	423	0.32	169	
8	292	241	218	459	0.47	184	
9	304	219	214	433	0.49	173	
10	320	255	220	475	0.46	190	
11	340	269	188	457	0.41	183	
12	372	331	136	467	0.29	187	
13	596	387	58	445	0.13	178	Cycle Ends

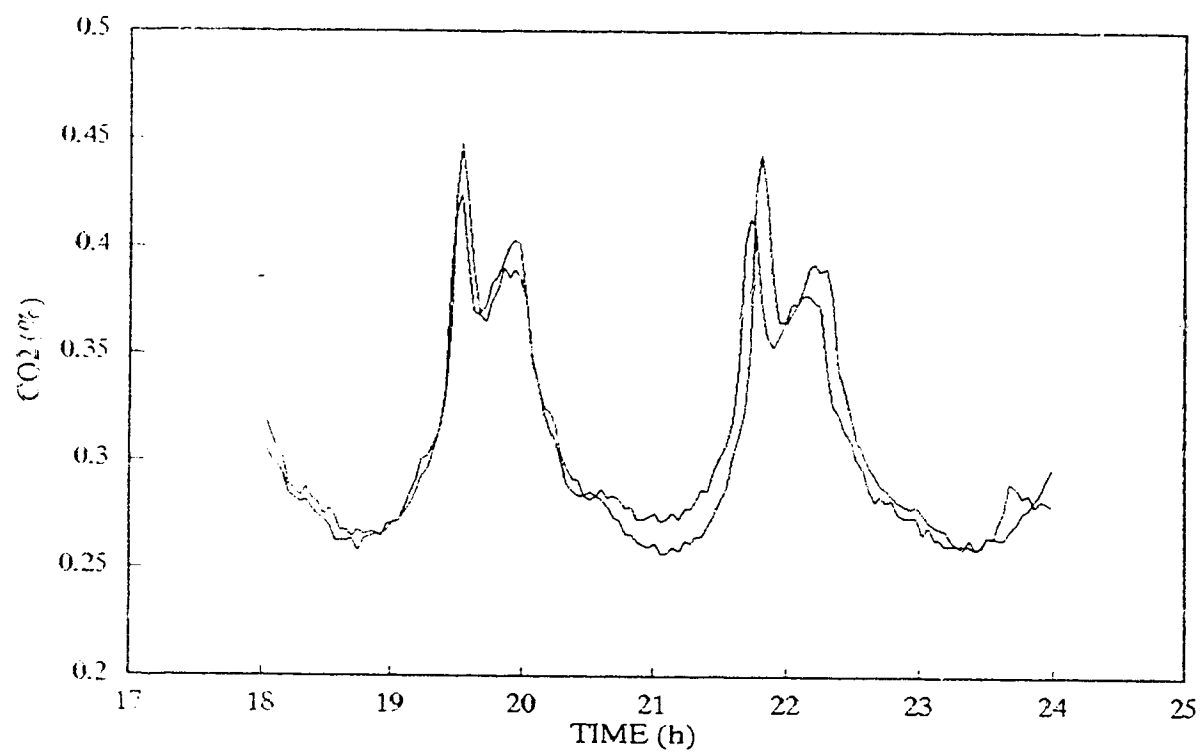


Figure D.1 Reproducibility of CO₂ profiles for chemostat fermentations at $D=0.2 \text{ h}^{-1}$.

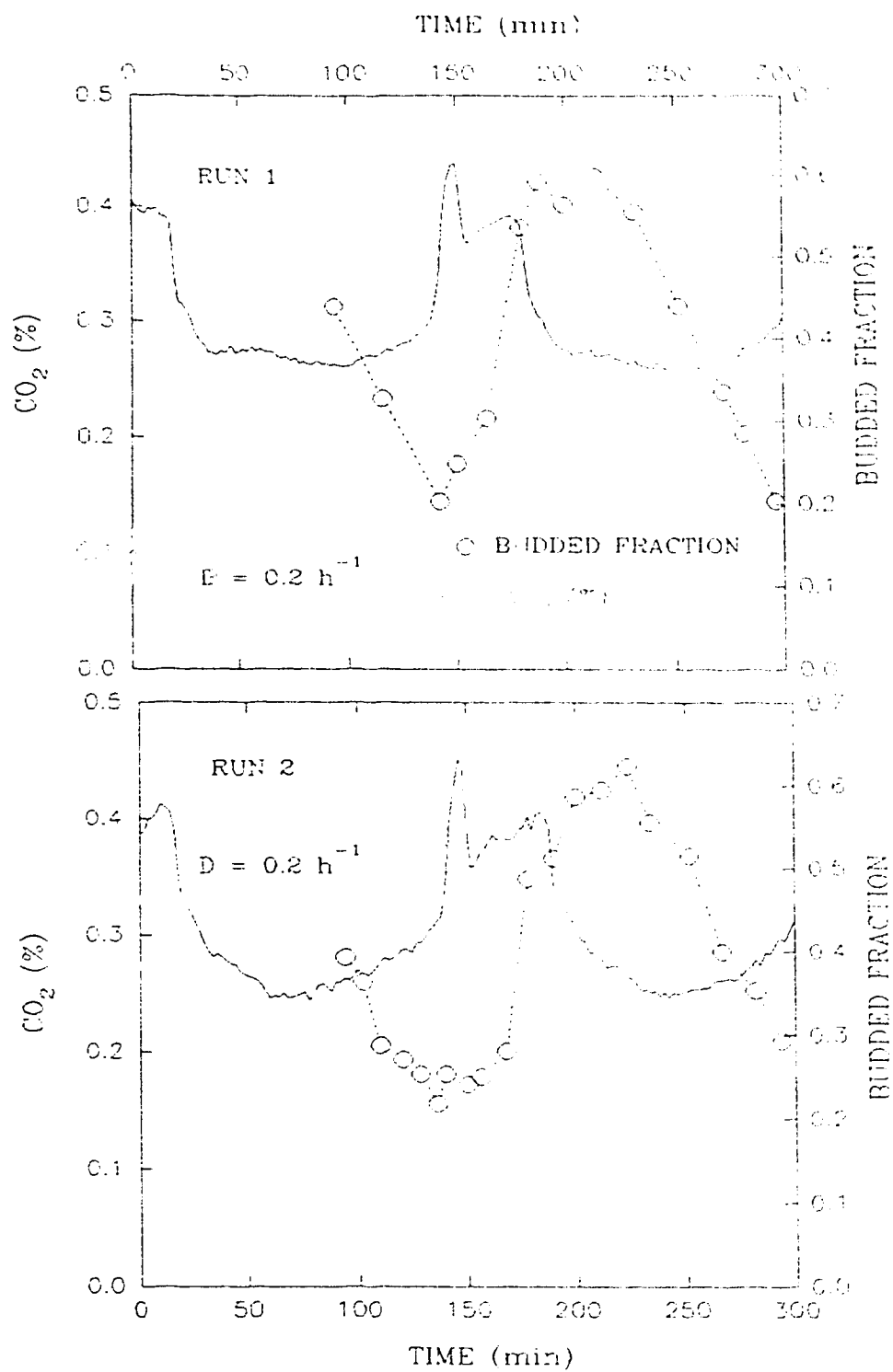


Figure D.2 CO₂-cycles during chemostat fermentations ($D=0.2 \text{ h}^{-1}$) as a measure of synchrony.

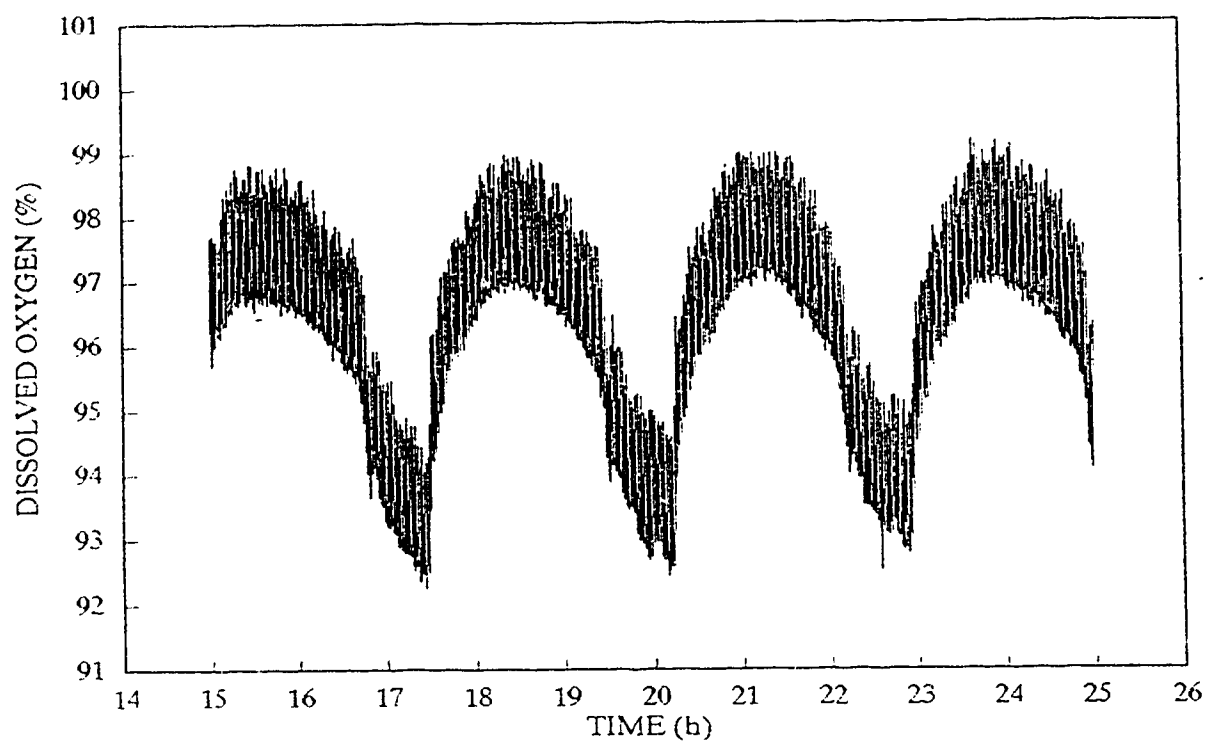


Figure D.3 Profile of Dissolved oxygen during a chemostat at $D=0.2 \text{ h}^{-1}$.

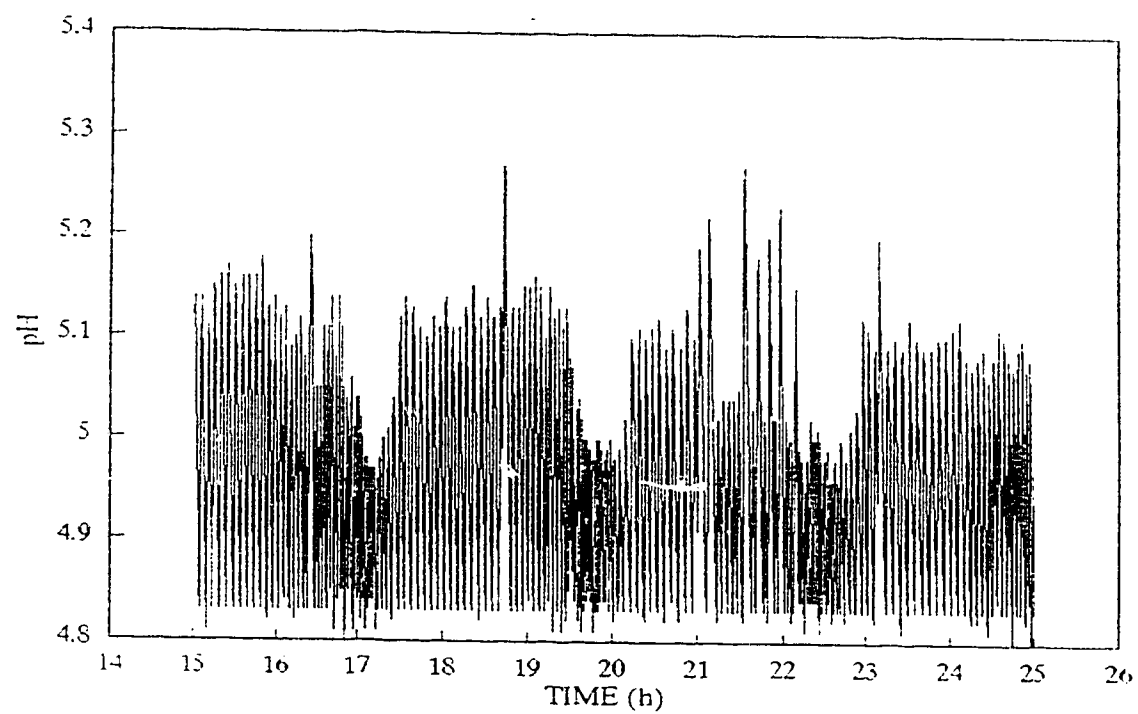


Figure D.4 Profile of pH during a chemostat at $D=0.2 \text{ h}^{-1}$.

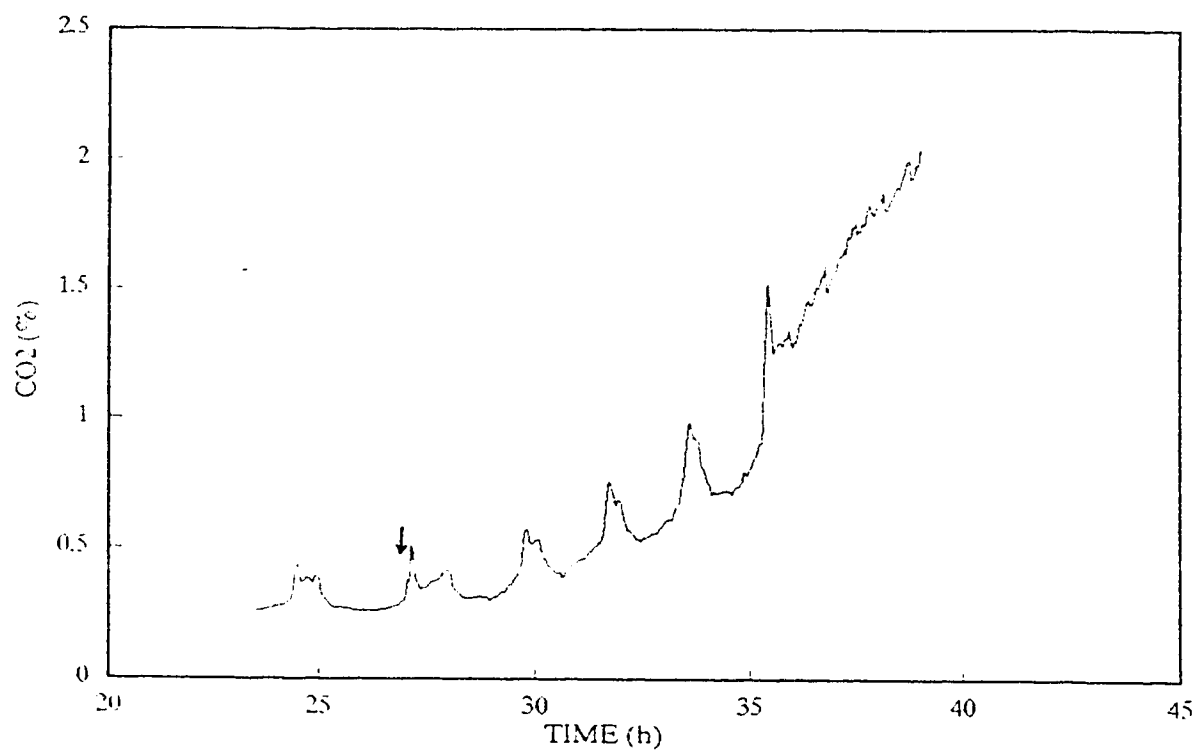


Figure D.5 Profile of CO₂ during a continuous fed-batch fermentation.

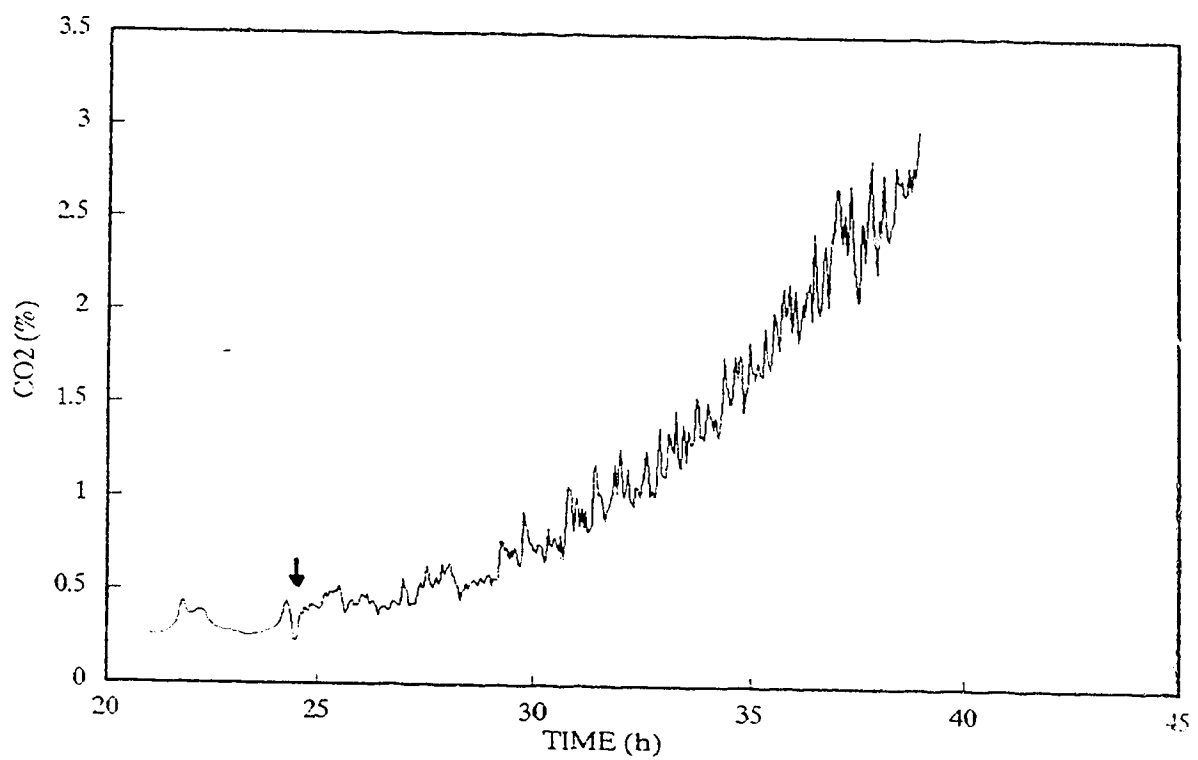


Figure D.6 Profile of CO₂ during a Monte Carlo fed-batch fermentation.

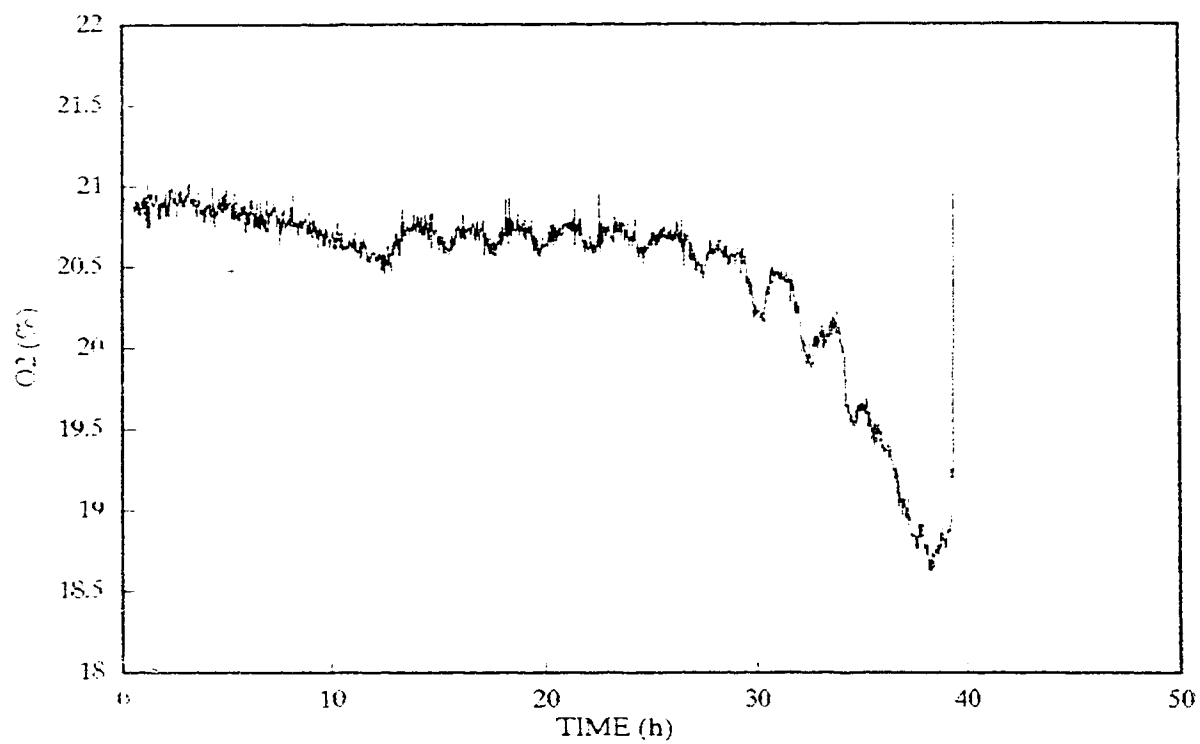


Figure D.7 Profile of O_2 during a batch-chemostat-continuous fed-batch fermentation.

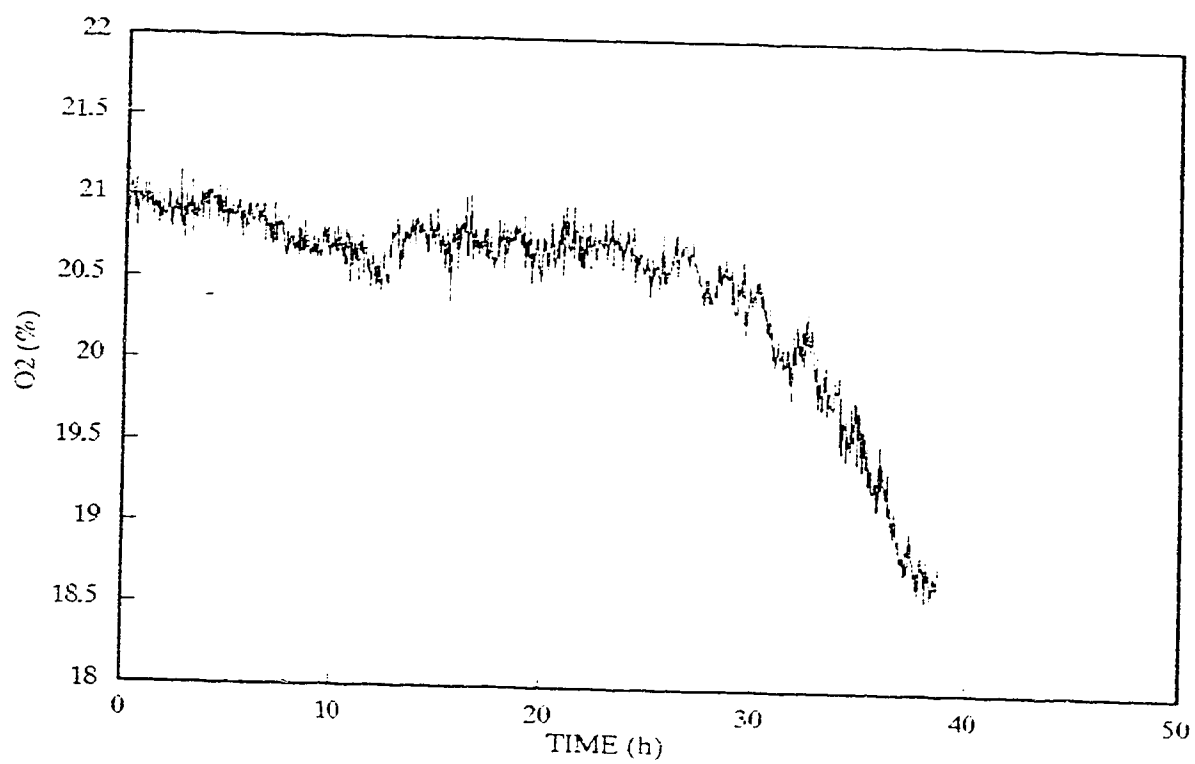


Figure D.8 Profile of O₂ during a batch-chemostat-Monte Carlo fed-batch fermentation.

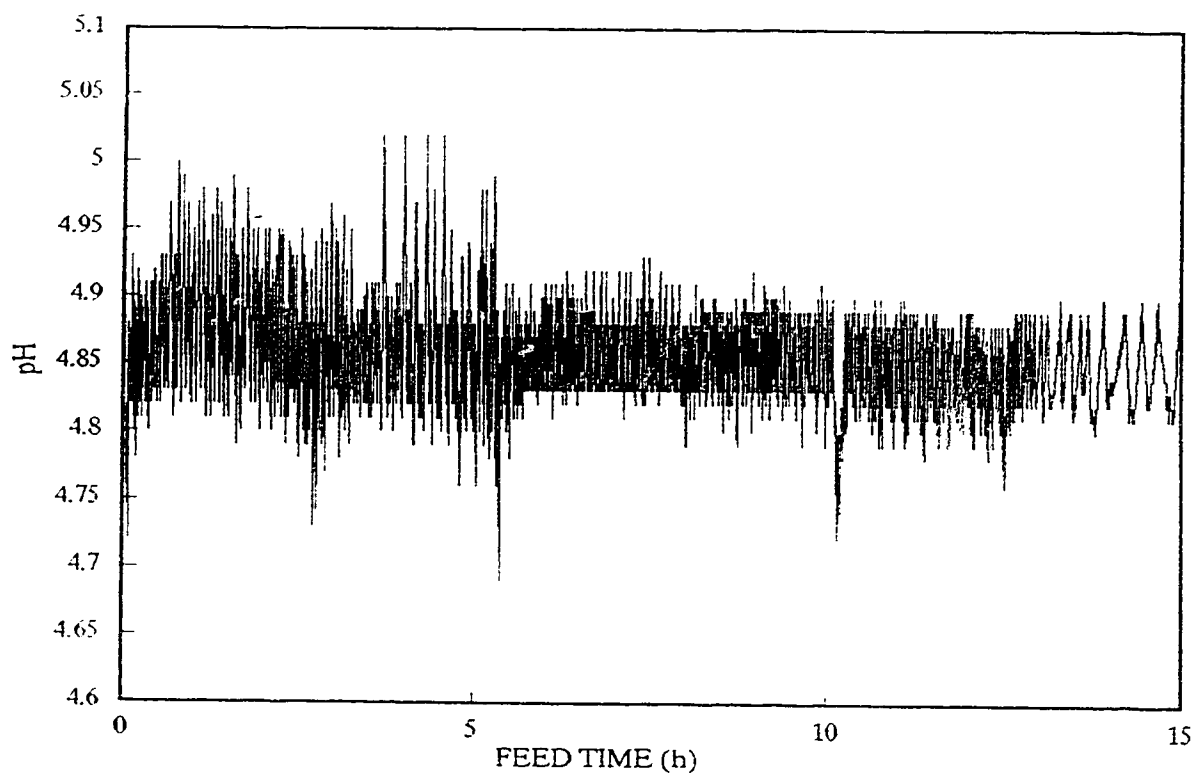


Figure D.9 Profile of pH during a batch-chemostat-continuous fed-batch fermentation.

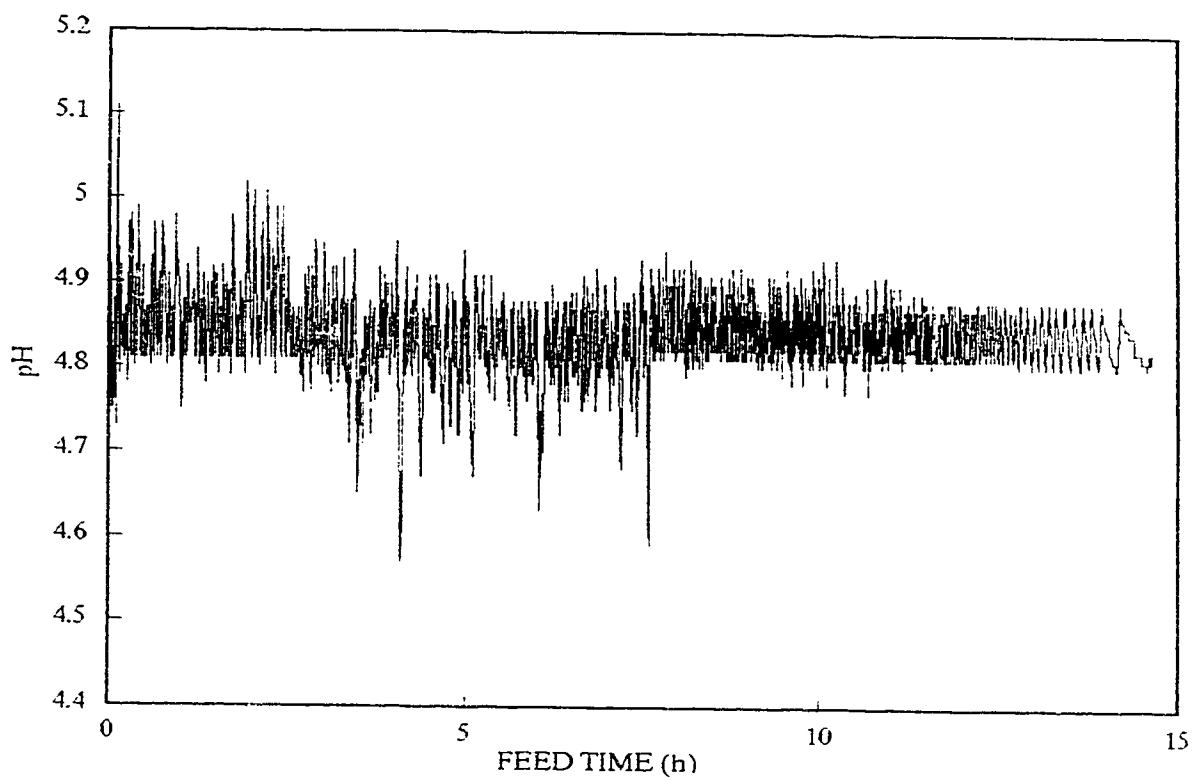


Figure D.10 Profile of pH during a batch—chemostat—Monte Carlo fed—batch fermentation.

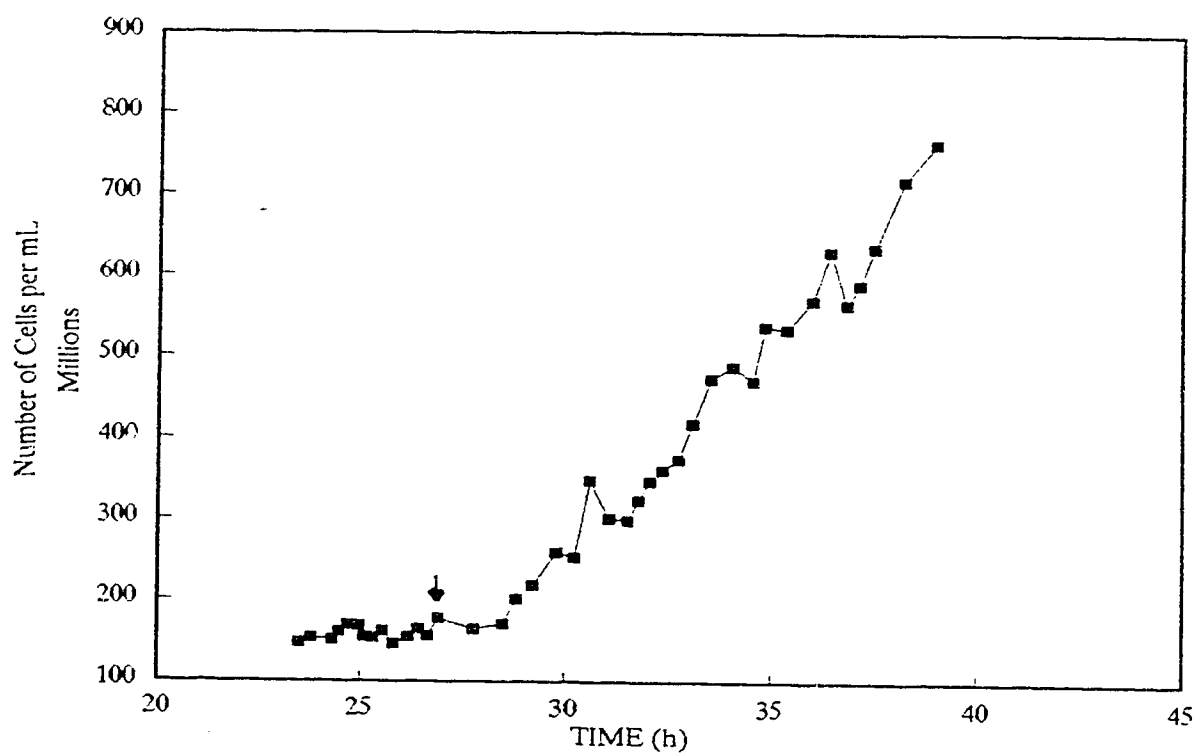


Figure D.11 Cell number density in chemostat-continuous fed-batch fermentation.

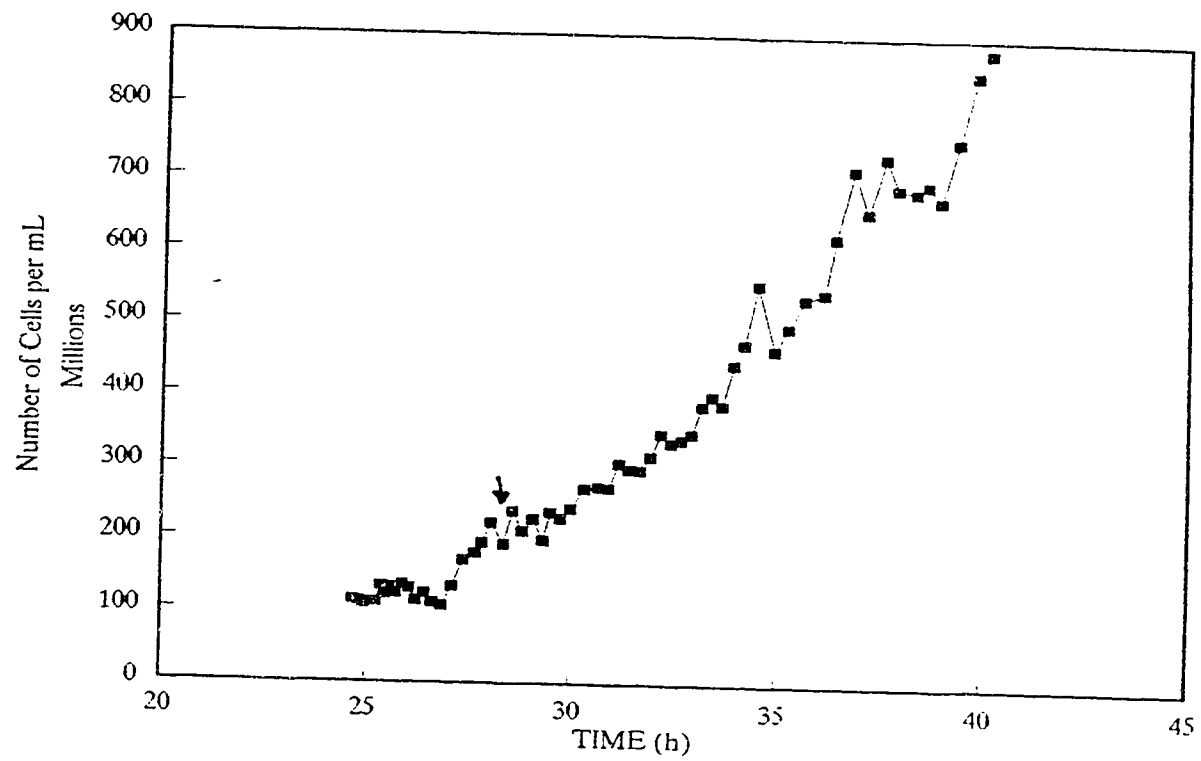


Figure D.12 Cell number density in chemostat-Monte Carlo fed-batch fermentation.